LIVING/CONTROLLED RADICAL POLYMERIZATION CONDUCTED IN AQUEOUS BASED SYSTEMS

by

RYAN W. SIMMS

A thesis submitted to the Department of Chemical Engineering

In conformity with the requirements for

The degree of Doctor of Philosophy

Queen's University

Kingston, Ontario, Canada

September 2007

ABSTRACT

In the last decade processes known as living/controlled radical polymerizations (L/CRP) have been developed which permit the synthesis of high-value specialty polymers. Currently, the three processes that have demonstrated the most potential are: reverse addition fragmentation chain transfer polymerization (RAFT), atom transfer radical polymerization (ATRP) and stable free radical polymerization (SFRP). While each process has their strengths and weaknesses with regard to specific polymers and architecture, the viability of these systems to industrial scale production all lie in the ability to perform the polymerization in a water based system because of process, environmental and economic advantages.

The most effective method of controlling the polymerization of vinyl acetate in bulk has been RAFT. We have developed a miniemulsion RAFT polymerization using the xanthate methyl (ethoxycarbonothioyl)sulfanyl acetate. The miniemulsion is stabilized with 3 wt% sodium lauryl sulfate, initiated with the azo-based water-soluble VA-060.

The main focus of this research was adapting ATRP to a miniemulsion system. It was determined that ionic surfactants can be successfully employed in emulsion-based ATRP. The cationic surfactant cetyltrimethylammonium bromide provides excellent stability of the latex over a range of surfactant loadings (allowing the particle size to be easily manipulated), at temperatures up to 90 ^{o}C, for a wide variety of ATRP formulations. A new method of initiation was developed for reverse ATRP, using the redox pair hydrogen peroxide/ascorbic acid. This nearly eliminated the induction period at the start of the polymerization, increased the polymerization rate 5 fold and,

surprisingly, enabled the formation of well-controlled polymers with a number-average molecular (M_n) weight approaching 1 million (typically ATRP is limited to ~200 000). The ability to control the particle size and the number of polymer chains (through the target M_n) over a wide range of values allowed us to determine that ATRP is influenced by compartmentalization effects.

The knowledge gained from our work in L/CRP was used to develop the surfactant-free SFRP of styrene. A multi-stage approach was adopted starting from dilute styrene/water solutions to favor the formation of the alkoxyamine and short chain SG1-oligomers (stage one) before the addition of the majority of the styrene (stage two).

ACKNOWLEDGEMENTS

I would like to thank Mike Cunningham for the opportunity to work in his lab over the last 4 years. I have learned a lot about science, dodgeball and the BBQing of salmon. Thanks to all my lab mates over the years who made the lab a fun place to work, and a great place to conduct research. To my family and friends, thanks for everything.

What gets us into trouble is not what we don't know,

it's what we know for sure that just ain't so.

- Mark Twain

TABLE OF CONTENTS

LIST OF SCHEMES

LIST OF TABLES

LIST OF FIGURES

NOMENCLATURE

3N	N,N,N',N',N'-Pentamethyldiethylenetriamine
AA	Ascorbic acid
AIBN	2,2'-azobis(isobutyronitrile)
ATRP	Atom transfer radical polymerization
BA	Butyl acrylate
BMA	Butyl methacrylate
BPO	Benzoyl peroxide
Bpy	2,2'-bipyridine
Brij98	Polyoxyethylene(20) oleyl ether
CMC	Critical micelle concentration
CTAB	Cetyltrimethylammonium bromide
dNbpy	4,4'-di(5-nonyl)-2,2'-bipyridine
EBiB	Ethyl 2-bromoisobutyrate
FRP	Free radical polymerization
HD	Hexadecane
HPO	Hydrogen peroxide
$[I]_0$	Initial concentration of initiator
KPS	Potassium persulfate
L/CRP	Living/controlled radical polymerization
MA	Methyl acrylate
MADIX	Macromolecular design via interchange of xanthates

MESA	Methyl (ethoxycarbonothioyl)sulfanyl acetate
MMA	Methyl methacrylate
$[M]_0$	Initial concentration of monomer at time = 0
$[M]_t$	Monomer concentration at time = t
NMRP	Nitroxide-mediated radical polymerization
PDI	Polydispersity index
$P_i^{\bullet}$	Propagating polymer radical
P_i-Y	Dormant chain
PVOH	Polyvinyl alcohol
RAFT	Reversible addition fragmentation transfer
SDS	Sodium dodecyl sulfate
SFRP	Stable free radical polymerization
SLS	Sodium lauryl sulfate
TREN	Tris(2-aminoethyl)amine
EHA_6TREN	Tris[2-di(2-ethylhexyl acrylate)aminoethyl]amine
V-50	2,2’azobis(2-methylpropionamidine) dihydrochloride
VA-044	2,2’azobis[2-(2-dimidazolin-2-yl)propane] dihydrochloride
VA-60	2,2'-Azobis{2-[1-(2-hydroxyethyl)-2-imidazolin-2-yl]propane}dihydrochloride
$Y^{\bullet}$	Persistent radical species

CHAPTER 1

1 INTRODUCTION

1.1 Aqueous Dispersed Polymerizations

1.1.1 Emulsion Polymerization

The benefits of emulsion polymerization include reduced volatile organic compounds, improved control over the heat evolved from the polymerization and reduced viscosity compared to solution/bulk systems. An emulsion polymerization consists of water, surfactant above its critical micelle concentration (CMC) and a water-insoluble monomer. These ingredients are vigorously agitated to form monomer droplets suspended in water. Surfactants are used to stabilize the emulsions through either electrostatic or steric (polymeric) mechanisms, and the micelles they form become the loci of polymerization. Most of the monomer is contained within the droplets that are 1-10 μm in diameter, while a small amount of monomer swells the micelles. Water-soluble initiators are used and decompose (thermally or chemically) in the aqueous phase to form primary radicals. The water-soluble primary radicals add 2-5 monomer units that are dissolved in the aqueous phase and become sufficiently hydrophobic to enter micelles thereby nucleating a particle. The micelles are predominately nucleated due to the large surface area of micelles relative to the monomer droplets. The monomer droplets act as a reservoir from which monomer diffuses to the growing polymer particles. The final product is a dispersion of polymer particles of uniform size with mean diameters ~50-500 nm.[1]

All living radical polymerizations that have been applied to emulsion polymerizations have suffered from colloidal instability. The cause of this instability has

yet to be determined but is attributed to one or a combination of: particle nucleation, polymerization within the droplets, stabilization of very small particles in the early stage of polymerization, and the high concentration of oligomeric chains. The shortcomings of the emulsion process have been overcome with the application of the miniemulsion process. The use of a miniemulsion has proven to be far more robust with respect to colloidal stability for conducting living radical polymerizations.[2]

1.1.2 Miniemulsion Polymerization

A miniemulsion[3,4] consists of water, water-insoluble monomer, surfactant (below the CMC) and a co-stabilizer. After the ingredients are mixed, the emulsion must be homogenized by a high shear device (microfluidizer or sonicator) to produce uniform monomer droplets that have diameters ~50-500 nm (controlled by the formulation). The costabilizer is a hydrophobe, usually hexadecane, which stabilizes the monomer droplets against diffusional degradation (Ostwald ripening). As with emulsions, water-soluble initiators are used (but oil-soluble initiators are compatible in miniemulsion formulations) which form oligoradicals in the aqueous phase that nucleate the monomer droplets. The surfactant concentration is kept below the CMC, eliminating micelles and allowing the monomer droplets to be the primary nucleation point. Droplet nucleation leads to simpler kinetic behavior by largely eliminating the early stages of conventional emulsion particle nucleation. The benefit of simpler kinetics in a miniemulsion has been very advantageous for conducting L/CRP, as well, miniemulsions are suitable for making particles containing additives or for polymerizing highly water-insoluble monomers that are difficult to polymerize in emulsion.

1.1.3 Colloidal Stability in Miniemulsion

One of the major obstacles in adapting "living" radical polymerizations to a miniemulsion process has been maintaining the colloidal stability throughout the polymerization. Colloidal instability can result from diffusional transfer (Ostwald ripening) of monomer droplets and/or particle coagulation (flocculation).

1.1.3.1 Diffusional Degradation

Diffusional degradation of monomer droplets is often called the Ostwald ripening effect. Monomer in the smaller droplets have a higher chemical potential then the monomer in the larger droplets, due to the Laplace pressure of the droplets, resulting in larger droplets growing at the expense of the smaller droplets. This effect can be minimized by producing a miniemulsion with a uniform droplet size and adding a hydrophobe. The hydrophobe creates an osmotic pressure inside the miniemulsion droplets that counterbalances the Laplace pressure.[5] Consequently, a change in the droplet size by diffusion of monomer causes the osmotic pressure to increase faster than the Laplace pressure, effectively preventing diffusion once the pressures are equal. The less water-soluble the hydrophobe the more effective it is as an osmotic pressure agent. Hexadecane can be used in any miniemulsion to effectively stabilize the monomer droplets against diffusional degradation. It has also been shown that for some systems a polymer can act as a costabilizer.[6]

1.1.3.2 Coagulation

Particles are constantly experiencing Brownian encounters with other particles which result in rapid coagulation (if the particles are unprotected). The particles clump

together when they collide because of the attractive London dispersion forces (van der Waals force) that exist between them.[7] To stabilize miniemulsion particles against coagulation a long range repulsive force must be imparted on the particles to oppose the attractive van der Waals force. Surfactants are used to stabilize the miniemulsions through either electrostatic or steric (polymeric) mechanisms. Miniemulsions have almost exclusively been prepared using electrostatic stabilization with ionic surfactants, for example sodium lauryl sulfate (SLS). The surfactant absorbs at the particle/water interface forming an electric double layer which provides electrostatic repulsion that stabilizes the miniemulsion.[8] The best steric (polymeric) stabilizers are amphipathic block copolymers. One segment must be soluble in the aqueous medium while the other is insoluble in water. The latter, called the anchor polymer, is soluble in monomer and serves to attach the surfactant to the monomer droplets. The hydrophilic block is the stabilizing moiety, which orients itself in the aqueous phase to provide stability for the colloidal particles. The most common class of non-ionic surfactants is based on the block copolymers of polyoxyethylene (POE) such as Brij 98.[9]

1.2 Living/Controlled Radical Polymerization (L/CRP)

Free radical polymerization is one of the most common and useful methods for making polymers from vinyl monomers. It has long been a cost effective way to produce commodity polymers due to its tolerance to impurities, adaptability to aqueous based systems and the wide variety of monomers that it can polymerize. Recent advances in the field have led to the development of L/CRP, which provides a facile route to the syntheses of polymers with narrow molecular weight distributions and complex microstructure, such as macromonomers, functional polymers, block polymers and graft

(comb or star) polymers. Such strict control of the polymer structure has previously been achieved using traditional living polymerizations (anionic, cationic and group transfer); however, none of these methods have found widespread application due to cost, narrow operating windows and/or lack of control over the structure. Irreversible termination reactions do occur in L/CRP, but the benefits include milder reaction conditions and a tolerance to impurities, including water, which is advantageous because it allows for aqueous based polymerizations. L/CRP has the potential to become commercially viable because it exhibits all the desirable traits of conventional free radical polymerization while providing the necessary control to produce polymers with complex architecture. The three L/CRP techniques appearing most frequently in the literature are: reverse addition fragmentation chain transfer polymerization (RAFT), atom transfer radical polymerization (ATRP) and stable free radical polymerization (SFRP).

1.2.1 Reverse Addition Fragmentation Transfer (RAFT)

Of all the L/CRP techniques RAFT has shown the most versatility in terms of the variety of monomers that can be polymerized in a controlled manner and the broad range of reaction conditions that can be employed.[10] The control of the polymerization is achieved through a reversible transfer mechanism, in which a chain transfer agent is repeatedly exchanged between the dormant polymer chains and polymeric radicals. The RAFT process originally referred to dithioesters as chain transfer agents (Figure 1-1), while the use of xanthates has been termed MADIX (macromolecular design via interchange of xanthates), although mechanistically the processes are identical. Chiefari *et al*.[11] showed that in the presence of the appropriate dithioester the polymerization of methyl methacrylate, butyl methacrylate, butyl acrylate and styrene all resulted in a linear

relationship between the molecular weight and conversion, and the polymers had very narrow final polydispersity index (*PDI*) of less than 1.2. The first MADIX article published by the Rhodia researchers[12] described the controlled polymerization of styrene, methyl acrylate, and vinyl acetate. For vinyl acetate the molecular weight grew with conversion (but in a non-linear manner), and the final *PDI* was relatively high for controlled polymerizations (ranging from 2.1 to 1.4). The MADIX process has since been refined and now provides excellent control over the polymerization for a variety of monomers.[13]

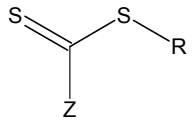

General RAFT Structure

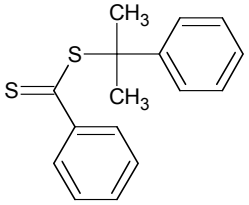

RAFT agent

(Cumyl dithiobenzoate)

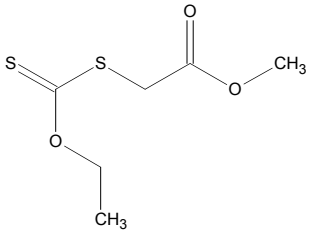

Xanthate

(Methyl (ethoxycarbonothioyl)sulfanyl acetate)

Figure 1-1: The Structure of RAFT/MADIX Agents

The ability of the RAFT agent to effectively mediate a radical polymerization depends on the leaving group, R, and the stabilizing group, Z (Figure 1-1). The R-group must be a good leaving group and also be able to re-initiate the polymerization, while the Z-group influences the stability and reactivity of the transfer agent. Different structures are more effective at controlling the polymerization of certain monomers.[14]

The basic reactions describing the RAFT process are shown in Scheme 1-1. The process begins with the formation and propagation of primary radicals from the

decomposition of the initiator. The number of radicals generated from the initiator will influence the rate of polymerization ($r_p \propto [R\bullet]$) and, critical to the control of the polymerization, the rate of termination ($r_t \propto [R\bullet]^2$). The short chain radical propagates by monomer addition until it reacts with the initial RAFT agent causing the release of the R leaving group, which itself propagates until it reacts with another RAFT species. The radical mediation step is the key equilibrium that determines the degree of control over the polymerization. Selecting a highly active transfer agent (one that is totally consumed within a few percent of monomer conversion) and adding a large amount of transfer agent relative to initiator (so that the total number of polymer chains is determined predominantly by the number of transfer agent molecules) will ensure that the final polymer has a narrow *PDI* because all the polymer chains originate from a transfer agent at the start of the polymerization (so that the polymer chains are approximately the same length because they have had equal time to propagate).

This is the generally accepted mechanism; however, there are still uncertainties about the kinetics of RAFT[15] In practice the number of free radicals is reduced whenever a RAFT agent is employed, leading to a lower polymerization rate than expected. This is termed rate retardation and is believed to arise from long-lived intermediates (Scheme 1-1, B). A mechanistically related event in these systems is inhibition, a period at the beginning of the reaction where no polymerization occurs. Inhibition is thought to occur because of the long-lived intermediate A in Scheme 1-1.[16] Another possibility is that the leaving group, R, may be slow to re-initiate.[17] Inhibition may also result from impurities in the system such as oxygen or residual inhibitor from the monomer. Buback and Vana have used mathematical modeling to suggest that a reaction step involving a propagating

radical and the long-lived intermediates (A and B) can resolve the RAFT polymerization kinetics.[18]

Initiation: $I_2 \longrightarrow 2I\bullet$ (decomposition)

$I\bullet + M \longrightarrow P_1\bullet$ (initiation)

RAFT Pre-equilibrium:

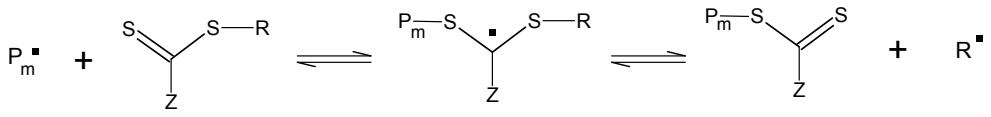

(**A**)

Propagation: $R^{\bullet} + M \longrightarrow P^{\bullet}_1$

$P^{\bullet}_m + M \longrightarrow P^{\bullet}_{m+1}$

Radical mediation:

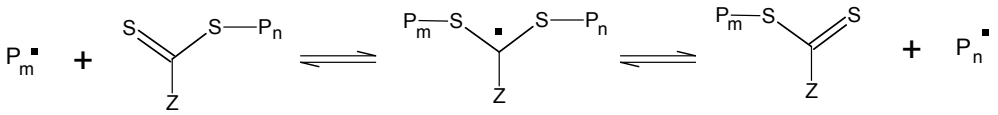

(**B**)

Transfer to monomer: $P_m\bullet + M \longrightarrow D_m + P_1\bullet$

Termination: $P_m\bullet + P_n\bullet \longrightarrow D_{n+m}$ (combination)

$P_n\bullet + P_m\bullet \longrightarrow D_n + D_m$ (disproportionation)

Scheme 1-1. The Reaction Mechanism of RAFT/MADIX

1.2.2 Atom Transfer Radical Polymerization (ATRP)

ATRP, also known as metal-mediated radical polymerization, controls the polymerization through a reversible termination mechanism of the growing polymer radicals, $P_i^{\bullet}$, with a persistent radical species, $Y^{\bullet}$, to form dormant chains, P_i-Y.[19] The mechanism is described by the following set of reactions:

$$P_i^{\bullet} + Y^{\bullet} \longrightarrow P_i - Y \qquad \text{(deactivation)}$$

$$P_i - Y \longrightarrow P_i^{\bullet} + Y^{\bullet} \qquad \text{(activation)}$$

Scheme 1-2. The Reversible Termination Mechanism

The foundation of control is the activation/deactivation cycle undertaken by all living chains during the polymerization. The fast and dynamic equilibrium that is established greatly favours the dormant chains over the growing polymer radicals. The resulting low concentration of radicals causes the rate of chain termination to become negligible, because it is proportional to the concentration of radicals in the system ($r_t \propto [R^{\bullet}]^2$).

The pioneering work was conducted by two groups that published their results in quick succession. Sawamoto's group[20] were able to polymerize methyl methacrylate with $RuCl_2(PPh_3)_3$/$MeAl(ODBP)_2$ as the radical mediating agent and CCl_4 as the initiator (ODBP = methylaluminum bis-(2,6-di-tert-butylphenoxide)). They showed that the molecular weight increased linearly with conversion while the polydispersity decreased with conversion, reaching a final value of less than 1.4. Shortly afterwards, Matyjaszewski's group[21,22] polymerized styrene using the initiator 1-phenylethyl chloride

and CuCl/2,2'-bipyridine as the radical mediating species. The resulting polymer exhibited an increasing molecular weight with conversion and a final polydispersity of less than 1.5. Extensive work has been performed to develop and expand an understanding of ATRP in bulk and solution.[23-27] Under appropriate conditions very good mediation of the radical polymerization may be achieved resulting in polymers with predetermined molecular weight, a narrow polydispersity and high end group purity.

1.2.2.1 Components of ATRP

The components of ATRP include the monomer, an initiator and a radical mediating complex. A variety of monomers have been polymerized successfully using ATRP, including (meth)acrylates, styenes and (meth)acrylamides. The initiators are alkyl halides with an activating substituent (such as aryl or carbonyl) on the α-carbon (Figure 1-2). The amount of initiator determines the number of polymer chains. If initiation is fast and termination negligible, the number of growing chains will equal the number of initiator molecules. This allows for a predetermined molecular weight equal to $[M]_0/[I]_0$.

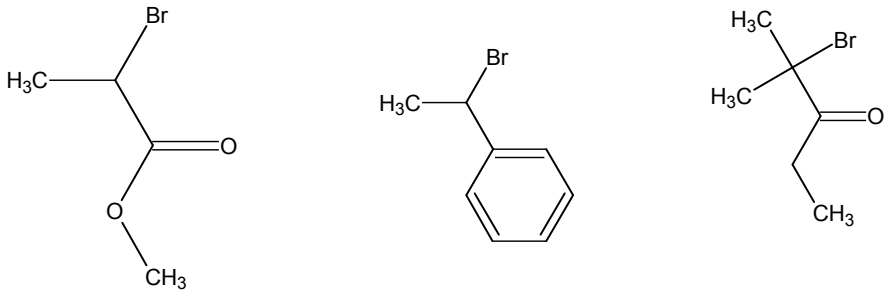

Methyl 2-bromopropanoate (MBrP) | Phenylethyl bromide | Ethyl α-bromoisobutyrate (EBiB)

Figure 1-2. Initiators Used in ATRP

The mediating complexes in ATRP control the activation/deactivation process during the polymerization. The frequency of the activation/deactivation cycle and the transient lifetime of the polymer radical species dictate not only the control of the polymerization but also the rate of the polymerization. A variety of metal complexes have been shown to be effective ATRP catalysts, with copper complexes exhibiting some of the highest activity in both homogeneous (bulk, solution) and heterogeneous (aqueous dispersed) systems.[28] Most of the copper systems utilize copper(I) bromide or chloride and a nitrogen based ligand. 2,2'-bipyridine was the first ligand used to form copper complexes; however, polydentate nitrogen-based ligands have been shown to be very effective in controlling the polymerization (Figure 1-3). The ligand tunes the activity of the complex predominantly through electronic and to a lesser extent steric effects. Long chain alkyl groups are often incorporated into the ligand structure to increase the solubility of the complex in organic media.

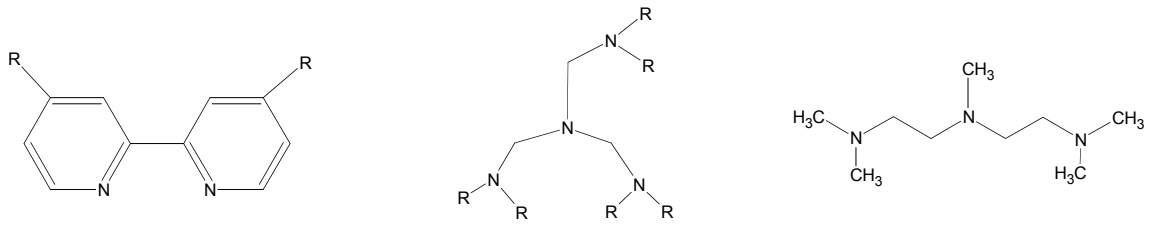

bipyridines
(bpy)
R = long chain alkyl group

tris(2-aminoethyl)amine
(TREN)
R = acrylate

N, N, N, N, N – penta-
methyldiethylenetriamine
(PMDETA)

Figure 1-3. Ligands Used in Copper Based ATRP Complexes

1.2.2.2 The Mechanism of ATRP

The elementary reactions in ATRP begin with initiation involving the transfer of the halide from the alkyl halide to the low oxidation state complex, M_t^n. The metal is oxidized via an electron transfer and abstracts the halogen to produce a primary radical and a metal complex in its higher oxidation state, XM_t^{n+1}. The radical propagates until it is terminated, transferred to monomer, or deactivated to create a dormant polymer chain. The oxidized metal complex will eventually donate a halogen to a polymeric radical and undergo a one-electron reduction to produce a dormant polymer chain with a halogen endgroup and metal complex in its lower oxidation state. The elementary reactions are shown in Scheme 1-3, where RX, M, M_t^n and XM_t^{n+1} represent the initiator, monomer, metal complex in lower oxidation state and metal complex is its higher oxidation state, respectfully; R•, P_i•, D_i and P_iX represent the active initiator, a propagating chain, a dead chain and a dormant chain, respectfully.

Initiation:	$RX + M_t^n \longrightarrow R^{\bullet} + XM_t^{n+1}$
	$R\bullet + M \longrightarrow P_1\bullet$
Propagation:	$P_i\bullet + M \longrightarrow P_{i+1}$
Termination:	$P_i\bullet + P_j\bullet \longrightarrow D_{i+j}$ (combination)
	$P_i\bullet + P_j\bullet \longrightarrow D_i + D_j$ (disproportionation)
Chain transfer to monomer:	$P_i\bullet + M \longrightarrow D_i + P_1\bullet$
Radical mediation:	$P_iX + M_t^n \longrightarrow P_i^{\bullet} + XM_t^{n+1}$ (activation)
	$P_i^{\bullet} + XM_t^{n+1} \longrightarrow P_iX + M_t^n$ (deactivation)

Scheme 1-3. The Reaction Mechanism of ATRP

1.2.2.3 Reverse ATRP

Reverse ATRP is another technique used to initiate ATRP systems (Scheme 1-4). A conventional radical initiator and a metal complex in its higher oxidation state are required. The radicals generated from the initiator combine with monomer to form polymeric radicals that are deactivated by the metal mediating complex. Ideally, the initiator should decompose instantaneously to ensure that all the polymer chains are initiated at the same time. Towards this end, a technique known as Activator Generated by Electron Transfer (AGET) employs a redox reaction to rapidly reduce the metal complex witch then reacts with an alkyl halide to initiate the polymerization.[29]

Reverse ATRP has proven to be an effective method of adapting ATRP to aqueous based systems. The formulation of aqueous dispersed systems requires that all the monomer soluble components be mixed in the monomer, then added to water and homogenized. For normal ATRP, the addition of the alkyl halide and the low oxidation state metal species to monomer and subsequent homogenization results in initiation of the system during the formation of the (mini)emulsion. This was not a concern with the early mediating complexes because they required elevated temperatures to abstract the halide from the alkyl halide compound. However, the highly active mediating complexes now applied to these systems are capable of abstracting a halide at room temperature. Thus, reverse ATRP is a preferred method of initiation in aqueous based ATRP systems.

Initiation: $I_2 \longrightarrow 2I\bullet$ (decomposition)

$I\bullet + M \longrightarrow P_1\bullet$ (initiation)

Radical mediation: $P_i^{\bullet} + XM_t^{n+1} \longrightarrow P_iX + M_t^n$ (deactivation)

$P_iX + M_t^n \longrightarrow P_i^{\bullet} + XM_t^{n+1}$ (activation)

Scheme 1-4. The Initiation Mechanism of Reverse ATRP

1.2.3 Stable Free Radical Polymerization (SFRP)

Similar to ATRP, the polymerization is controlled through a reversible termination mechanism (Scheme 1-2), with the propagating radical species being deactivated by a stable free radical. A variety of stable radicals have been investigated, with the nitroxide class of compounds proving to be the most effective (Figure 1-4). The technique is referred to as nitroxide-mediated radical polymerization (NMRP),[30] and the term is often used interchangeably with SFRP. The distinguishing feature of NMRP is the reversible termination of the polymeric radicals by the nitroxide species forming an alkoxyamine (the dormant polymer chain), and the subsequent homolytic cleavage of the C-O bond to reform the polymeric radical and the free nitroxide. Radical termination reactions are suppressed because the equilibrium greatly favors the formation of the alkoxyamine, which allows for controlled polymerizations to be conducted. The original investigations by Solomon[31] and Georges[32] employed the nitroxide 2,2,6,6-tetramethylpiperidinyl-1-oxy (TEMPO, Figure 1-4) to produce well-controlled polymerizations of styrene. The drawbacks of TEMPO are that it requires elevated temperatures (~120 ^{o}C) for reasonable rates of polymerization to occur because of the

low dissociation rate constant of the alkoxyamine, as well, TEMPO has largely been limited to styrene based monomers. Other nitroxides have been developed in recent years, with one of the more successful being *N*-*tert*-butyl-*N*-(1-diethylphosphono-2,2-dimethylpropyl) nitroxide (DEPN, also known as SG1).[33] SG1 can effectively control the polymerization of acrylates, and styrene polymerizations can be conducted at temperatures as low as 90 ^{o}C.

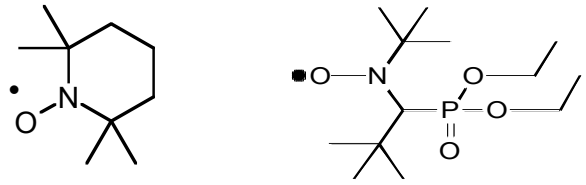

TEMPO SG1

Figure 1-4. Nitroxides Employed in SFRP

1.3 Objective

The objective of this research was to develop L/CRP techniques in aqueous based systems. Research was initially focused on the application of ATRP to a miniemulsion process, but the scope evolved as the knowledge gained in ATRP was used to exploit opportunities in the similar fields of aqueous based RAFT and SFRP.

Each L/CRP has their strengths and weaknesses with regard to specific monomers employed. The application of L/CRP to vinyl acetate has proven to be difficult because of the high reactivity of the propagating radicals and their tendency to undergo chain transfer and chain termination reactions. Xanthates have been shown to effectively

mediated vinyl acetate polymerization though a RAFT mechanism of control. Chapter 2 explains the development of the RAFT polymerization of vinyl acetate.

The early work in miniemulsion ATRP centered on overcoming the colloidal instability of the latex in these systems, and determining a formulation that would allow for a controlled polymerization. Chapter 3 presents the work that led to the development of a robust miniemulsion ATRP process, which also greatly expanded the window of operating temperatures (important for increasing the polymerization rate and improving the properties of the final polymer). With the problems of latex stability and control of the polymerization understood, the issue of a relatively long inhibition period at the beginning of a miniemulsion ATRP was addressed. Chapter 4 describes the development of a redox initiation system applied to miniemulsion ATRP that eliminates the induction period and, unexpectedly, allows for significantly faster rates of polymerization and the formation of well-controlled polymers approaching one-million molecular weight (a result believed not possible with ATRP, due to the unavoidable termination reactions that occur). The techniques described in chapters 3 and 4 provided the opportunity to investigate the influence on the kinetics of the polymerization and properties of the polymer when ATRP is conducted in a confined space (ie. miniemulsion droplets). Chapter 5 provides evidence that conducting the polymerization in a confined space influences both the rate of the polymerization and degree of control. The experiments reveal why it has not been seen previously, the important parameters that need to be considered, and the influence that compartmentalization has on both the rate and control of the polymerization.

The use of a miniemulsion has proven to be far more effective for conducting L/CRP compared to conventional emulsion polymerization because it eliminates the issue of transporting the mediating agent to the site of polymerization and avoids particle nucleation. The ability to conduct L/CRP in an emulsion is desirable because it simplifies the formulation by removing the need for a hydrophobe (which has to be removed from the final product) and the application of high shear to form the initial emulsion. Chapter 6 describes the development of a surfactant-free emulsion polymerization of styrene, mediated with the nitroxide SG1.

1.4 References

1. Gilbert R. G. *Emulsion Polymerization – A Mechanistic Approach*; Academic Press: New York, 1995.
2. Cunningham, M. F. *Prog. Polym. Sci.* **2002**, 27, 1039.
3. Landfester, K. *Macromol. Rapid Commun.* **2001**, 22, 896. Capek, I.; Chern, C. S. *Advances in Polym. Sci.* **2001**, 155, 101. Asua, J. M. *Prog. Polym. Sci.* **2002**, 27, 1283.
4. Lovell, P. A.; El-Aasser, M. S., Eds. *Emulsion polymerization and Emulsion Polymers*; Wiley: New York, 1997.
5. Landfester, K. *Macromolecules* **1999**, 32, 5222.
6. Reimers, J.; Schork, F. J. *J. Appl. Polym. Sci.*, **1996**, 59, 1833.
7. Van Oss, C. J. *Interfacial Forces in Aqueous Media*; Marcel-Dekker: New York, 1994.
8. Hunter, R. J. *Foundations of Colloidal Science*; Oxford University Press: New York, 1986.

9. Osipow, L. I. *Surface Chemistry: Theory and Industrial Applications*; Robert E. Krieger Publishing Company: New York, 1977.
10. Moad, G.; Chiefari, J.; Chong, Y. K.; Kristina, J.; Mayadunne, R. T. A.; Postma, A.; Rizzardo, E.; Thang, S. H. *Polymer International* **2000**, 993.
11. Chiefari, J.; Chong, Y. K.; Erole, F.; Krstina, J.; Jeffery, J.; Le, T. P. T.; Mayadunne, R. T. A.; Meijs, G. F.; Moad, C. L.; Moad, G.; Rizzardo, E.; Thang, S. H. *Macromolecules* **1998**, 31, 5559.
12. Charmot, D.; Corpart, P.; Adam, H.; Zard, S. Z.; Biadatti, T.; Bouhadir, G. *Macromol. Symp.* **2000**, 150, 23.
13. Favier, A.; Barner-Kowollik, C.; Davis, T. P.; Stenzel, M. H. *Macromol. Chem. Phys.* **2004**, 205, 925.
14. Moad, G.; Rizzardo, E.; Thang, S. H. *Aust. J. Chem.* **2006**, 59, 669.
15. Barner, C.; Davis, T. P.; Heuts, J. P. A.; Stenzel, M. H.; Vana, P.; Whittaker, M. *J. Polym. Sci.: Part A: Polym. Chem.* **2002**, 41, 365.
16. Kwak, Y.; Goto, A.; Tsujii, Y.; Murata, Y.; Komatsu, K.; Fukuda, T. *Macromolecules* **2002**, 35, 3026. Monteiro, M. J.; de Brouwer, H. *Macromolecules* **2001**, 34, 349.
17. Vana, P.; Davis, T. P.; Barner-Kowollik, C. *Macromol. Theory Simul*. **2002**, 11, 823.
18. Buback, M.; Vana, P. *Macromol. Rapid Commun.* **2006**, 27, 1299.
19. Fischer, H. *Chem. Rev.* **2001**, 101, 3581.
20. Kato, M.; Kamigaito, M.; Sawamoto, M.; Higashimura, T. *Macromolecules* **1995**, 28, 1721.
21. Patten, T. E.; Xia, J.; Abernathy, T.; Matyjaszewski, K. *Science* **1996**, 272, 866.
22. Wang, J.; Matyjaszewski, K. *J. Am. Chem. Soc.* **1995**, 117, 5614.

23. Matyjaszewski, K.; Xia, J. *Chem. Rev.* **2001**, 101, 2921.

24. Kamigaito, M.; Ando, T.; Sawamoto, M. *Chem. Rev.* **2001**, 101, 3689.

25. Pintauer, T.; Matyjaszewski, K. *Coord. Chem. Rev.* **2005**, 249, 1155.

26. Braunecker, W. A.; Matyjaszewski, K. *J. Molecul. Catal. A: Chem.* **2006**, 254, 155.

27. Tsarevsky, N. V.; Braunecker, W. A.; Matyjaszewski, K. *J. Organomet. Chem.* **2007**, 692, 3212.

28. Bisht, H.; Chatterjee, A. K. *J. Macromol. Sci., Polym. Rev.* **2001**, C41(3), 139.

29. Min, K.; Jakubowski, W.; Matyjaszewski, K. *Macromol. Rapid Commun.* **2006**, 27, 594.

30. Hawker, C. J.; Bosman, A.; Harth, E. *Chem. Rev.* **2001**, 101, 3661.

31. Solomon, D. H.; Rizzardo, E.; Cacioli, P. US Patent 4581429, 1985

32. Georges, M. K.; Veregin, R. P. N.; Kazmaier, P. M.; Hamer, G. K. *Macromolecules* **1993**, 26, 2987.

33. Grimaldi, S.; Finet, J. –P.; Le Moigne, F.; Zeghdaoui, A.; Tordo, P.; Benoit, D.; Fontanille, M.; Gnanou, Y. *Macromolecules* **2000**, 33, 1141.

CHAPTER 2

2 Xanthate-Mediated Living Radical Polymerization of Vinyl Acetate in Miniemulsion

published in Macromolecular Rapid Communications 2005, 26, 592-596.

2.1 Preface

The primary focus of my research was the development of ATRP in miniemulsion. While the different types of living radical polymerizations (ATRP, RAFT/MADIX, SFRP) have features that are unique to the specific technique, many of the issues that arise when conducting these polymerizations in aqueous based systems are universal. My preliminary work developing ATRP in miniemulsion focused on maintaining the stability of the latex during the polymerization and the knowledge gained from this work could be directly applied to RAFT/MADIX systems. When it was reported in the literature that xanthates could effectively mediate the polymerization of vinyl acetate (a commercially significant monomer, those polymerization was notoriously difficult to control) I took the opportunity to apply this system to a miniemulsion. The results of the investigation are presented here and are reproducible. This is the first report of the controlled polymerization of vinyl acetate in an aqueous based system.

2.2 Abstract

The MADIX/RAFT mechanism, employing a xanthate as the reversible chain-transfer agent, has been shown to facilitate the living radical polymerization of vinyl acetate in miniemulsion. Methyl (ethoxycarbonothioyl)sulfanyl acetate (MESA) successfully mediated the polymerization which was initiated with either of the water-soluble initiators 2,2-azobis{2-[1-(2-hydroxyethyl)-2-imidazolin-2-yl]propane} dihydrochloride (VA-060) or 2,2-azobis[2-(2-dimidazolin-2-yl)propane] dihydrochloride (VA-044). The polymerizations exhibit living characteristics, demonstrated by the evolution of molecular weight distributions. The formulation of the miniemulsion produced stable latexes with no coagulum.

2.3 Introduction

Living/controlled radical polymerization (L/CRP) techniques provide exceptional control of radical polymerizations, allowing for the production of specialty polymers such as macromonomers, functional polymers, block polymers, and graft (comb or star) polymers. Three variations of the L/CRP system that receive extensive attention in the literature are: reversible addition fragmentation transfer (RAFT),[1] atom transfer radical polymerization (ATRP),[2] and nitroxide-mediated radical polymerization (NMRP).[3] The RAFT process originally referred to dithioesters as controlling agents, while the use of xanthates as controlling agents was coined MADIX (macromolecular design via interchange of xanthates).[4] The MADIX technique mediates the polymerization through a reversible addition fragmentation chain-transfer mechanism and the term RAFT is applied to the mechanism of control when xanthates are used as chain-transfer agents.

The application of L/CRP to vinyl acetate (VA) has proven to be very difficult, and there are few reports in the literature of controlled VA polymerizations.[5] The difficulties in adapting LRP to VA result from the high reactivity of the propagating radicals and their tendency to undergo chain-transfer and chain-termination reactions.[6] Recently, the controlled polymerization of VA was reported using the RAFT mechanism with both dithiocarbamates and xanthates.[7-12] Eight xanthates were investigated by Stenzel *et al.*[10] to determine the effect of the xanthate structure on the properties of the living radical polymerization of VA in bulk. Of the xanthates in the study, methyl (ethoxycarbonothioyl)sulfanyl acetate (MESA, Figure 2-1) provided the most desirable combination of properties, with high rates of polymerization, low polydispersities, and minimal inhibition times.

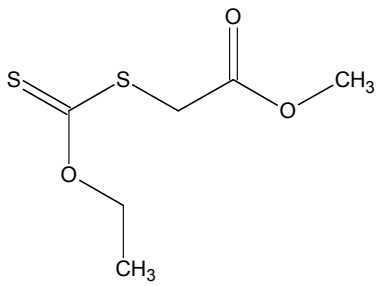

Figure 2-1. The MADIX (RAFT) agent Methyl (ethoxycarbonothioyl)sulfanyl acetate (MESA)

Application of the RAFT polymerization of VA to an aqueous dispersed system, such as an emulsion or miniemulsion process, is expected to provide process advantages over a bulk or solution polymerization. Benefits, such as reduced volatile organic compounds, improved control over the heat evolved from the polymerization, and reduced viscosity, are important aspects to consider if the process is to become commercially viable. A further incentive to adapt the xanthate-mediated polymerization of VA to a (mini)emulsion process arises from the reversible transfer method of control in the RAFT mechanism. Since the radical concentration in the RAFT process is expected to be the same as its conventional free radical counterpart, the phenomenon of compartmentalization[13] is expected to influence the kinetics of the polymerization. The advantages from compartmentalization that could be realized in a RAFT polymerization include increased rates of polymerization and decreased irreversible biradical termination.[13,14] In general, the adaptation of L/CRP to emulsion polymerization has met with only limited success, the problems have been attributed to one or a combination of: particle nucleation, polymerization within the droplets, stabilization of very small particles in the early stage of polymerization, and the high concentration of oligomeric

chains. The shortcomings of the emulsion process have been overcome with the application of the miniemulsion process. The use of a miniemulsion has proven to be far more robust with respect to maintaining control over the growth of the living chains and the stability of the latex.[14,15] The RAFT process has been applied to emulsion[16-18] and miniemulsion[19-24] processes. Successful application of xanthate-mediated polymerizations to aqueous dispersed systems has been reported for the emulsion process.[8,25] During the preparation of this manuscript, we have learned that Russum *et al.* have also reported on a miniemulsion vinyl acetate polymerization using MADIX.[26]

Most VA polymerizations are performed in emulsion, with VA latexes having considerable commercial importance for a variety of applications including adhesives, paints, and coatings. This paper describes the initial results from the RAFT polymerization of VA in miniemulsion using the xanthate MESA. Living/comtrolled polymerizations were initiated with either of the water-soluble initiators VA-060 or VA-044.

2.4 Experimental

Materials. Vinyl acetate (VA, Aldrich) was purified by passing through a column packed with inhibitor remover (Aldrich). The compounds 2,2-azobis[2-(2-dimidazolin-2-yl)propane] dihydrochloride (VA-044, Wako Chemicals), 2,2-azobis{2-[1-(2-hydroxyethyl)-2-imidazolin-2-yl]propane} dihydrochloride (VA-060, Wako Chemicals), hexadecane (HD, Aldrich), and sodium lauryl sulfate (SLS, Aldrich) were used as received. The synthesis of methyl (ethoxycarbonothioyl)sulfanyl acetate (MESA) was adapted from literature methods.[10]

Polymerization Procedure. The organic phase was prepared by adding hexadecane (HD, 1.48 g, 3.8 wt% vs. monomer) and MESA to VA (39 g, 15 wt% vs. water) and was stirred for 15 min. The aqueous phase consisted of sodium lauryl sulfate (SLS, 1.17 g, 3 wt% vs. monomer) in deionized water (DIW, 221 g) which was stirred for 30 min. The organic phase was added to the aqueous phase and stirred for 30 min prior to passing through a Microfluidizer-110S (Microfluidics International Corporation) operating at an inlet pressure of 40 psi. The miniemulsion (200 g) was transferred to a 500 mL round-bottom flask fitted with a condenser and was purged with ultra-high-purity nitrogen for 30 min to deoxygenate the system. The flask was immersed in an oil bath that was preheated to 60 °C. Thirty minutes elapsed before the initiator was added, which marked the start of the polymerization. The initiator (VA-060 or VA-044) was dissolved in 2 mL of DIW, deoxygenated by purging with ultra-high-purity nitrogen for 20 min and then added to the miniemulsion with a deoxygenated syringe. Samples were withdrawn with a deoxygenated syringe and immediately added to a hydroquinone solution to prevent further polymerization. The polymer samples were dried under the air manifold overnight than placed in a vacuum overnight to remove all volatile compounds. All polymerizations were repeated to ensure reproducibility.

Characterization. Monomer conversions were determined gravimetrically. Size Exclusion Chromatography (SEC) was used to measure the molecular weight and polydispersity of polymer samples. The SEC was equipped with a Waters 2960 separation module containing four Styragel columns of pore sizes 100, 500, 10^3, and 10^4 Å, coupled with a differential refractive index detector maintained at 40 °C.

Tetrahydrofuran was used as the eluant and the flow rate was set to 1.0 $mL \cdot min^{-1}$. The system was calibrated using narrow polystyrene standards ranging from 870 to 355 000 $g \cdot mol^{-1}$. The universal calibration was used to correct the molecular weights obtained for polystyrene to poly(vinyl acetate). The Mark-Houwink parameters for polystyrene are $K = 14.1 \times 10^{-3}$ $mL \cdot g^{-1}$ and $a = 0.70$, and for poly(vinyl acetate) $K = 16 \times 10^{-3}$ $mL \cdot g^{-1}$ and $a = 0.70$.[27] The particle size of the latex was measured using a Matec Applied Sciences Capillary Hydrodynamic Fractionation (CHDF) 2000. The UV detector was set to 220 nm. The eluent was a 20:1 mixture of DIW and GR500-1X (Matec). Samples were diluted with the eluent to approximately 3.5 wt% solids and sonicated for 5 min. Samples were then passed through a 0.5 m pore size filter prior to injection. A 2 wt% solution of sodium benzoate was used as the marker. A calibration curve was generated using six Seradyn Uniform Microparticle standards.

2.5 Results and Discussion

The experiments are summarized in Table 2-1. The use of VA-060 as the initiator and MESA as the chain-transfer agent produced a living polymerization of VA in a miniemulsion (Exp. 2). Figure 2-2 shows a plot of the number-average molecular weight (M_n) and polydispersity index (PDI) versus conversion. The polydispersity obtained a minimum value of 1.13 at 17% conversion, which then increased with conversion, reaching a final value of 1.67 at 74% conversion. The number-average molecular weight grew linearly with conversion and was slightly less than twice the theoretical value. The theoretical number-average molecular weight was calculated with Equation 2-1, and

represents the ideal MADIX polymerization, in that each polymer chain has an end group that originated from the chain-transfer process.

$$M_{n,theory} = \frac{[VA]_0 \times MW(VA) \times conversion}{[MADIX]_0} \quad \text{(eq 2-1)}$$

The experimental data indicate that approximately 55% of the MADIX molecules do not form polymer chains. A distinct possibility for the low MESA efficiency, but one for which we have no direct evidence at this time, is that there is a significant amount of oligo-MESA present in the aqueous phase. This is a possibility because of the use of a water-soluble initiator and the comparatively high water solubility of VA.

Table 2-1. Summary of experimental conditions for the RAFT miniemulsion polymerization of VA

Exp	Initiator	n(I_2)	n(MESA)	MESA/I_2	Time	Conversion	final		
					(min)	(%)	M_n	*PDI*	M_n(theory)
1	VA-060	9.7×10^{-5}	0	0	90	86	--	--	--
2	VA-060	9.7×10^{-5}	9.0×10^{-4}	9.2	200	74	45400	1.67	24400
3	VA-060	9.7×10^{-5}	5.1×10^{-4}	5.3	200	72	68500	1.93	41900
4	VA-044	4.3×10^{-5}	0	0	< 30	93	--	--	--
5	VA-044	4.3×10^{-5}	5.6×10^{-4}	13.0	160	87	55000	1.69	46600
6	VA-044	4.3×10^{-5}	2.2×10^{-4}	5.1	135	85	159600	2.02	103700
7	VA-044	2.4×10^{-4}	7.7×10^{-4}	3.2	45	73	61200	1.96	28400

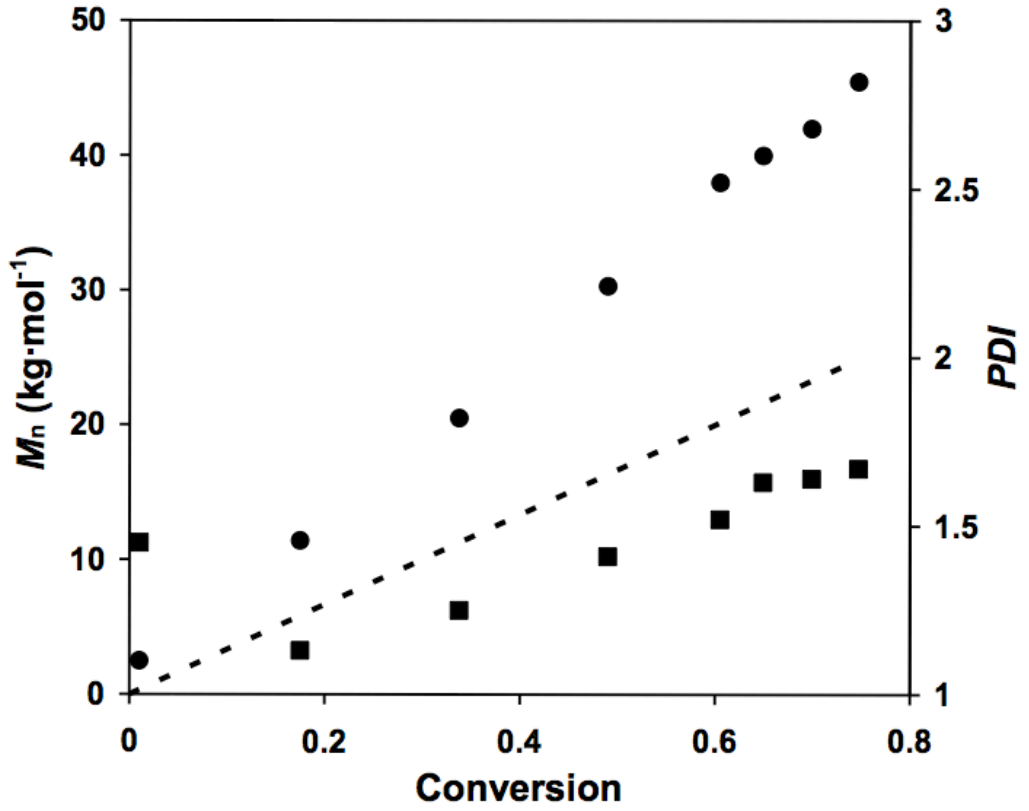

Figure 2-2. Number average molecular weight (M_n, ●) and polydispersity (*PDI*, ■) as a function of monomer conversion for the RAFT miniemulsion polymerization of VA (exp 2). The dashed line illustrates the theoretical M_n

The living nature of the VA miniemulsion polymerization is further demonstrated by the evolution of molecular weight distributions with monomer conversion shown in Figure 2-3. The addition of MESA also reduced the maximum conversion obtained for the polymerization. The conventional free radical polymerization of VA in miniemulsion (Exp. 1) achieved a maximum conversion of 86% after 1.5 h. In experiment 2 the conversion reached 74% in 3.5 h, and after 10 h of polymerization the monomer

conversion was unchanged (75%). The RAFT polymerization of VA in miniemulsion produced a colloidally stable latex. There was no evidence of coagulum formation and the particle diameter distribution was monomodal. The final weight-average particle diameter was 141 nm with a standard deviation of 90 nm.

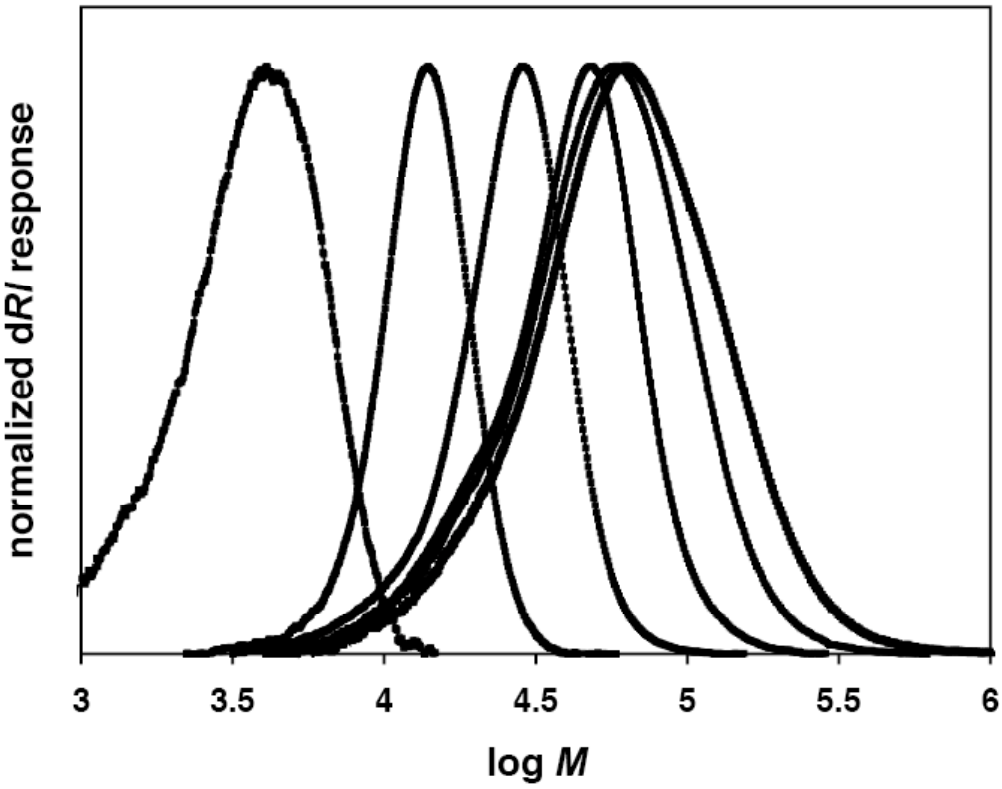

Figure 2-3. Evolution of molecular weight as measured by SEC for the RAFT miniemulsion polymerization of VA (exp 2). Molecular weight increases from left to right. The conversions are 1%, 17%, 34%, 49%, 61%, 70%, respectfully.

The conversion versus time data in Figure 2-4 compares the kinetic results from the RAFT polymerization (Exp. 2) and the identical conventional free radical

polymerization (Exp. 1). Both inhibition and rate retardation were present in the miniemulsion RAFT polymerization of VA. The addition of MESA produces an inhibition period, where no polymerization occurs, of approximately 15 min. Rate retardation was indicated by the lower rate of polymerization in the presence of MESA when compared with the free radical polymerization. The previous work with RAFT miniemulsion polymerization has shown that radical exit can play an important role in decreasing the rate of the polymerizations.[21,28] We note that some of the early work with bulk xanthate-mediated VA polymerization suffered inhibition and retardation,[10] which has subsequently been attributed to trace impurities.[11]

As expected from Equation 2-1, a decrease in the amount of MESA (Exp. 3) resulted in an increased number-average molecular weight at any given conversion. Similar to experiment 2, a comparison between the experimental (68 500 $g \cdot mol^{-1}$) and theoretical (42 300 $g \cdot mol^{-1}$) number-average molecular weight, at a conversion of 72%, indicated that approximately 40% of the MADIX molecules do not form polymer chains. The polydispersity obtained a minimum value of 1.22 at 14% conversion, and then increased with conversion to reaching a final value of 1.93 at 72% conversion. The increase in polydispersity is likely influenced by chain transfer to polymer, which is an important consideration in VA polymerization. The conversion versus time profile in Figure 2-4 illustrates that both the degree of rate retardation and the inhibition period were essentially identical for the experiments with different MESA loadings.

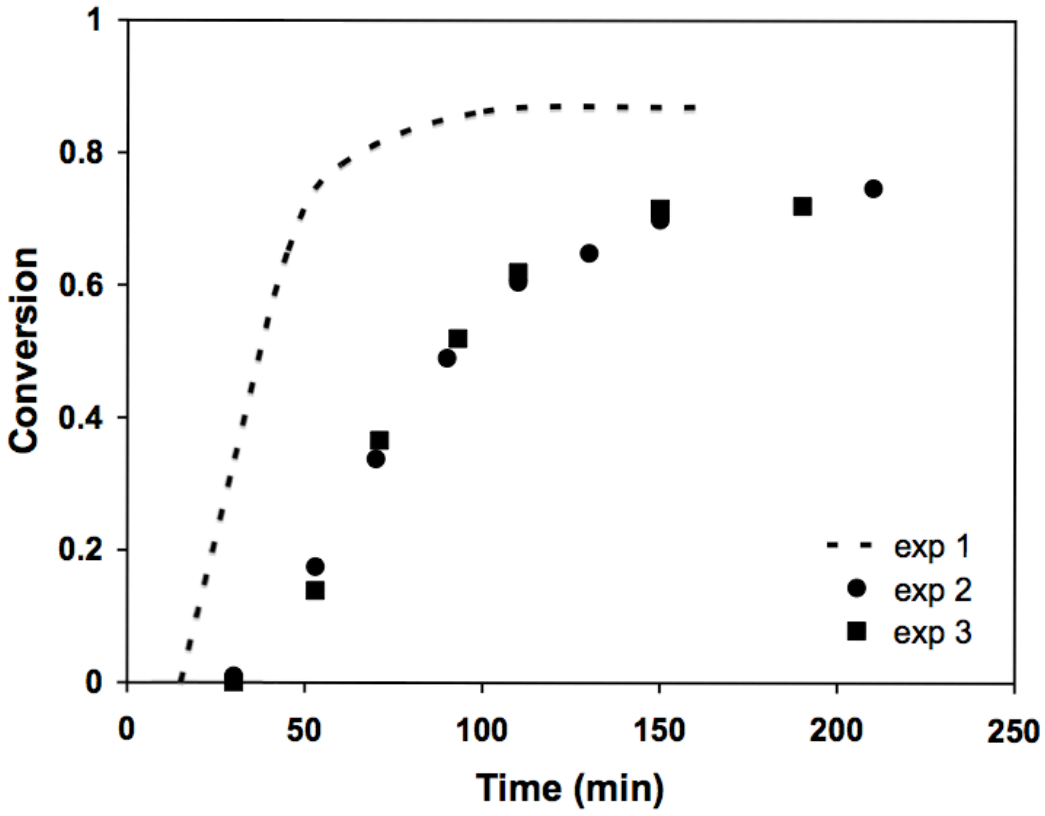

Figure 2-4. Conversion as a function of time for the RAFT miniemulsion polymerization of VA.

I was interested to see how the system would respond to the water-soluble initiator VA-044 when the polymerization temperature was maintained at 60 °C. VA-044 has a 10 h half-life temperature of 44 °C, whereas VA-060 has a 10 h half-life temperature of 60 °C. In qualitative terms, VA-060 will slowly decompose over the course of the polymerization, whereas VA-044 will decompose faster, creating more primary radicals in a narrower timeframe. The conventional free radical polymerization of VA in miniemulsion initiated with VA-044 reached complete conversion (92%) in less

than 30 min (Exp. 4). VA-044 was able to initiate the living polymerization of VA when MESA was used as the chain-transfer agent (Exp. 5-7). The number-average molecular weight grew linearly with conversion, and the polydispersity followed the same trend as the VA-060 initiated systems. The final values are summarized in Table 2-1. In both experiment 5 and 6 the incorporation of MESA appears to be greater than when VA-060 is used to initiate the polymerizations; however, in experiment 7 the apparent incorporation of MESA is similar to that of the VA-060 initiated polymerizations. At this time, the factors that influence the incorporation of MESA during the miniemulsion polymerization of VA are unknown, and are currently under investigation.

2.6 Conclusions

The xanthate-mediated radical polymerization of vinyl acetate has been successfully carried out in miniemulsion. The number-average molecular weight increased linearly with conversion. Polydispersity at lower conversions was good (<1.2), while at higher conversions the polydispersity was relatively high for a controlled polymerization (1.6-1.9). The increase in polydispersity is likely influenced by chain transfer to polymer. The evolution of the molecular weight distribution with conversion confirms the controlled nature of these polymerizations. Kinetics indicated that both inhibition and rate retardation are present in these systems. The formulation of the polymerization produced stable latexes with no coagulum present.

2.7 References

1. Chiefari, J.; Chong, Y. K.; Ercole, F.; Krstina, J.; Jeffery, J.; Le, T. P. T.; Mayadunne, R. T. A.; Meijs, G. F.; Moad, C. L.; Moad, G.; Rizzardo, E.; Thang, S. H. *Macromolecules* **1998**, 31, 5559.
2. (a) Kato, M.; Kamigaito, M.; Sawamoto, M.; Higashimura, T. *Macromolecules* **1995**, 28, 1721. (b) J. Wang, K. Matyjaszewski, *J. Am. Chem. Soc.* 1995, 117, 5614.
3. Georges, M. K.; Veregin, R. P. N.; Kazmaier, P. M.; Hamer, G. K. *Macromolecules* **1993**, 26, 2987.
4. Taton, D.; Wilczewska, A.-Z.; Destarac, M. *Macromol. Rapid Commun.* **2001**, 22, 1497.
5. Iovu, M. C.; Matyjaszewski, K. *Macromolecules* **2003**, 36, 9346.
6. Moad, G.; Solomon, D. H. *The Chemistry of Free Radical Polymerization*; Pergamon: Oxford, 1995.
7. Destarac, M.; Charmot, D.; Franck, X.; Zard, S. Z. *Macromol. Rapid Commun.* **2000**, 21, 1035.
8. Charmot, D.; Corpart, P.; Adam, H.; Zard, S. Z.; Biadatti, T.; Bouhadir, G. *Macromol. Symp.* **2000**, 150, 23.
9. Coote, M. L.; Radom, L. *Marcomolecules* **2004**, 37, 590.
10. Stenzel, M. H.; Cummins, L.; Roberts, E.; Davis, T. P.; Vana, P.; Barner-Kowollik, C. *Macromol. Chem. Phys.* **2003**, 204, 1160.
11. Favier, A.; Barner-Kowollik, C.; Davis, T. P.; Stenzel, M. H. *Macromol. Chem. Phys.* **2004**, 205, 925.
12. Stenzel, M. H.; Davis, T. P.; Barner-Kowollik, C. *Chem. Commun.* **2004**, 1546.

13. Butte, A.; Storti, G.; Morbidelli, M. *Macromolecules* **2000**, 33, 3485.

14. Cunningham, M. F. *Prog. Polym. Sci.* **2002**, 27, 1039.

15. Qiu, J.; Charleux, B.; Matyjaszewski, K. *Prog. Polym. Sci.* **2001**, 26, 2083.

16. Smulders, W.; Gilbert, R. G.; Monteiro, M. J. *Macromolecules* **2003**, 36, 4309.

17. Prescott, S. W.; Ballard, M. J.; Rizzardo, E.; Gilbert, R. G. *Macromolecules* **2002**, 35, 5417.

18. Uzulina, I.; Kanagasabapathy, S.; Claverie, J. *Macromol. Symp.* **2000**, 150, 33.

19. Mcleary, J. B.; Tonge, M. P.; De Wet Roos, D.; Sanderson, R. D.; Klumperman, B. *J. Polym. Sci., Part A: Polym. Chem.* **2004**, 42, 960.

20. Luo, Y. W.; Liu, X. *J. Polym. Sci., Part A: Polym. Chem.* **2004**, 42, 6248.

21. Lansalot, M.; Davis, T. P.; Heuts, J. P. A. *Macromolecules* **2002**, 35, 7582.

22. Butté, A.; Storti, G.; Morbidelli, M. *Macromolecules* **2001**, 34, 5885.

23. Tsavalas, J. G.; Schork, F. J.; De Brouwer, H.; Monteiro, M. J. *Macromolecules* **2001**, 34, 3938.

24. De Brouwer, H.; Tsavalas, J. G.; Schork, F. J.; Monteiro, M. J. *Macromolecules* **2000**, 33, 9239.

25. Smulders, W.; Monteiro, M. J. *Macromolecules* **2004**, 37, 4474.

26. Russum, J. P.; Barbre, N. D.; Jones, C. W.; Schork, F. J. *J. Polym. Sci., Part A: Polym. Chem.* **2005**, 43, 2188.

27. Cane, F.; Capaccioli, T. *Eur. Polym. J.* **1978**, 14, 185.

28. Luo, Y.; Yu, B. *Polym. Plastics Tech. Eng.* **2004**, 43, 1299.

CHAPTER 3

3 Reverse Atom Transfer Radical Polymerization of Butyl Methacrylate in Miniemulsion Stabilized with a Cationic Surfactant

published in the Journal of Polymer Science: Part A: Polymer Chemistry, 2006, 44, 1628-1634, 2006.

3.1 Preface

From the reports in the literature at the time when I began research into miniemulsion ATRP (in 2004) the major issues that had to be addressed were the stability of the latex and the degree of control over the polymerization were. It had been determined that anionic surfactants, typically used to stabilize aqueous based radical emulsion polymerizations, poisoned the ATRP catalyst. Cationic surfactants were also reported to be incompatible with ATRP, so that only non-ionic surfactants could be used in conjunction with ATRP. The drawback of non-ionic surfactants is that their ability to stabilize a latex is known to decrease at elevated temperatures.

Although cationic surfactants were reported to cause poorly controlled polymerizations, their structures appear to be compatible with ATRP. The investigation revealed that the cationic surfactant cetyltrimethylammonium bromide (CTAB) provides a robust latex (ie. no coagulum formation) that does not interfere with the control over the polymerization. Polymerizations can be conducted at temperatures up to 90 ^{o}C, which is beneficial for reverse ATRP systems because it dramatically reduces the inhibition time (time required for the initiators to thermally decompose) and increases the overall polymerization rate. As well, the particle size of the latex can be easily manipulated between 100-200 nm at surfactant levels below the CMC, which is important when investigating the kinetic affects of dispersed system on ATRP (Chapter 5).

The ligand EHA_6-TREN was selected for this work because it provides enough hydrophobicity to ensure that the copper species resides in the organic phase (critical because this is where the polymerization occurs) while still providing relatively fast rates of polymerization.

3.2 Abstract

The miniemulsion reverse atom transfer radical polymerization (ATRP) of butyl methacrylate (BMA) was carried out with cetyltrimethylammonium bromide (CTAB) as the sole surfactant. The polymerizations were initiated with 2,2′-azobis[2-(2-imidazolin-2-yl)propane] dihydrochloride (VA-044) and mediated with copper(II) bromide ($CuBr_2$)/Tris[2-di(2-ethylhexyl acrylate)aminoethyl]amine (EHA_6-TREN). The living character was demonstrated by the linear increase in the number-average molecular weight with conversion and decreasing polydispersity index (PDI) with conversion. The polymerizations could be conducted at 90 ^oC with 1 wt % CTAB based on monomer, producing a coagulum free latex with a mean particle diameter of 155 nm. The resulting latexes exhibited good shelf life stability.

3.3 Introduction

Living/controlled radical polymerization (L/CRP) techniques (atom transfer radical polymerization (ATRP)[1-3], reverse addition fragmentation chain transfer polymerization (RAFT) [4,5] and stable free radical polymerization (SFRP)[6,7]) provide a facile route to the syntheses of polymers with predetermined microstructure and narrow molecular weight distributions. The techniques have been successfully developed in both bulk and solution processes, and their application to aqueous dispersed systems (suspension, emulsion and miniemulsion) continues to evolve.[8,9] The incentives to adapt L/CRP to aqueous-based systems include reduced environmental impact and more attractive process economics. Aqueous-based polymerizations provide reaction engineering advantages such as better mixing, improved heat transfer, and easier removal of residual monomer. The adaptation of ATRP and reverse ATRP to aqueous based systems has not been without its challenges. The difficulties encountered include effectively controlling the polymerization and maintaining the colloidal stability of the latex.[10-19] The miniemulsion process has been a valuable technique used to improve the performance of these systems.[20-26] Miniemulsion eliminates some of the complicating factors thought to negatively impact the colloidal instability of reverse ATRP latexes made by emulsion polymerization, such as, micelle nucleation, simultaneous polymerization within droplets and particles, and stabilization of very small particles at the beginning of the polymerization.

Although significant progress has been made developing ATRP and reverse ATRP in aqueous dispersed systems with nonionic surfactants, the stability of the latexes is still a concern. Nonionic surfactants stabilize the latex by thermodynamically favorable

steric interactions, the effectiveness of which diminishes as the temperature rises. In contrast to nonionic surfactants, the electrostatic stabilization provided by ionic surfactants is not dependant on temperature. The drawback to ionic surfactants is that their effectiveness is dependent on the ionic strength and possibly the pH of the solution.[27]

To date, ionic surfactants have not been successfully incorporated into miniemulsion ATRP systems. Anionic surfactants deactivate the metal complexes,[28] and until now, cationic surfactants, which are not expected to have an adverse effect on the metal center, were reported to be incompatible with ATRP. Matyjaszewski et al. commented on the use of dodecyltrimethylammonium bromide (DTAB) as a surfactant for aqueous based ATRP. The system reportedly allowed for a controlled polymerization, but the latex coagulated when the stirring was stopped.[13] An investigation by Eslami and Zhu into the emulsion ATRP of 2-ethylhexyl methacrylate found that DTAB was unable to stabilize the latex, whereas the use of myristyltrimethylammonium bromide (MTAB) resulted in an uncontrolled polymerization.[29] Recently, Limer et al. had success with both nonionic and cationic surfactants when conducting ATRP under suspension polymerization conditions. The cationic surfactant was a block copolymer of poly(2-(dimethylamino)ethyl methacrylate) (PDMAEMA) and poly(methyl methacrylate) (PMMA) (Mn=8000 g/mol) with the PDMAEMA quaternized with methyl iodide.[30]

In this article we report that the cationic surfactant cetyltrimethylammonium bromide (CTAB) is capable of effectively stabilizing the miniemulsion reverse ATRP of butyl methacrylate (BMA). Compared to the nonionic surfactant Brij 98, the use of CTAB requires a lower surfactant concentration and allows the polymerization to be

conducted at higher temperatures, which reduces in half the time required to reach the maximum conversion.

3.4 Experimental

Materials. n-Butyl methacrylate (BMA, Aldrich) and 2-ethylhexyl acrylate were purified by passing each through a column packed with inhibitor remover (Aldrich). The compounds copper(II) bromide ($CuBr_2$, Aldrich), tris(2-aminoethyl)amine (TREN, Aldrich), cetyltrimethylammonium bromide (CTAB, Aldrich), polyoxyethylene(20) oleyl ether (Brij 98, Aldrich), hexadecane (HD, Aldrich), basic alumina (Aldrich), and 2,2′-azobis[2-(2-imidazolin-2-yl)propane] dihydrochloride (VA-044, Wako Chemicals) were used as received. The synthesis of tris[2-di(2-ethylhexyl acrylate)aminoethyl]amine (EHA_6-TREN) was adapted from literature methods.[31, 32]

Miniemulsion Polymerization. The organic phase was prepared by adding copper(II) bromide ($CuBr_2$, 0.153 g, 6.85×10^{-4} mol), tris[2-di(2-ethylhexyl acrylate)aminoethyl]amine (EHA_6-TREN, 0.901 g, 7.20×10^{-4} mol), hexadecane (HD, 1.48 g, 3.8 wt % vs. monomer) and butyl methacrylate (BMA, 39 g, 0.274 mol, 15 wt % vs. deionized water) to a beaker and stirring overnight at room temperature to form a homogeneous solution. The aqueous phase that consisted of the surfactant cetyltrimethylammonium bromide (CTAB, 0.5 – 2.5 wt % vs. monomer) and deionized water (DIW, 221 g) was stirred for 30 min. When polyoxyethylene(20) oleyl ether (Brij 98) was used as the surfactant the solution was stirred overnight at room temperature. The organic phase was added to the surfactant solution and stirred for approximately 30

min prior to passing through a Microfluidizer 110S (Microfluidics International Corporation) operating at an inlet pressure of 275 kPa. The miniemulsion (200 g) was transferred to a 500 mL round-bottom flask fitted with a condenser and was purged with ultra-high-purity argon for 30 min. The flask was immersed in an oil bath that was preheated to the desired temperature and the magnetic stirring speed was set to 250 rpm. Thirty minutes elapsed before the initiator was added, which marked the start of the polymerization. The water soluble initiator 2,2′-azobis[2-(2-imidazolin-2-yl)propane] dihydrochloride (VA-044, 0.07 g, 2.16×10^{-4} mol) was dissolved in 2 mL of deionized water, and purged with ultra-high-purity argon for 20 min prior to injection into the miniemulsion with a deoxygenated syringe. Samples were withdrawn with a deoxygenated syringe and placed in an ice bath. The polymer samples were dried under the air manifold overnight than placed in a vacuum overnight to remove all volatile compounds. All polymerizations were repeated to ensure reproducibility.

Characterization. After the polymerizations were complete the latexes were passed through a filter paper (Fisherbrand P8 creped) to collect any coagulum. The amount of coagulum, if present, was determined gravimetrically. Monomer conversions were determined gravimetrically. Gel permeation chromatography (GPC) was used to measure the molecular weight and polydispersity of the polymer samples. The dried polymer samples from the miniemulsion were dissolved in tetrahyrdofuran and passed through a column packed with basic alumina to remove the residual copper. The GPC was equipped with a Waters 2960 separation module containing four Styragel columns of pore sizes 100, 500, 10^3 and 10^4 Å, coupled with a differential refractive index detector

maintained at 40 ^{o}C. Tetrahydrofuran was used as the eluant and the flow rate was set to 1 mL·min^{-1}. The system was calibrated with 9 narrow poly(methyl methacrylate) standards. The particle size of the latexes was measured using a Matec Applied Sciences Capillary Hydrodynamic Fractionation (CHDF) 2000 unit. The UV detector was set to 220 nm. The eluant was a 20:1 mixture of deionized water and GR500-1X (Matec Applied Sciences). Samples were diluted with the eluant to approximately 3.5 wt % solids and sonicated for 5 minutes. Samples were passed through a 0.5 μm pore size filter prior to injection. The marker was a 2 wt % solution of sodium benzoate. The system was calibrated with 6 Seradyn Uniform Microparticle standards.

3.5 Results and Discussion

The objective of this study was to expand the conditions under which miniemulsion reverse ATRP can be conducted while maintaining latex stability, specifically by preparing latexes using electrostatic stabilization. To be considered colloidally stable there should be no coagulum formation and the final latex must have good shelf life (i.e., three weeks following the polymerization there is no change in mean particle diameter or particle size distribution).

Employing the nonionic surfactant Brij 98 in the miniemulsion reverse ATRP of BMA required a minimum surfactant loading of 10 wt % based on monomer, when the polymerization temperature was 60 ^{o}C (exp 1). The resulting latex had 1.5 wt % coagulum and a final weight average particle diameter of 126 nm. Figure 3-1 illustrates the living nature of the polymerization. The number average molecular weight (M_n) increases with conversion and the polydispersity index (*PDI*) decreases with conversion.

A decrease in the amount of Brij 98 to 5 wt % resulted in severe coagulation of the latex, but control of the polymerization was maintained.

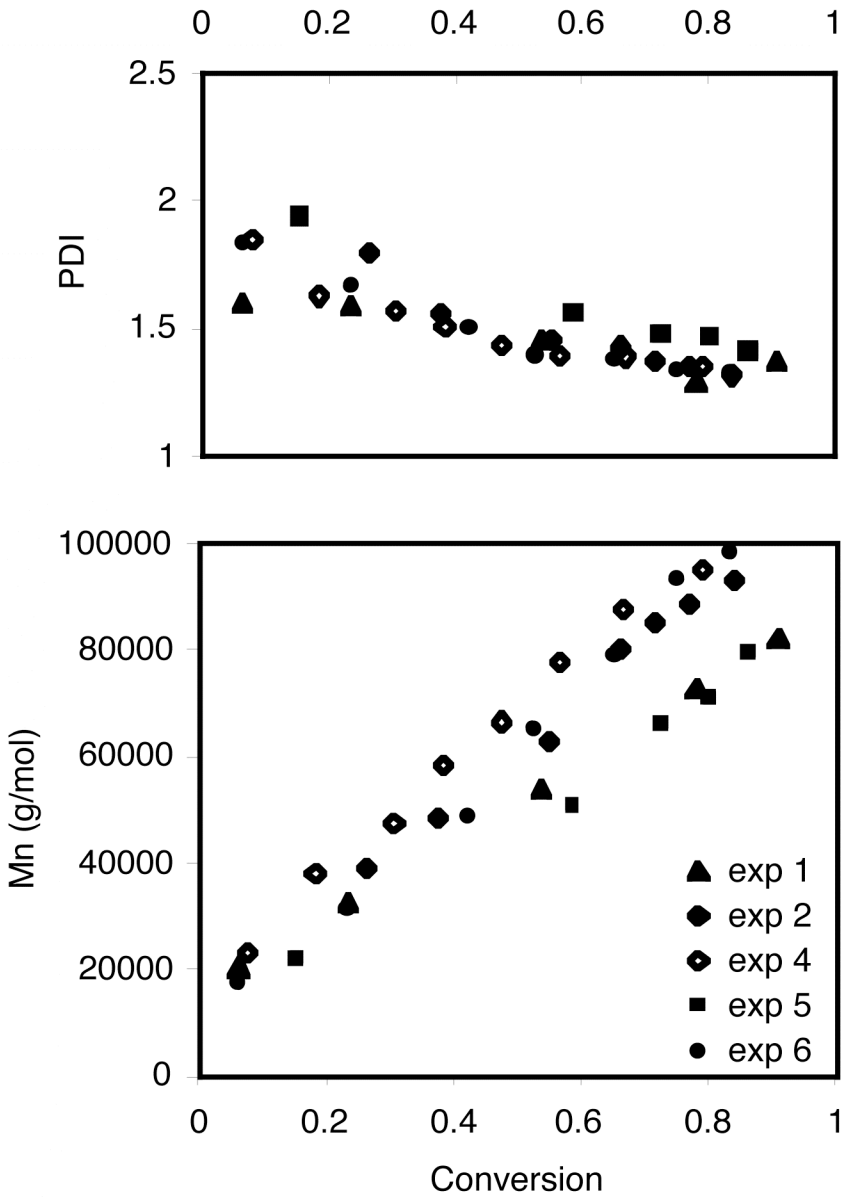

Figure 3-1. Number-average molecular weight (M_n) and polydispersity (PDI) as a function of conversion for the reverse ATRP in miniemulsion of BMA

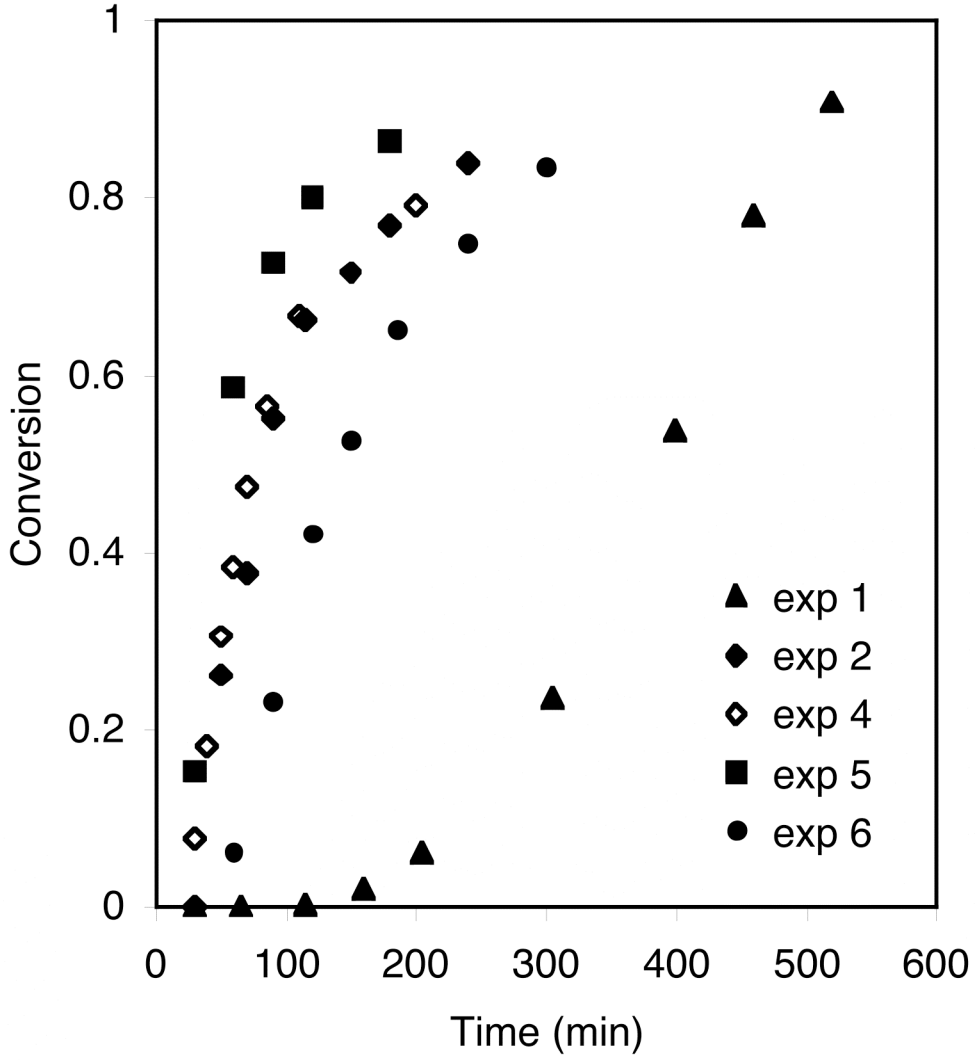

Figure 3-2. Conversion as a function of time for the miniemulsion reverse ATRP

Table 3-1. Summary of the experimental conditions and results for the reverse ATRP in miniemulsion of BMA

Exp.	CTAB	*n*(VA-044)[c]	Temp.	Inhib. Time	Final Polymer			Final Latex	
	(wt %)[a]	(mmol)	(^{o}C)	(min)	Conv. (%)	M_n (g·mol^{-1})	PDI	D_w (nm)	St. Dev.
1	10[b]	2.16	60	120	91	82320	1.37	126	40
2	2.5	2.16	90	30	87	91980	1.32	146	25
3	1.0	2.16	90	30	84	92250	1.34	155	32
4	0.5	2.16	90	30	79	95240	1.35	196	45
5	2.5	3.10[d]	90	30	86	79740	1.47	152	37
6	2.5	2.16	80	40	88	98480	1.33	150	19

(Inhib. Time: inhibition time; Conv.: conversion; D_w: weight-average particle diameter; St. Dev.: standard deviation of the weight-average particle diameter)

[a] based on monomer

[b] nonionic surfactant Brij 98

[c] $[BMA]_o/[Cu^{II}]_o/[VA\text{-}044]_o = 400/1/0.32$

[d] $[BMA]_o/[Cu^{II}]_o/[VA\text{-}044]_o = 400/1/0.46$

Raising the temperature to 70 ^{o}C also led to severe coagulation, even with a Brij 98 loading of 20 wt %. These results are significantly different from those reported by Li and Matyjaszewski who produced stable latexes with a Brij 98 loading of only 2.3 wt %.[22] This apparent discrepancy is rationalized by comparing the particle diameter of the final latexes. Our formulation of the miniemulsion generates a final particle diameter of 126 nm, compared to the previous reported values of 200-250 nm[22] (2.3 wt % Brij 98) and 195 nm[11] (13.5 wt % Brij 98). For a given miniemulsion recipe, a smaller droplet diameter increases the oil/water interfacial area and increases the surface tension, both of which increase the amount of surfactant required to stabilize the system. The initial droplet size of a miniemulsion is determined by many factors, including the recipe of the miniemulsion and choice of homogenizer.[33-36] We presume that our use of a microfluidizer rather than the sonification technique used by the Matyjaszewski lab is the reason for the significantly different particle diameters in these two similar systems. Our investigation found that Brij 98 is unable to stabilize the latex for the miniemulsion reverse ATRP of BMA when the temperature is greater than 60 ^{o}C and the particle diameter is approximately 130 nm.

The use of the cationic surfactant CTAB proved to be very effective at stabilizing the reverse ATRP of BMA in miniemulsion, while still allowing for control of the polymerization (Table 3-1, exp 2-6). All of the reverse ATRP systems, including when Brij 98 was used, exhibited some phase separation. The clear colorless monomer layer formed during the inhibition period (the time at the beginning of the polymerization during which there is no conversion) and remained until a conversion of approximately 75 %. The lack of color indicates the absence of any copper species, which suggests that

the monomer layer does not originate from droplet coalescence, but rather that the layer formed from monomer extracted from the droplets. For the CTAB stabilized systems the monomer layer did not form when the miniemulsion was held at 90 ^{o}C for 100 minutes, without initiator, discounting the high temperature as the primary cause of the destabilization. Additionally, the monomer layer was not observed when the conventional miniemulsion free radical polymerization (FRP) was conducted (Table 3-2, exp 7-9). It is presumed that the mechanism of the reverse ATRP process during the initial stages of the polymerization is the origin of the instability. Instability of the miniemulsion early in the polymerization has been reported in some LRP systems,[37] but its presence does not lead to coagulum formation in these systems.

Table 3-2. Summary of the experimental conditions and results for the conventional miniemulsion FRP of BMA

Exp.	CTAB (wt %)	Minutes elapsed at 60 % conv.	Final Latex D_w (nm)	St. Dev.
7	2.5	14	126	12
8	1.0	21	142	6
9	0.5	28	162	13

[a] based on monomer

The effect of the CTAB concentration was investigated by conducting polymerizations at surfactant loadings of 0.5, 1.0 and 2.5 wt % based on monomer. Figure 3-1 shows that the number-average molecular weight grows linearly with

conversion and that the polydispersity index decreases with conversion. The evolution of the molecular weight showed little dependence on the amount of CTAB added to the system. Similar to the experiment when Brij 98 was used to stabilize the systems, all the experiments using CTAB (exp 2-6) have a rapid increase in the molecular weight at the beginning of the polymerization, a trend that is commonly reported in the reverse ATRP literature.[20, 22, 24] As expected, the amount of surfactant influences the particle diameter in these systems. A decrease in the amount of CTAB results in an increase of the particle diameter of the final latex (Table 3-1, exp 2-4). The weight-average particle diameter was determined to be 146 nm, 155 nm and 196 nm for CTAB loadings of 2.5, 1.0 and 0.5 wt %, respectively. A similar trend is seen in the FRP process (Table 3-2, exp 7-9), but for a given CTAB loading, the reverse ATRP system had a larger particle diameter as well as a larger standard deviation (Figure 3-3). In the FRP systems the rate of polymerization was faster when the particle diameter was decreased, due to the phenomenon known as compartmentalization.[38] The advantage of compartmentalization, which reduces the rate of termination and significantly affects the kinetics of the polymerization, are not realized in reverse ATRP systems,[39] evident from the comparable conversion verse time profiles for CTAB loadings of 2.5 wt % (exp 2) and 0.5 wt % (exp 4) in Figure 3-2.

The use of CTAB produces latexes that are free of coagulum upon completion of the polymerization and showed no evidence of colloidal instability after 3 weeks. The one exception was when 0.5 wt % CTAB was used to stabilize the miniemulsion (exp 4). The use of 0.5 wt % CTAB for both the reverse ATRP (exp 4) and FRP (exp 9) systems exhibited no coagulum formation during the polymerization, however, their shelf lives were dramatically different. The reverse ATRP latex formed coagulum after 2 days,

while the FRP latex showed no evidence of instability after 3 weeks. An important difference between the latexes is the distribution of the particle diameters; the standard deviations were 45 nm for the ATRP latex and 13 nm for the FRP latex. The broad and asymmetrical particle diameter distribution for the reverse ATRP system (Figure 3-3, exp 4) is believed to be the cause of the poor shelf-life stability of the latex. (The FRP latex has a much higher molecular weight than the ATRP latex but this is not expected to significantly affect stability.)

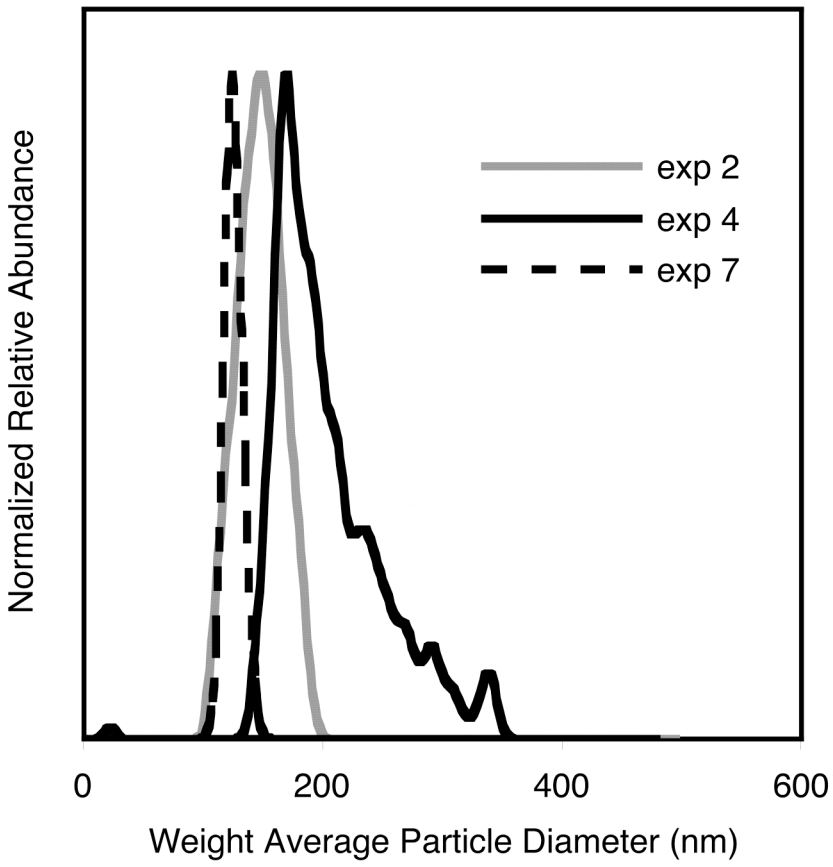

Figure 3-3. The particle diameter of the final latex

Within a reverse ATRP that is functioning properly the amount of initiator determines the number of polymer chains and subsequently the ratio of activator (Cu^{I}) to deactivator (Cu^{II}). This controls the ATRP equilibrium, which in turn influences the rate of polymerization. Increasing the amount of VA-044 from 2.16×10^{-4} mol (exp 2) to 3.10×10^{-4} mol (exp 5) increased the number of polymer chains, which is evident from the reduced molecular weight of the polymer in exp 5 (Figure 3-1). The presence of more polymer chains also decreases the amount of deactivator, both of which contribute to the observed increase in the polymerization rate (Figure 3-2). The increased rate of polymerization was accompanied by an increase in the polydispersity of the polymer from 1.32 (exp 2) to 1.47 (exp 5). The broader polydispersity results from combination of reduced deactivation efficiency and increased formation of dead chains because the number of polymer chains was increased while the total copper concentration remained constant.

The temperature of the polymerization influences the rate of initiator decomposition, the equilibrium constant of the atom transfer reaction and the propagation rate constant of the polymer. As well, the stability of latexes formed with nonionic surfactants are known to be compromised at high temperature.[29] The nonionic surfactant Brij 98 could provide reasonable stability of the latex up to a maximum temperature of 60 ^{o}C when the surfactant loading was 10 wt % based on monomer. In Figure 3-2 it can be seen that the Brij 98 system has an inhibition period of approximately 120 minutes and the maximum conversion is reached after 530 minutes. The length of the inhibition period depends on the time required for the initiator to decompose and establish an atom transfer equilbrium that will permit a reasonable rate of propagation. Using the water soluble

initiator VA-044, which has a 10 hour half life temperature of 44 ^{o}C, will always result in an inhibition period, the length of which is a function of the polymerization temperature. The use of CTAB allows for the polymerization to be conducted at temperatures as high as 90 ^{o}C, reducing the inhibition time to 30 minutes and the time required to reach maximum conversion to only 250 minutes. A comparison of the CTAB stabilized system conducted at 90 ^{o}C (exp 2) and 80 ^{o}C (exp 6) showed the expected dependence on temperature. A decrease in the temperature from 90^{o}C to 80 ^{o}C had no significant effect on the molecular weight or polydispersity of the polymer but did affect the rate of the polymerization. At 80 ^{o}C the inhibition period of the polymerization was approximately 40 minutes, compared to only 30 minutes when the polymerization was run at 90 ^{o}C. The slower decomposition rate of VA-044 at the lower temperature could account for the increased time of the inhibition period. In addition, from a comparison of the slopes in the conversion verse time plots in Figure 3-2 the expected decrease in the polymerization rate at the lower temperature is seen. The decrease in the rate of polymerization is attributed to a combination of the effect of the temperature on the equilibrium constant of the atom transfer reaction and the propagation rate constant of the monomer.

3.6 Conclusions

The miniemulsion reverse ATRP of BMA initiated VA-044 and mediated with $CuBr_2$/EHA_6-TREN can be stabilized with cationic surfactant CTAB. There is no coagulum produced at CTAB loading as low as 1 wt % based on monomer, which is significantly lower than the 10 wt % of Brij 98 that is required to stabilize the miniemulsion when the particle diameter of the latex is approximately 130 nm. The

resulting latexes are stable for more than three weeks after the polymerization. With CTAB as the surfactant the polymerizations can be conducted at temperatures as high as 90 ^{o}C, while Brij 98 allows for a maximum temperature of only 60 ^{o}C. The ability to conduct the polymerization at higher temperatures dramatically reduces the length of the inhibition period and increases the polymerization rate, which allows for the polymerization to be completed in half the time compared to systems stabilized with the nonionic surfactant Brij 98.

3.7 References

1. Kato, M.; Kamigaito, M.; Sawamoto, M.; Higashimura, T. *Macromolecules* **1995**, 28, 1721.
2. Wang, J.; Matyjaszewski, K. *J. Am. Chem. Soc.* **1995**, 117, 5614.
3. Matyjaszewski, K.; Xia, J. *Chem.. Rev*. **2001**, 101, 2921.
4. Chiefari, J.; Chong, Y. K.; Ercole, F.; Krstina, J.; Jeffery, J.; Le, T. P. T.; Mayadunne, R. T. A.; Meijs, G. F.; Moad, C. L.; Moad, G.; Rizzardo, E.; Thang, S. H. *Macromolecules* **1998**, 31, 5559.
5. Perrier, S.; Takolpuckdee, P. *J. Polym. Sci. Part A: Polym. Chem*. **2005**, 43, 5347.
6. Georges, M. K.; Veregin, R. P. N.; Kazmaier, P. M.; Hamer, G. K. *Macromolecules* **1993**, 26, 2987.
7. Hawker, C. J.; Bosman, A. W.; Harth, E. *Chem. Rev.* **2001**, 101, 3661.
8. Cunningham, M. F. *Prog. Polym. Sci.* **2002**, 27, 1039.
9. Qiu, J.; Charleux, B.; Matyjaszewski, K. *Prog. Polym. Sci*. **2001**, 26, 2083.
10. Qiu, J.; Gaynor, S. G.; Matyjaszewski, K. *Macromolecules* **1999**, 32, 2872.

11. Qiu, J.; Pintauer, T.; Gaynor, S. G.; Matyjaszewski, K.; Charleux, B.; Vairon, J. *Macromolecules* **2000**, 33, 7310.

12. Chambard, G.; de Man, P.; Klumperman, B. *Macromol. Symp*. **2000**, 150, 45.

13. Matyjaszewski, K.; Qiu, J.; Shipp, D. A.; Gaynor, S. *Macromol. Symp*. **2000**, 155, 15.

14. Wan, X.; Ying, S. *J. Appl. Polym. Sci.* **2000**, 75, 802.

15. Jousset, S.; Qiu, J.; Matyjasewski, K. *Macromolecules* **2001**, 34, 6641.

16. Peng, H.; Cheng, S.; Feng, L. *J. Appl. Polym. Sci.* **2003**, 89, 1542.

17. Okubo, M.; Minami, H.; Zhou, J. *Colloid. Polym. Sci*. **2004**, 282, 747.

18. Yoo, S. H.; Lee, J. H.; Lee, J-C.; Jho, J. Y. *Macromolecules* **2002**, 35, 1146.

19. Peng, H.; Cheng, S.; Feng, L. *Polym. Int.* **2004**, 53, 828.

20. Matyjaszewski, K.; Qiu, J.; Tsarevsky, N. V.; Charleux, B. *J. Polym. Sci. Part A: Polym. Chem.* **2000**, 38, 4724.

21. Matyjaszewski, K.; Shipp, D. A.; Qiu, J.; Gaynor, S. G. *Macromolecules* **2000**, 33, 2296.

22. Li, M.; Matyjasewski, K. *Macromolecules* **2003**, 36, 6028.

23. Li, M.; Matyjaszewski, K. *J. Polym. Sci. Part A: Polym. Chem.* **2003**, 41, 3606.

24. Li, M.; Min, K.; Matyjaszewski, K. *Macromolecules* **2004**, 37, 2106.

25. Li, M.; Jahed, N. M.; Min, K.; Matyjaszewski, K. *Macromolecules* **2004**, 37, 2434.

26. Min, K.; Gao, H.; Matyjaszewski, K. *J. Am. Chem. Soc.* **2005**, 127, 3825.

27. Fitch, R. M. *Polymer Colloids: A Comprehensive Introduction*; Academic Press: New York, 1997.

28. Gaynor, S. G.; Qiu, J.; Matyjaszewski, K. *Macromolecules* **1998**, 31, 5951.

29. Eslami, H.; Zhu, S. *Polymer* **2005**, 46, 5484.

30. Limer, A.; Heming, A.; Shirley, I.; Haddleton, D. *European Polymer Journal* **2005**, 41, 805.

31. Klee, J. E.; Neidhart, F.; Flammersheim, H. J.; Mülhaupt, R. *Macromol. Chem. Phys.* **1999**, 200, 517.

32. Zeng, F.; Shen, Y.; Zhu, S.; Pelton, R. *Macromolecules* **2000**, 33, 1628.

33. Asua, J. M. *Prog. Polym. Sci.* **2002**, 27, 1283.

34. Capek, I.; Chern, C. S. *Adv. Polym. Sci.* **2001**, 155, 101.

35. Landfester, K. *Macromol. Rapid. Commun.* **2001**, 22, 896.

36. Schork, F. J.; Luo, Y.; Smulders, W.; Russum, J. P.; Butté, A.; Fontenot, K. *Adv. Polym. Sci.* **2005**, 175, 129.

37. Luo, Y.; Tsavalas, J.; Schork F. J. *Macromolecules* **2001**, 34, 5501.

38. Gilbert, R. G. *Emulsion Polymerization – A Mechanistic Approach*; Academic Press: New York, 1995.

39. Butté, A.; Storti, G.; Morbidelli, M. *Macromolecules* **2001**, 34, 5885.

CHAPTER 4

4 High Molecular Weight Poly(Butyl Methacrylate) by Reverse Atom Transfer Radical Polymerization in Miniemulsion Initiated by a Redox System

published in Macromolecules 2007, 40, 860-866.

4.1 Preface

While investigating ways to increase the rate of aqueous based ATRP I explored the use of a redox initiation system. Using a redox initiation system would allow for a more ideal initiation since all the polymer chains would be generated over a narrow time range. It would also allow for the polymerization to be conducted at low temperature because you would no longer be restricted to initiators that thermally decompose (which require high temperatures). The drawback to this technique is that ATRP controls the polymerization through a redox process, leading to a potentially complex system. The experiments revealed that the redox initiating pair hydrogen peroxide/ascorbic acid did influence the control over the polymerization because I was able to synthesize very high molecular weight polymers. Typically, the molecular weight is limited in ATRP because of side reactions such as termination (which builds up the copper(II) species and prevents further conversion) and transfer to monomer and polymer. In addition to the high molecular weight, the system also had high rates of polymerization. These observations can be explained by an advantageous ratio of copper(I) to copper(II) which is known to be a key component of both the rate of the polymerization and the degree of control over the polymer.

4.2 Abstract

The reverse atom transfer radical polymerization of butyl methacrylate in miniemulsion, initiated with the redox pair hydrogen peroxide/ascorbic acid and mediated with copper(II) bromide tris[2-di(2-ethylhexyl acrylate)aminoethyl]amine produced high-molecular weight poly(butyl methacrylate) (M_n = 989900, PDI = 1.25). The miniemulsion was carried out with 15% solids (based on 100% conversion), 10 wt% of the nonionic surfactant Brij 98 (based on monomer), and 3.8 wt% hexadecane (based on monomer), with the final weight-average particle diameter less than 110 nm. The use of the redox pair to initiate the polymerization also facilitated a relatively fast rate of polymerization. The polymerizations were carried out at 60^{o}C and typically reached their maximum conversion (with degrees of polymerization up to 6900) of approximately 80% in only 8 hours. Additionally, the polymerization of methyl methacrylate produced well-defined high-molecular weight polymers with a controlled degree of polymerization and narrow molecular weight distribution.

4.3 Introduction

Atom transfer radical polymerization (ATRP)[1-4] provides a facile route to the syntheses of polymers with predetermined microstructure and narrow molecular weight distributions. Regardless of how well suppressed the radical reactions are in the ATRP system the radicals undergo the same side reactions (termination and transfer) that occur in conventional free radical polymerizations. The lifetime of the growing end, and consequently the molecular weight, are limited by the rate of the radical side reactions. Typically, for linear polymers produced by ATRP the number-average molecular weight (M_n) is limited to ~200 000, after which the effect of the radical side reactions become significant and the livingness of the system is decreased.[3,4] Well-defined high-molecular weight poly(methyl methacrylate) (PMMA) was achieved by Xue et al.[5] using the phenyl 2-bromomethylpropionate/CuCl/4,4'-*n*-nonyl-2,2'-bipyridine initiator/mediating complex in xylene. After 500 minutes the conversion reached approximately 55% resulting in PMMA with a M_n of 360 000 with a polydispersity index (PDI) of approximately 1.20. Recently, Mao et al.[6] produced high-molecular weight poly[2-(dimethylamino)ethyl methacrylate] employing *p*-toluenesulfonyl chloride/CuCl/1,1,4,7,10,10-hexamethyl-triethylenetetramine as the initiator/mediating complex in a methanol/water mixture. After 24 hours at 50°C the conversion reached 85% and the resulting polymer had a M_n of 1100 000 with a PDI of 1.26.

The application of ATRP to an aqueous dispersed system such as an emulsion or miniemulsion process provides advantages such as better mixing, improved heat transfer, and easier removal of residual monomer. Compared to ATRP conducted in emulsion, the miniemulsion process has proven to be far more robust in terms of colloidal stability and

maintaining control of the polymerization.[7-13] Miniemulsion eliminates some of the complicating factors thought to negatively impact ATRP latexes made by emulsion polymerization, such as, micelle nucleation, simultaneous polymerization within droplets and particles, and stabilization of very small particles at the beginning of the polymerization.[14,15] In addition, nucleation of the miniemulsion droplets that already contain the mediating complex avoids the need to transport the very hydrophobic mediating complex to the polymerization site. Reverse ATRP has proven to be an effective method of adapting ATRP to miniemulsion. It employs the mediating complex in its higher oxidation state, which is not easily oxidized during the high shear required to formulate the 100-200 nm droplets of a miniemulsion. We have previously observed that a thermal initiator which decomposes readily at low temperature is required since miniemulsion ATRP with particles sizes less than 200 nm are typically not colloidally stable above 60^{o}C.[16] The azo initiator 2,2'-azobis[2-(2-dimidazolin-2-yl)propane] dihydrochloride (VA-044) is employed since it has one of the lowest 10 hour half-life temperatures commercially available (44^{o}C). Using VA-044 as the initiator at 60^{o}C leads to an induction period, in which no polymer is formed, at the beginning of the polymerization. This had been attributed to the time required for the initiator to thermally decompose and consume the copper(II) complex to levels where polymerization can proceed at an appreciable rate.

Initiators used for conventional free radical polymerizations, including azo compounds,[17,18] peroxides[19] and thermal iniferters,[20] have all been successful applied to reverse ATRP; however, relatively high polymerization temperatures (> 90^{o}C) are required to ensure the rapid decomposition of the initiator. Reverse ATRP employing a

redox initiation system would allow the polymerization to be run at lower temperatures, as well as afford a more ideal reverse ATRP initiation, with all the polymer chains initiated almost instantaneously. The use of the redox pair, such as hydrogen peroxide (HPO)/ascorbic acid (AA) was expected to reduce the length of the induction period and lower the polydispersity index of the polymer. In addition to the expected results, the HPO/AA redox initiation system applied to the reverse ATRP of butyl methacrylate (BMA) and methyl methacrylate (MMA) in miniemulsion produced well-defined high-molecular weight polymers ranging from 300 000 to 1000 000. The preliminary results of the investigation are presented here.

4.4 Experimental

Materials. n-Butyl methacrylate (99%, Aldrich), methyl methacrylate (99%, Aldrich) and 2-ethylhexyl acrylate (98%, Aldrich) were purified by passing each through a column packed with inhibitor remover (Aldrich). The compounds copper(II) bromide ($CuBr_2$, 99%, Aldrich), tris(2-aminoethyl)amine (96%, Aldrich), polyoxyethylene(20) oleyl ether (Brij 98, Aldrich), hexadecane (99%, Aldrich), basic alumina (Aldrich), ascorbic acid (99%, Aldrich), hydrogen peroxide (3 wt% in water, Aldrich) and 2,2′-azobis[2-(2-imidazolin-2-yl)propane] dihydrochloride (Wako Chemicals) were used as received. The synthesis of tris[2-di(2-ethylhexyl acrylate)aminoethyl]amine (EHA_6TREN) was adapted from literature methods.[21,22]

Miniemulsion Polymerization. The organic phase was prepared by adding $CuBr_2$ (0.153 g, 6.85×10^{-4} mol), EHA_6TREN (0.901 g, 7.20×10^{-4} mol), hexadecane (1.48 g, 3.8

wt% vs. monomer) and BMA (39 g, 0.274 mol, 15 wt% vs. deionized water) to a beaker and stirring overnight at room temperature to form a homogeneous solution. The aqueous phase that consisted of the surfactant Brij 98 (3.9 g, 10 wt% vs. monomer) and deionized water (221 g) was stirred overnight at room temperature. The organic phase was added to the surfactant solution and stirred for approximately 30 min prior to passing through a Microfluidizer 110S (Microfluidics International Corporation) operating at an inlet pressure of 275 kPa. The miniemulsion (200 g) was transferred to a 500 mL round-bottom flask fitted with a condenser and was purged with ultra-high-purity nitrogen for 30 min before being immersed in a 60^{o}C oil bath with the magnetic stirring speed set to 250 rpm. Fifteen minutes elapsed before the addition of the initiator. The AA (0.0227 g, 1.29×10^{-4} mol) and HPO (0.02916 g, 2.57×10^{-4} mol) were added to separate Schlenk tubes, mixed with 2 mL of deionized water, and purged with ultra-high-purity nitrogen for 20 min prior to injection. Using a deoxygenated syringe, the HPO was added prior to the AA, which was added dropwise over 5 minutes. Samples were withdrawn with a deoxygenated syringe and placed in an ice bath. The polymer samples were dried under the air manifold overnight than placed in a vacuum overnight to remove all volatile compounds. All polymerizations were repeated to ensure reproducibility.

Characterization. After the polymerizations were complete the latexes were filtered (Fisherbrand P8 creped) to collect any coagulum. The amount of coagulum, if present, was determined gravimetrically. Monomer conversions were determined gravimetrically. Size exclusion chromatography (SEC) was used to measure the molecular weight distribution of the polymer samples. The dried polymer samples from the miniemulsion were dissolved in tetrahydrofuran (THF) and passed through a column

packed with basic alumina to remove the residual copper. The SEC was equipped with a Waters 2960 separation module containing four Styragel columns (100, 500, 10^3, 10^4 Å) maintained at 40^{o}C, coupled with a Waters 410 differential refractive index (RI) detector and a Wyatt Technology DAWN EOS photometer multi-angle light scattering (LS) detector (690 nm, 30 mW Ga-As laser). THF was used as the eluant and the flow rate was set to 1 mL·min^{-1}.The LS detector was calibrated with toluene, normalized with 30 000 g·mol^{-1} narrow polystyrene standard and the data was processed using Astra (version 4.90.08) software. A Wyatt Optilab DSP 690 nm refractometer was used determine the d*n*/d*c* values of poly(butyl methacrylate) (PBMA) and PMMA. There was good agreement between the RI data and the LS data up to ~ 400 000 g·mol^{-1}, after which the RI data underestimated the molecular weight of the polymer (due to differences in the type of polymer used in the calibration and the samples). Before running the samples, the instrument was first calibrated with sodium chloride. Six samples of 1-10 mg·mL^{-1} were prepared in THF for each polymer and injected sequentially to construct a curve with slope d*n*/d*c*. The d*n*/d*c* value for PBMA and PMMA were 0.075 and 0.081 respectively. The particle sizes of the latexes reported in this paper were measured using a Matec Applied Sciences Capillary Hydrodynamic Fractionation (CHDF) 2000 unit. The UV detector was set to 220 nm. The eluant was a 20:1 mixture of deionized water and GR500-1X (Matec Applied Sciences). Samples were diluted with the eluant to approximately 3.5 wt% solids and sonicated for 5 minutes. Samples were passed through a 0.5 μm pore size filter prior to injection. The marker was a 2 wt% solution of sodium benzoate. To ensure that there were no particles greater than 0.5 μm the particle size distributions were also measured using a Malvern Mastersizer 2000 equipped with a

Hydro 2000S optical unit. The refractive index value for water, PBMA and PMMA were 1.33, 1.48 and 1.49 respectfully.

4.5 Results and Discussion

4.5.1 Reverse ATRP initiated with the water-soluble initiator VA-044

The polymerization of BMA was carried out in a miniemulsion system using the reverse ATRP process with VA-044 as the radical initiator and $CuBr_2$-EHA_6TREN as the mediating complex. The ratio of $[BMA]_o$:$[CuBr_2$-$EHA_6TREN]_o$:$[VA\text{-}044]_o$ = 400:1:1 (exp 1) afforded a well-controlled polymerization (Figure 4-1a) after an inhibition period of approximately 130 minutes (Figure 4-1b). After 480 minutes the conversion was 85% and the polymer had a M_n of 67 900 with a PDI of 1.34. The weight-average particle diameter was 82 nm with a standard deviation of 34 nm. The evolution of the molecular weight and the rate of the polymerization is consistent with earlier reports of copper-mediated ATRP in aqueous dispersed systems using nonionic surfactants.[8-10,23-27]

4.5.2 Redox initiation system for reverse ATRP

The use of the HPO/AA redox pair to initiate ATRP, which controls the polymerization through a reversible redox process, creates a potentially complex system. The AA is oxidized by HPO forming hydroxyl radical and ascorbate radical intermediates that initiate the polymerization. Dehydroascorbic acid, a product of the reaction between AA and HPO, can be hydrolyzed to products that are reducing agents[28] and reactions of these secondary products could influence the reverse ATRP process. In addition to the

generation of primary radicals from the reaction between AA and HPO, both AA and HPO can react with other species in the system. Jakubowski and Matyjaszewski

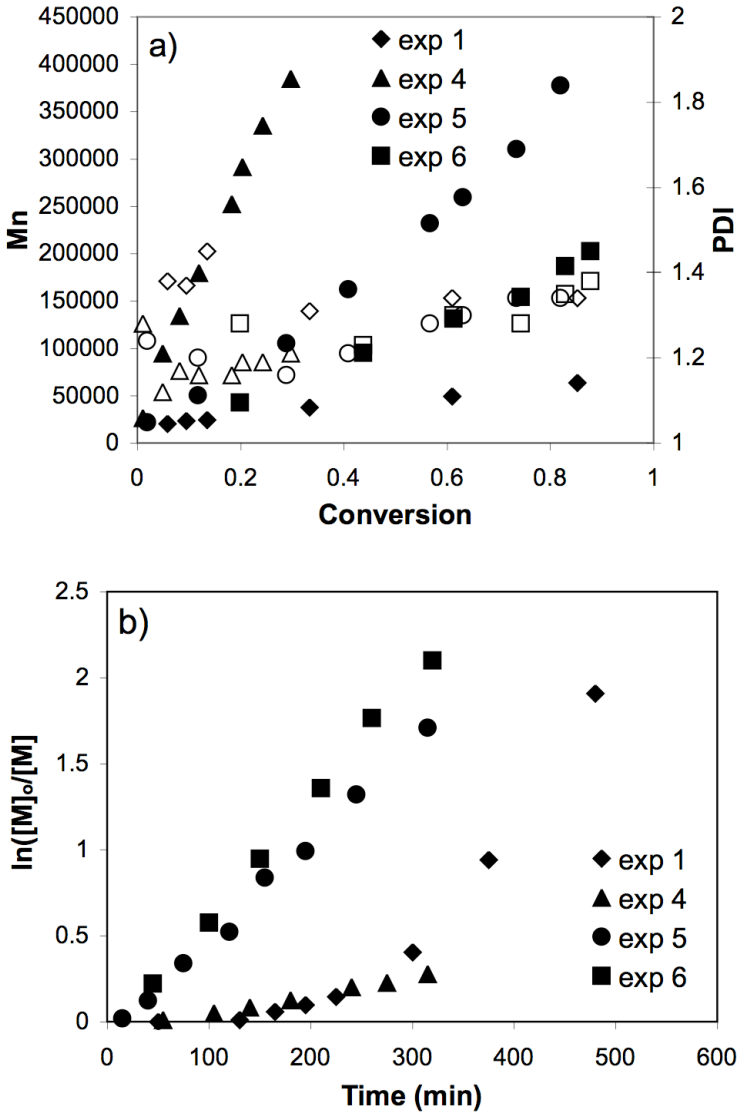

Figure 4-1. Evolution of M_n (filled symbols) and PDI (open symbols) with conversion (a) and the kinetic plots (b) for the reverse ATRP of BMA

exp 1: $[CuBr_2\text{-}EHA_6TREN]_0:[VA\text{-}044]_0 = 1:1$;

exp 4: $[CuBr_2\text{-}EHA_6TREN]_0:[HPO]_0:[AA]_0 = 1:0.25:0.25$;

exp 5: $[CuBr_2\text{-}EHA_6TREN]_0:[HPO]_0:[AA]_0 = 1:0.5:0.25$;

exp 6: $[CuBr_2\text{-}EHA_6TREN]_0:[HPO]_0:[AA]_0 = 1:1:0.25$.

developed a process called activator generated by electron transfer (AGET) ATRP using a reducing agent, tin(II) 2-ethylhexanoate, in combination with a copper(II) complex (in the presence of an alkyl halide initiator) to produce well-defined polymers.[29] The system has also been successfully applied to miniemulsion[30] and microemulsion[31] processes using AA as the reducing agent. In another process, referred to as activators regenerated by electron transfer (ARGET),[32] the presence of a reducing agent regenerates the copper(I) complex from the copper(II) complex, allowing for a significant reduction in the amount of copper in the system. As well, the decomposition of peroxides by copper(I) complexes occurs,[33] and this reaction has been used to initiate ATRP.[34,35]

When BMA was polymerized with 1.0 equivalent of the $CuBr_2$-EHA_6TREN complex relative to the HPO/AA redox initiating system, $[BMA]_0$:$[CuBr_2$-$EHA_6TREN]_0$:$[HPO]_0$:$[AA]_0$ = 400:1:1:1 (exp 3), there was inefficient deactivation of the radicals generated in the system, evident from the uncontrolled polymerization that reached complete conversion in less than 30 minutes with the polymer obtaining a M_n of 424 000 g·mol^{-1} with a PDI of 2.3. A reduction in the amount of initiator (HPO/AA) relative to the copper(II) complex, $[BMA]_0$:$[CuBr_2$-$EHA_6TREN]_0$:$[HPO]_0$:$[AA]_0$ = 400:1:0.25:0.25 (exp 4, Figure 4-1), resulted in a controlled polymerization that unexpectedly produced high-molecular weight polymer (Mn = 384 600 g·mol^{-1}, PDI = 1.21). The rate of the polymerization was slow, attaining only 30% conversion after 360 minutes. As shown in Figure 4-1, the effect of the $[HPO]_0$:$[AA]_0$ ratio was investigated by maintaining $[BMA]_0$:$[CuBr_2$-$EHA_6TREN]_0$:$[AA]_0$ at 400:1:0.25 and varying $[HPO]_0$. All the polymerizations were controlled and a trend of decreasing molecular weight was seen when the ratio of $[HPO]_0$:$[AA]_0$ was increased from 1:1 (exp 4) to 2:1 (exp 5) to 4:1

(exp 6), indicating that more polymer chains were created. The M_n increased linearly with conversion and the PDI remained low. The molecular weight vs conversion data does not pass through the origin, and the rapid increase of molecular weight at the beginning of the polymerization is a trend that is common in reverse ATRP systems.[7,10,11,16] This indicates that chains are either initiated slowly (unlikely with redox initiation) or more probably in a miniemulsion system, chains initiated in the aqueous phase do not all immediately enter droplets/particles thereby resulting in a lower number of chains at low conversions.

From the kinetic plots of $\ln([M]_0/[M])$ vs time shown in Figure 4-1b it can be seen that employing the redox initiating system significantly reduced the inhibition period when compared to the VA-044 initiated system. The inhibition time of less than 20 minutes is attributed to the initiation of the majority of the polymer chains early in the polymerization, which consumes the copper(II) complex to levels where polymerization can proceed at an appreciable rate. An increase in the $[HPO]_0$:$[AA]_0$ ratio from 1:1 (exp 4) to 2:1 (exp 5) to 4:1 (exp 6) increased the rate of the polymerization. An increase in the rate of the polymerization is expected when the number of propagating chains are increased and the copper(II) complex loading is held constant. This is attributed not only to the increase in the number of polymer chains, but also the subsequent increase in the ratio of copper(I) complex to copper(II) complex during the polymerization. A $[HPO]_0$:$[AA]_0$ ratio of 2:1 (exp 5) resulted in the polymerization obtaining 82% conversion in 315 minutes compared to 30% conversion in 360 minutes when the $[HPO]_0$:$[AA]_0$ ratio was 1:1 (exp 4). However, increasing the $[HPO]_0$:$[AA]_0$ ratio to 4:1 (exp 6), which resulted in approximately double the number of polymer chains relative to

exp 5, had only a minimal effect on the rate of the polymerization.

Table 4-1. Summary of Experiments for the Reverse ATRP of BMA and MMA in Miniemulsion at 60 ^{o}C initiated with the redox pair HPO/AA

Exp	Monomer	$[monomer]_0:[CuBr_2]_0:[HPO]_0:[AA]_0$	Conv[b] (%)	M_n[c] ($g \cdot mol^{-1}$)	PDI[d]	D_w[e] (nm)	SD[f]
5	BMA	400:1:0.5:0.25	82	377500	1.34	103	24
7	BMA	800:1:0.5:0.25	83	604600	1.29	99	27
8	BMA	1200:1:0.5:0.25	83	989900	1.24	113	19
9	BMA	800:1:0.4:0.20	80	850800	1.23	102	20
10	BMA	800:1:0.6:0.30	78	447600	1.23	107	26
11	MMA	800:1:0.5:0.25	69	333400	1.22	89	16
12	MMA	1136:1:0.5:0.25	70	502200	1.27	99	24
13	MMA	1685:1:0.5:0.25	59	629200	1.17	97	21

[a] [Brij 98]:[hexadecane] = 10:3.8 wt% based on monomer; 15% solid content. [b] conv = conversion, determined gravimetrically. [c] M_n = number-average molecular weight, determined from size exclusion chromatography. [d] PDI = polydispersity index, determined from size exclusion chromatography. [e] D_w = weight-average particle diameter, determined with capillary hydrodynamic fractionation (CHDF 2000). [f] SD = standard deviation of the weight-average particle diameter, determined with capillary hydrodynamic fractionation (CHDF 2000).

4.5.3 High-molecular weight PBMA

The ratio of $[BMA]_0:[CuBr_2\text{-}EHA_6TREN]_0:[HPO]_0:[AA]_0$ = 400:1:0.5:0.25 produced well-controlled polymers at high rates of polymerization, subsequently this ratio was studied in further detail. As seen in Table 4-1, varying the amount of

copper/initiator relative to BMA targeted high-molecular weight polymer. Figure 4-2a illustrates that the M_n increased with conversion while the PDI remained relatively low. The evolution of the molecular weight distributions with conversion in Figure 4-3 (exp 8) further demonstrates that the polymerization was controlled. The entire molecular weight distribution shifted to higher molecular weight during the polymerization and the distributions remained narrow. At low conversion the molecular weight distribution is broad, and there is a slight shoulder in the SEC trace at a conversion of 23%, attributed to variation in number of activation/deactivation cycles that polymer chains undergo at low conversions. There is no low molecular weight tail indicating that all the polymer chains are created during the early stages of the polymerization and that termination and transfer reactions involving the polymer chains are minimal. Xue et al.[5] reported a low molecular weight tail in the SEC distribution when the molecular weight of the PMMA reached 367 000 $g \cdot mol^{-1}$, attributed to slow propagation of a fraction of the chains.

As expected, a decrease in the amount of copper/initiator relative to the initial amount of monomer resulted in an increase in the molecular weight of the polymer. The $[BMA]_o$:$[CuBr_2\text{-}EHA_6TREN]_o$ ratios of 400, 800, and 1200 produced polymers with M_n of 377 500, 604 600 and 989 900 and PDI of 1.34, 1.29 and 1.24, respectively. The trend of decreasing PDI with a higher targeted molecular weight could be attributed to the decreased concentration of radicals that would result in less termination, or from the expected decrease in PDI with increasing molecular weight in ATRP systems. After an induction period of less than 20 minutes, the kinetic plots of $\ln([M]_o/[M])$ vs time in Figure 4-2b were relatively linear up to 70% conversion, which demonstrates the first order dependence of monomer consumption with respect to time. The induction period

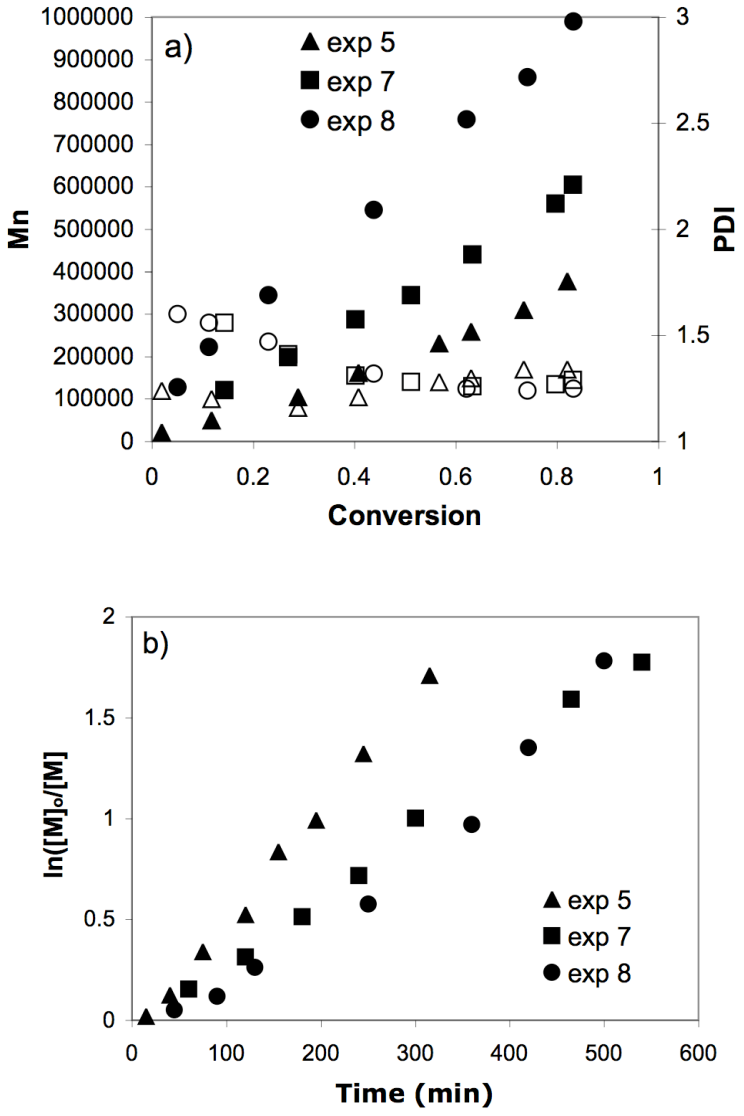

Figure 4-2. The effect of varying the $[BMA]_0/[CuBr_2\text{-}EHA_6TREN]_0$ ratio. Evolution of M_n (filled symbols) and PDI (open symbols) with conversion (a) and the kinetic plots (b) for the reverse ATRP of BMA

exp 5: $[BMA]_o:[CuBr_2\text{-}EHA_6TREN]_o$ = 400:1;
exp 7: $[BMA]_o$: $[CuBr_2\text{-}EHA_6TREN]_o$= 800:1;
exp 8: $[BMA]_o$: $[CuBr_2\text{-}EHA_6TREN]_o$= 1200:1.

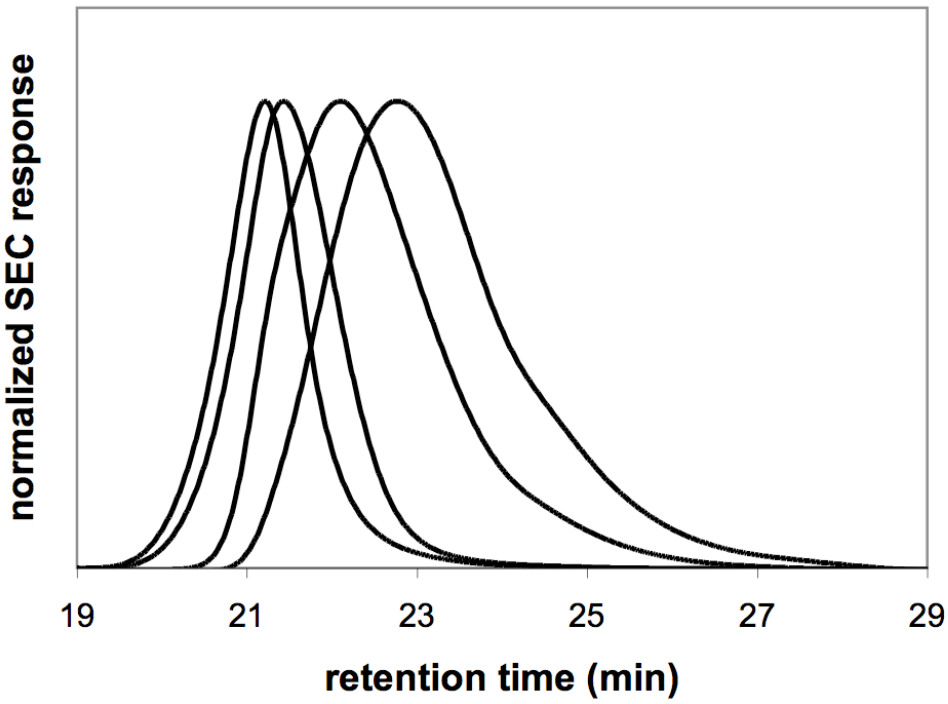

Figure 4-3. Size exclusion chromatography (SEC) traces of experiment 8 for the reverse ATRP of BMA at 60°C in miniemulsion.

Conversion increases from right to left;
conversion = 11%, M_n = 222 500, PDI = 1.56;
conversion = 23%, M_n = 345000, PDI = 1.47;
conversion = 74%, M_n = 859000, PDI = 1.24;
conversion = 83%, M_n = 989900, PDI = 1.24.

suggests that the initial concentration of $CuBr_2$-EHA_6TREN was sufficient to capture all the radicals generated by the redox initiation system.

From the basic ATRP mechanism, Matyjaszewski et al. developed a rate law that is first order with respect to time,[36] which can be used when there is an excess of copper(II) complex and if it assumed that the concentration of the other species remain constant (eq 1-2).[37,38] This simple mechanistic model allows an apparent rate constant

(k^{app}) of the polymerization to be estimated and the relative rate of the polymerizations to be compared; however, no specific mechanistic information is drawn from the data. The model neglects the persistent radical effect on the kinetics for ATRP, which was first developed by Fischer[39] and has since been refined by Tang et al.[38] As well, the reduction of the termination rate during the polymerization due to the gel effect is neglected.[40]

$$R_p = k_p[M][P^*] = k_p[M]K_{eq}[chain]\frac{[Cu(I)]}{[Cu(II)]} = k^{app}[M] \qquad (1)$$

$$\ln\left(\frac{[M]_o}{[M]}\right) = k^{app}t \qquad (2)$$

$$\frac{k^{app}}{[chain]} = k_pK_{eq}\frac{[Cu(I)]}{[Cu(II)]} \qquad (3)$$

The k^{app} was determined from the slope of the kinetic plot between approximately 10-70% conversion. As seen in Table 4-2, the k^{app} of the polymerization was found to decrease as higher molecular weight polymer was targeted. The $[BMA]_o$:$[CuBr_2$-$EHA_6TREN]_o$ ratios of 400, 800, and 1200 resulted in a k^{app} of $9.3\times10^{-5}s^{-1}$, $7.5\times10^{-5}s^{-1}$ and $4.9\times10^{-5}s^{-1}$, respectfully. The decrease in k^{app} results from the decrease in the number of polymer chains in the system (Table 4-2) which influences the rate of the polymerization (eq 1). The fast rate of polymerization for the redox initiated systems is highlighted by a comparison of the k^{app} per polymer chain (eq 3, Table 4-2). Typically, the redox initiated systems have an apparent rate constant per polymer chain which is greater than five times that of the VA-044 systems. Since the k_p and K_{eq} values should not be influenced by the initiation system, the conclusion is that the HPO/AA

Table 4-2. Kinetic Parameters for the Reverse ATRP of BMA and MMA initiated with the redox pair HPO/AA

Exp	monomer	VA-044 ($mol\times10^{-4}$)	HPO ($mol\times10^{-4}$)	$CuBr_2$ ($mol\times10^{-4}$)	k^{app} [a] ($s^{-1}\times10^{-5}$)	chain[b] ($mol\times10^{-5}$)	chain/HPO	$CuBr_2$/chain	k^{app}/chain
1	BMA	5.15	-	5.15	11.7	37.5	-	1.4	0.31
2	BMA	2.58	-	5.15	2.8	19.4	-	2.7	0.14
5	BMA	-	2.57	5.15	9.3	6.5	0.25	7.9	1.43
7	BMA	-	1.29	2.58	7.5	4.1	0.32	6.3	1.83
8	BMA	-	0.86	1.72	4.9	2.5	0.29	6.9	1.96
9	BMA	-	1.03	2.58	7.8	2.8	0.27	9.2	2.76
10	BMA	-	1.54	2.58	8.0	5.2	0.34	5.0	1.54
11	MMA	-	1.83	3.66	5.9	6.0	0.32	6.3	0.98
12	MMA	-	1.29	2.58	6.3	4.1	0.31	5.3	1.54
13	MMA	-	0.87	1.74	3.4	2.7	0.31	6.3	1.25

[a] k^{app} = apparent rate constant.

[b] moles of polymer chains = moles(monomer)×molarmass(monomer)×conversion/number-average molecular weight.

system yields an advantageous ratio of [Cu(I)]/[Cu(II)] that allows the polymerization to proceed at higher rates and to much higher molecular weights, while preserving control, than has previously been observed. While the exact nature of this behavior is currently not understood, it is possible that the concentration of the deactivating species ($CuBr_2$-EHA_6TREN) is regulated by the presence of the AA. This kinetic analysis also allowed for a comparison between the redox initiated systems, for which the apparent rate constant per polymer chain increased as the number of chains in the system decreased.

The desired molecular weight of the polymer can be targeted by selecting the $[BMA]_0$:$[CuBr_2$-$EHA_6TREN]_0$ ratio. The theoretical M_n can not be readily determined since the number of species that produce a polymer chain is not accurately known; however, an initiator efficiency ([polymer chains]/$[initiator]_0$) can be calculated. The initiator efficiency for the VA-044 systems is 0.36 and 0.38 for experiment 1 and 2, respectively. These values are typical of the VA-044 initiated reverse ATRP, and consistent with the initiation efficiency of nonionic azo initiators,[41] although we note that VA-044 is cationic. For redox initiated systems it can be seen from Table 4-2 that for every mole of HPO (when $[HPO]_0$:$[AA]_0$ = 2:1) approximately 0.3 moles of polymer chains are produced. To produce a well-controlled polymerization a greater than five fold excess of initial $CuBr_2$-EHA_6TREN relative to the moles of polymer chains produced is required. Compared to the VA-044 initiated systems in which the initial moles of $CuBr_2$-EHA_6TREN relative to the moles of polymer chains are 1.4 (exp 1) and 2.7 (exp 2) it would be expected that such a large excess of $CuBr_2$-EHA_6TREN would result in no polymer formation, or very slow rates of polymerization. Attempts at targeting high-molecular weight polymers with VA-044 as the initiator have so far been unsuccessful.

Targeting high-molecular weight polymer ($[BMA]_0$:$[CuBr_2$-$EHA_6TREN]_0$:$[VA\text{-}044]_0$ = 1000:1:1) led to poor control of the polymerization. The amount of the copper(II) complex was increased in an attempt to improve control over the polymerization ($[BMA]_0$:$[CuBr_2$-$EHA_6TREN]_0$:$[VA\text{-}044]_0$ = 1000:3:1), however, after 24 hours no polymer had formed. It appears that the use of the HPO/AA redox pair is required to create well-controlled, high-molecular weight polymer at relatively high rates of polymerization, however, the reason for this interesting behavior is unknown and currently under investigation.

Typically, the final latexes were monomodal and ranged in particle size from 90-110 nm, with less than 2 wt% coagulum at the end of the polymerization. The particle sizes were confirmed with a Malvern Mastersizer 2000, which also verified the absence of large particles in the system. All the experiments exhibited some initial phase separation. A clear, colorless monomer layer was present from the beginning of the experiment until the system reached approximately 75% conversion. Instability of the miniemulsion early in living radical polymerizations has been reported[16,42] but its presence does not lead to coagulum formation in these systems.

4.5.4 Effect of the Initiator Concentration

The relationship between the initial concentration of $CuBr_2$-EHA_6TREN and the initiator (HPO/AA) was studied. If the amount of copper remains constant, an increase in the concentration of initiator should produce more chains that would result in a lower M_n. Table 4-2 summarizes the experimental results of varying the initiator concentration (maintaining $[HPO]_0$:$[AA]_0$ = 2:1) on the system. The plots of M_n and PDI are displayed

in Figure 4a. All the polymerizations were well-controlled, with the M_n increasing linearly with conversion and the PDI remaining low. As well, there was no low-molecular weight tail in the molecular weight distribution. From Figure 4-4a it can be seen that the molecular weight of the polymer was dependent on the amount of initiator, with a higher initiator concentration resulting in lower molecular weight polymer due to the increased number of polymer chains (Table 4-2). The molecular weight of the polymer responded to changes in the amount of the redox initiator as would be expected for a typical reverse ATRP process.

The kinetic plots for the different initiator concentrations are shown in Figure 4-4b. The plots are first order with respect to monomer consumption up to approximately 70% conversion, except for the high initiator experiment (exp 10) which shows curvature for the entire duration of the polymerization. The k^{app} for the high (exp 10), medium (exp 7), and low (exp 9) initiator concentrations were $8.0\times10^{-5}s^{-1}$, 7.5×10^{-5} s^{-1} and $7.8\times10^{-5}s^{-1}$, respectively. The expected trend of increased polymerization rate with increased initiator concentration, due to the increase in the number of polymer chains in combination with the increase in the ratio of copper(I) complex to copper(II) complex (eq 1), was not observed. Contrary to this expected trend, when based on the k^{app} per polymer chain (eq 3, Table 4-2) the rate increased as the amount of the initiator decreased. The reason for this is unknown, but the results are consistent with the observations from the high-molecular weight set of experiments (exp 5, exp 7, exp 9).

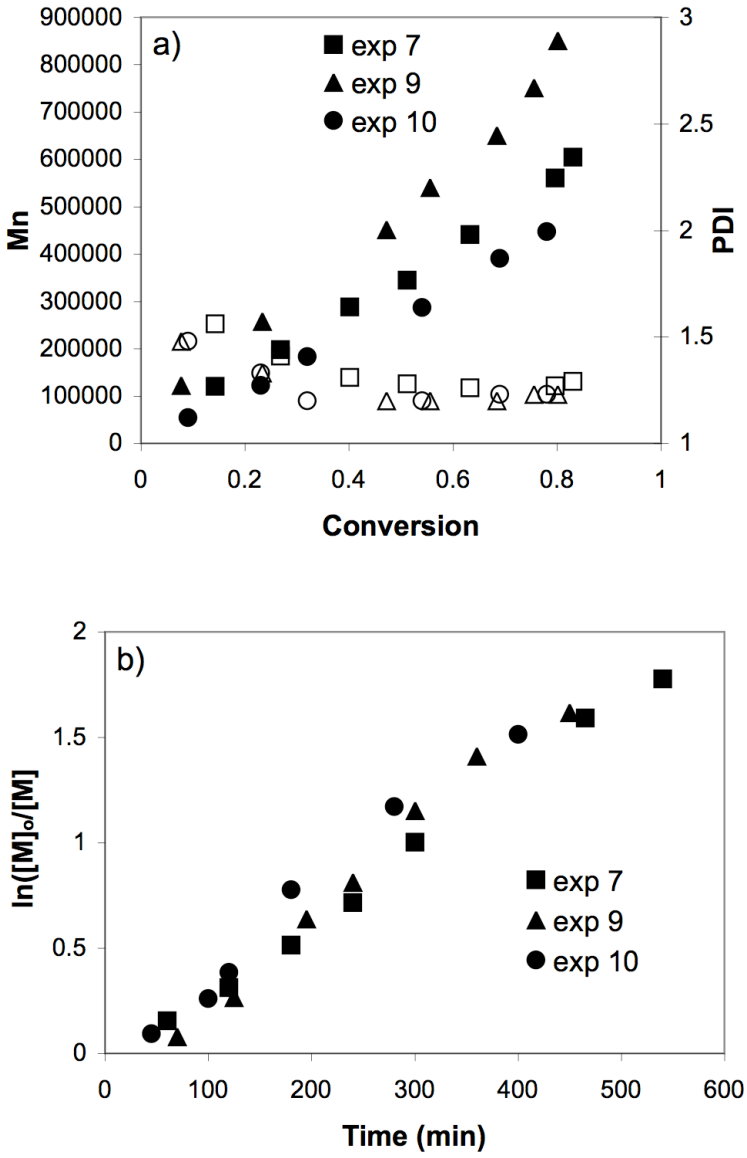

Figure 4-4. The effect of the amount HPO/AA on the evolution of M_n (filled symbols) and PDI (open symbols) with conversion (a) and the kinetic plots (b) for the reverse ATRP of BMA

exp 7: $[CuBr_2\text{-}EHA_6TREN]_0:[HPO]_0:[AA]_0 = 1:0.5:0.25$;

exp 9: $[CuBr_2\text{-}EHA_6TREN]_0:[HPO]_0:[AA]_0 = 1:0.4:0.2$;

exp 10: $[CuBr_2\text{-}EHA_6TREN]_0:[HPO]_0:[AA]_0 = 1:0.6:0.3$.

4.5.5 Reverse ATRP of MMA initiated with HPO/AA

A similar study was carried out with MMA, with the total solids content maintained at 15 wt%. Figure 4-5 is a plot of the M_n and PDI vs conversion. The molecular weight increased linearly with conversion, while the PDI remained relatively low, with no low-molecular weight tail in the SEC trace. The M_n ranged from 333 400 - 629 200, depending on the conditions of the polymerization (Table 4-1). From Table 4-2, the number of polymer chains for the MMA polymerizations were similar to their BMA

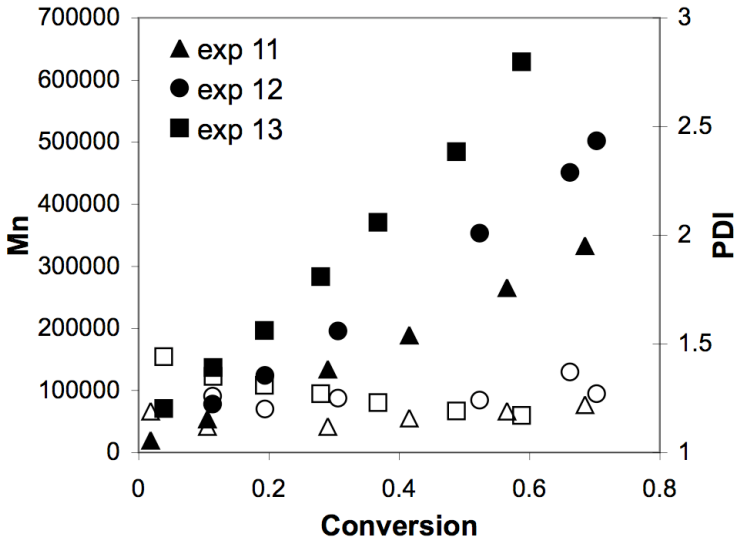

Figure 4-5. The effect of varying the $[MMA]_0$:$[CuBr_2$-$EHA_6TREN]_0$ ratio. Evolution of M_n (filled symbols) and PDI (open symbols) with conversion for the reverse ATRP of MMA

exp 11: $[MMA]_0$:$[CuBr_2$-$EHA_6TREN]_0$ = 800:1;
exp 12: $[MMA]_0$:$[CuBr_2$-$EHA_6TREN]_0$ = 1136:1;
exp 13: $[MMA]_0$:$[CuBr_2$-$EHA_6TREN]_0$ = 1685:1.

counterpart (exp 7 and 12, exp 8 and 13), as well, the initiator efficiency was approximately 0.3 moles of growing polymer chains per mole of HPO. The use of MMA resulted in some coagulum formation during the polymerization, ranging from 5-9 wt% based on total solids. The final particle diameter distribution was monomodal and the resulting latex showed no further instability after 3 weeks on the shelf. Compared to BMA, the polymerizations had lower final conversions (typically 70%), attributed in part to the coagulum formation that would cause the measured conversion to be lower than the actual conversion.

4.6 Conclusions

The miniemulsion reverse ATRP using $CuBr_2$-EHA_6TREN as the mediating complex and HPO/AA as the initiator has been carried out for BMA and MMA. The use of the HPO/AA redox pair as the initiator enables the production of well-controlled polymers with M_n ranging from 300 000 to 1000 000. A polymer with M_n of 989 900 and a PDI of 1.25 can be produced in approximately 8 hours of reaction time at 60^oC. The origin of the high-molecular weight polymers is currently unknown, however, the polymerizations behave like a typical reverse ATRP system. Kinetic analyses suggest the HPO/AA system provides an advantageous ratio of [Cu(I)]/[Cu(II)] compared to conventional initiators. The molecular weight of the polymer can be controlled by varying the initial amount of initiator (HPO/AA), as well, the desired molecular weight can be predetermined by selecting the initial ratio of monomer to $[CuBr_2$-$EHA_6TREN]_0/[HPO]_0/[AA]_0$.

The kinetics of HPO/AA initiated reverse ATRP appear to be complex. The overall rates of the polymerizations initiated with HPO/AA were similar to the VA-044 initiated polymerizations. However, when the k^{app} was based on the number of polymer chains in the system there was a greater 5-fold increase in the rate of the HPO/AA initiated polymerization compared to the VA-044 initiated polymerization. As well, there appears to be a trend of increasing k^{app} when the number of chains in the system decreased. This includes the set of experiments where the amount of HPO/AA was increased while the amount of $CuBr_2$-EHA_6TREN remained constant, for which the opposite trend was expected.

The latexes had weight-average particle diameters typically less than 110 nm. All of the final particle diameter distributions were monomodal and the resulting latex showed no further instability after 3 weeks on the shelf. The formation of coagulum was minimal during the polymerization of BMA (less than 2 wt% based on total solids), while the polymerization of MMA resulted in coagulum formation that ranged between 5-9 wt% based on total solids.

4.7 References

1. Kato, M.; Kamigaito, M.; Sawamoto, M.; Higashimura, T. *Macromolecules* **1995**, *28*, 1721.
2. Wang, J. –S.; Matyjaszewski, K. *J. Am. Chem. Soc.* **1995**, *117*, 5614.
3. Matyjaszewski, K.; Xia, J. *Chem. Rev.* **2001**, *101*, 2921.
4. Kamigaito, M.; Ando, T.; Sawamoto, M. *Chem. Rev.* **2001**, *101*, 3689.
5. Xue, L.; Agarwal, U. S.; Lemstra, P. J. *Macromolecules* **2002**, *35*, 8650.

6. Mao, B. W.; Gan, L. H.; Gan, Y. Y. *Polymer* **2006**, *47*, 3017.
7. Matyjaszewski, K.; Shipp, D. A.; Qiu, J.; Gaynor, S. G. *Macromolecules* **2000**, *33*, 2296.
8. Qiu, J.; Pintauer, T.; Gaynor, S. G.; Matyjaszewski, K.; Charleux, B.; Vairon, J. *Macromolecules* **2000**, *33*, 7310.
9. Li, M.; Matyjaszewski, K. *J. Polym. Sci., Part A: Polym. Chem.* **2003**, *41*, 3606.
10. Li, M.; Matyjaszewski, K. *Macromolecules* **2003**, *36*, 6028.
11. Li, M.; Min, K.; Matyjaszewski, K. *Macromolecules* **2004**, *37*, 2106.
12. Li, M.; Jahed, N. M.; Min, K.; Matyjaszewski, K. *Macromolecules* **2004**, *37*, 2434.
13. Min, K.; Gao, H.; Matyjaszewski, K. *J. Am. Chem. Soc.* **2005**, *127*, 3825.
14. Cunningham, M. F. *Prog. Polym. Sci.* **2002**, *27*, 1039-1067.
15. Qiu, J.; Charleux, B.; Matyjaszewski, K. *Prog. Polym. Sci.* **2001**, *26*, 2083.
16. Simms, R. W.; Cunningham, M. F. *J. Polym. Sci., Part A: Polym. Chem.* **2006**, *44*, 1628.
17. Wang, J. –S.; Matyjaszewski, K. *Macromolecules* **1995**, *28*, 7572.
18. Xia, J.; Matyjaszewski, K. *Macromolecules* **1997**, *30*, 7692.
19. Zhu, S.; Wang, W.; Tu, W.; Yan, D. *Acta Polym.* **1999**, *50*, 267.
20. Qin, D. –Q.; Qin, S. –H.; Qiu, K. –Y. *Macromolecules* **2000**, *30*, 6987.
21. Klee J. E.; Neidhart F.; Flammersheim H. –J.; Mülhaupt, R. *Macromol. Chem. Phys.* **1999**, *200*, 517.
22. Zeng, F.; Shen, Y.; Zhu, S.; Pelton, R. *Macromolecules* **2000**, *33*, 1628.
23. Qiu, J.; Gaynor, S. G.; Matyjaszewski, K. *Macromolecules* **1999**, *32*, 2872.

24. Matyjaszewski, K.; Qiu, J.; Tsarevsky, N. V.; Charleux, B. *J. Polym. Sci., Part A: Polym. Chem.* **2000**, *38*, 4724.

25. Jousset, S.; Qiu, J.; Matyjaszewski, K.; Granel, C. *Macromolecules* **2001**, *34*, 6641.

26. Peng, H.; Cheng, S.; Feng, L. *J. Appl. Polym. Sci.* **2003**, *89*, 1542.

27. Peng, H.; Cheng, S.; Feng, L.; Fan, Z. *J. Appl. Polym. Sci.* **2003**, *89*, 3175.

28. Deutsch, J. C. *Anal. Biochem.* **1998**, *255*, 1.

29. Jakubowski, W.; Matyjaszewski, K. *Macromolecules* **2005**, *38*, 4139.

30. Min, K.; Gao, H.; Matyjaszewski, K. *J. Am. Chem. Soc.* **2005**, *127*, 3825.

31. Min, K.; Matyjaszewski, K. *Macromolecules* **2005**, *38*, 8131.

32. Jakubowski, W.; Min, K.; Matyjaszewski, K. *Macromolecules* **2006**, *39*, 39.

33. Moad, G.; Solomon, D. H. *The Chemistry of Free radical Polymerization;* Elsevier Science Inc.: New York, 1995.

34. Wang, W.; Yan, D.; Jiang, X.; Detrembleur, C.; Lecomte, P.; Jérôme, R. *Macromol. Rapid Commun.* **2001**, *22*, 439.

35. Xia, J.; Matyjaszewski, K. *Macromolecules* **1999**, *32*, 5199.

36. Matyjaszewski, K.; Patten, T. E.; Xia, J. *J. Am. Chem. Soc.* **1997**, *119*, 674.

37. Zhang, H.; Klumperman, B.; Ming, W.; Fischer, H.; Linde, R. v. d. *Macromolecules* **2001**, *34*, 6169.

38. Tang, W.; Tsarevsky, N. V.; Matyjaszewski, K. *J. Am. Chem. Soc.* **2006**, *128*, 1598.

39. Fischer, H. *Chem. Rev.* **2001**, *101*, 3581.

40. Shipp, D. A.; Matyjaszewski, K. *Macromolecules* **1999**, *32*, 2948.

41. Torii, H.; Fujimoto, K.; Kawaguchi, H. *J. Polym. Sci., Part A: Polym. Chem.* **1996**, *34*, 1237.

42. Luo, Y.; Tsavalas, J.; Schork, F. J. *Macromolecules* **2001**, *34*, 5501.

CHAPTER 5

5 Compartmentalization of Atom Transfer Radical Polymerization in Miniemulsion

5.1 Preface

The ability to easily control the particle size in miniemulsion ATRP and the ability to make high molecular weight polymers allowed for an investigation into confined space effects. To identify confined space affects you need to be able to systematically vary the size of the particle and observe what (if any) influence there is on the kinetics or degree of control over the polymerization. It was important to target high molecular weight polymers because this allowed for the number of chains and the persistent radical species ($CuBr_2$-EHA_6TREN) to be limited in each particle. (Another way to limit the amount of reactants would be to reduce the particle size to diameters less than 100 nm, but going to smaller and smaller particle sizes in ATRP become increasing difficult due to issues of latex stability and control of the polymerization.) Confined space effects, also known as compartmentalization in radical polymerization, have two distinct consequences in a radical polymerization. First, the segregation of the radicals in different particles prevents mutual termination, with the degree of segregation increasing as the particle size decreases. Second, the size of the particle influences the reaction rate between radicals, with smaller particles increasing the reaction rate. The experiments show that confined space effects are present in miniemulsion ATRP, observed by a decrease the polymerization rate and improved control over the polymerization as the particle size decreases.

5.2 Abstract

Compartmentalization of an ATRP system was found to reduce the overall polymerization rate and improve the control over the polymerization. Both the particle size and the number of polymer chains contained in the particle are important parameters to control when formulating an ATRP system that exhibits compartmentalization effects. It was determined that a particle size of less than 200 nm is sufficiently small to affect ATRP provided that each particle contains less than ~ 4000 polymer chains because compartmentalization requires that the reactants (active polymeric radicals and $CuBr_2$-EHA_6TREN) be limited by the volume of the particle. The difference between a conventional free radical polymerization and ATRP are highlighted by the opposing impact that compartmentalization has on the kinetic of the polymerizations. In a conventional system it is the segregation effects that cause an increase in the polymerization rate, while the confined space effect dominates the kinetics in ATRP.

5.3 Introduction

Progress in living/controlled radical polymerization (L/CRP) conducted in aqueous based systems has highlighted the significant differences of L/CRP conducted in bulk versus (mini)emulsion, and between conventional free radical (mini)emulsion and CRP (mini)emulsion systems. To effectively perform an aqueous based L/CRP it is important to determine the suitability of the controlling species and initiator (phase partitioning, stability) and the potential influence of the CRP mechanism on the kinetics of the polymerization, particle nucleation, radical entry and exit from the particle, and stability of the latex. [1,2] For CRP based on the reversible termination mechanism of control, atom transfer radical polymerization (ATRP)[3-11] and nitroxide-mediated polymerization (NMP),[12-17] a complete understanding of the kinetics has been concealed by the complexity of the system. Most notably is whether conducting ATRP/NMP in a small reaction volume can result in compartmentalization and to what degree it will influence the system.

Compartmentalization in conventional free radical polymerizations dramatically increases the rate of the (mini)emulsion polymerization and the molecular weight of the polymer compared to its bulk counterpart. This is a consequence of the segregation effect in compartmentalization, in which radicals in different particles are unable to mutually terminate, decreasing the termination rate and therefore increasing the overall polymerization rate of the system. Another important aspect of compartmentalization is the confined space effect, where the reaction rate between two radicals in the same particle increases with decreasing particle volume.[18]

Under the right conditions compartmentalization has been identified in CRP based on reversible transfer reactions (reversible addition fragmentation transfer (RAFT) and macromolecular design via interchange of xanthates (MADIX)) by an increase in the polymerization rate with decreasing particle size.[19-23] The influence of compartmentalization in RAFT/MADIX is similar to a conventional free radical polymerization because of the mechanistic similarity of the two techniques. The mechanism of control in an ideal RAFT/MADIX process maintains the same population of free radicals as the conventional free radical polymerization, and both techniques involve the steady release of primary radicals from an initiator source for the duration of the polymerization. Therefore, under the right conditions, small reaction volumes in a RAFT/MADIX system result in segregated propagating radicals leading to the reduced termination of propagating polymer chains and an increase in the overall polymerization rate.

While compartmentalization is present in RAFT/MADIX, it has been generally accepted that in reversible termination systems (ATRP/NMP) compartmentalization does not exist because of the method of controlling the polymerization in these techniques. The polymer chains are reversibly terminated through repeated activation/deactivation cycles, with the vast majority of chains being in the dormant state at any one time. Compared to a conventional free radical polymerization, the probability of mutual termination in ATRP is kept to a minimum because the concentration of active radical species is maintained at a very low level, dictated by the ATRP equilibrium (determined by the ATRP equilibrium constant K_{eq}, Equation 5-1) that is established in the system. Another particular aspect of ATRP is that after the initiation period at the start of the

polymerization (in which all the polymer chains are formed) there are no primary (short chain) radicals in the system (excluding transfer reactions and thermally generated radicals) so that radical entry and exit are of minimal importance. Therefore, ATRP should behave as a pseudo-bulk system because the very low concentration of active radicals coupled with no short chain radicals (entry/exit effects) means that the size of the particle should not influence the system.

$$K_{eq} = \frac{[\text{active radicals}][\text{deactivator}]}{[\text{dormant chains}][\text{activator}]} \qquad (5\text{-}1)$$

A limited number of modeling studies of NMP that suggest under the right set of conditions compartmentalization may occur, although the effect on systems are not all in agreement. Charleux considered the segregation of propagating radicals, using a Smith-Ewart approach for the model that predicted faster rates of polymerization for smaller particle sizes.[24] Butte *et al.*[25] accounted for the segregation of the nitroxide as well as the propagating radicals and concluded that the polymerization rate would decrease in smaller particles, which was expanded on by Zetterlund and Okubo.[26] The size of the particle has been reported to influence NMP in miniemulsion, due to interfacial effects on the system.[27] Recently, experimental evidence for compartmentalization in miniemulsion NMP has been reported by Maehata *et al.*[28] who found that decreasing the particle size resulted in lower rates of polymerization and superior livingness of the polymer chains.

A theoretical study on compartmentalization in ATRP predicted that at sufficiently small particle sizes compartmentalization should cause a decrease in the polymer chain termination rate and an increase in the ATRP deactivation rate, leading to better control and lower polymerization rates.[29] The present paper provides experimental evidence of particle size effects in ATRP conducted in miniemulsion that influence the

rate and control of the polymerization. It was found that particles with diameters in the 100-200 nm range are small enough to cause the system to be compartmentalized, provided that the number of propagating polymer chains in each particle is sufficiently low that compartmentalization can influence the concentration of active radicals in the particle.

5.4 Experimental

Materials. n-Butyl methacrylate (BMA, 99%, Aldrich) and 2-ethylhexyl acrylate (98%, Aldrich) were purified by passing each through a column packed with inhibitor remover (Aldrich). The compounds copper(II) bromide ($CuBr_2$, 99%, Aldrich), tris(2-aminoethyl)amine (96%, Aldrich), cetyltrimethylammonium bromide (CTAB, Aldrich), hexadecane (99%, Aldrich), ascorbic acid (AA, 99%, Aldrich), hydrogen peroxide (HPO, 3 wt% in water, Aldrich), basic alumina (Aldrich), and 2,2′-azobis[2-(2-imidazolin-2-yl)propane] dihydrochloride (VA-044, Wako Chemicals) were used as received. The synthesis of tris[2-di(2-ethylhexyl acrylate)aminoethyl]amine (EHA_6TREN) was adapted from literature methods.[30, 31]

Miniemulsion Polymerization. In a typically experiment, the organic phase was prepared by adding $CuBr_2$ (0.0766 g, 3.43×10^{-4} mol), EHA_6TREN (0.4399 g, 3.51×10^{-4} mol), hexadecane (1.48 g, 3.8 wt% vs. monomer) and BMA (39 g, 0.274 mol, 15 wt% vs. deionized water) to a beaker and stirring overnight at room temperature to form a homogeneous solution. The aqueous phase that consisted of the surfactant CTAB (1.17 g, 3 wt% vs. BMA) and deionized water (221 g) was stirred overnight at room temperature. The organic phase was added to the surfactant solution and stirred for approximately 30

min prior to passing through a Microfluidizer 110S (Microfluidics International Corporation) operating at an inlet pressure of 275 kPa. The miniemulsion (200 g) was transferred to a 500 mL round-bottom flask fitted with a condenser and was purged with ultra-high-purity nitrogen for 30 min before being immersed in a 90 ^{o}C oil bath with the magnetic stirring speed set to 250 rpm. Fifteen minutes elapsed before the addition of the initiator. The AA (0.0143 g, 1.65×10^{-4} mol) and HPO (0.1876 g of 3 wt% HPO, 8.12×10^{-5} mol) were added to separate Schlenk tubes, mixed with 2 mL of deionized water, and purged with ultra-high-purity nitrogen for 20 min prior to injection. Using a deoxygenated syringe, the HPO was added prior to the AA, which was added dropwise over 5 minutes. Samples were withdrawn with a deoxygenated syringe and placed in an ice bath. The polymer samples were dried under the air manifold overnight than placed in a vacuum overnight to remove all volatile compounds. All polymerizations were repeated to ensure reproducibility.

Characterization. After the polymerizations were complete the latexes were filtered (Fisherbrand P8 creped) to collect any coagulum. The amount of coagulum was determined gravimetrically (all experiments had less than 2 wt% coagulum). Monomer conversions were determined gravimetrically. Size exclusion chromatography (SEC) was used to measure the molecular weight distribution of the polymer samples. The dried polymer samples from the miniemulsion were dissolved in tetrahydrofuran (THF) and passed through a column packed with basic alumina to remove the residual copper. The SEC was equipped with a Waters 2960 separation module containing four Styragel columns (100, 500, 10^3, 10^4 Å) maintained at 40 ^{o}C, coupled with a Waters 410 differential refractive index detector and a Wyatt Technology DAWN EOS photometer

multi-angle light scattering (LS) detector (690 nm, 30 mW Ga-As laser). THF was used as the eluant and the flow rate was set to 1 $mL \cdot min^{-1}$. The LS detector was calibrated with toluene, normalized with 30 000 $g \cdot mol^{-1}$ narrow polystyrene standard and the data was processed using Astra (version 4.90.08) software. A d*n*/d*c* value of 0.075 was used for poly(butyl methacrylate) (PBMA).[32] There was good agreement between the refractive index (RI) data and the LS data up to ~ 400 000 $g \cdot mol^{-1}$, after which the RI data underestimated the molecular weight of the polymer (due to differences in the type of polymer used in the calibration and the samples). The particle sizes of the latexes were measured using a Matec Applied Sciences Capillary Hydrodynamic Fractionation (CHDF) 2000 unit. The UV detector was set to 220 nm. The eluant was a 20:1 mixture of deionized water/GR500-1X (Matec Applied Sciences). Samples were diluted with the eluant to approximately 3.5 wt% solids and sonicated for 5 minutes. Samples were passed through a 0.5 μm pore size filter prior to injection. The marker was a 2 wt% solution of sodium benzoate. To ensure that there were no particles greater than 0.5 μm the particle size distributions were also measured using a Malvern Mastersizer 2000 equipped with a Hydro 2000S optical unit. The refractive index value for water and PBMA were 1.33 and 1.48, respectfully.

Determining the number of radicals. The average number of free radicals per latex particle ($\bar{n}$) was calculated at approximately 30% conversion from the observed polymerization rate (as d(*fractional conversion*)/d*t*, d*x*/d*t*) and the calculated value of monomer concentration [M] using the following rate equation for an emulsion polymerization:[18]

$$\mathrm{d}x/\mathrm{d}t = k_p[\mathrm{M}]\bar{n}N_c \Big/ n_M^0 N_A \qquad (5\text{-}2)$$

where n_M^0 is the initial number of moles of monomer present, N_c is the number concentration of particles, N_A is Avogadro's constant, and the propagation rate coefficient k_p was calculated from the following equation: [33]

$$k_p = 10^{6.58} \exp\left(-22.9/RT\right) \qquad (5\text{-}3)$$

While $\bar{n}$ is an informative parameter used in conventional free radical emulsion systems, for an ATRP system the number of active radicals is dictated by the ATRP equilibrium, and is a function of the number of polymer chains present (Equation 5-1). Therefore, in an ATRP system the value of $\bar{n}$ would be a function of both the particle size and the number of polymer chains per particle (N_{chain}). For example, doubling the volume of a particle would double the value of $\bar{n}$ because N_{chain} also doubles, not due to any compartmentalization effect. To normalize the value of $\bar{n}$ against the number of polymer chains, the average number of radicals per particle per polymer chain ($\bar{n}_{chain}$) was calculated using the following equation:

$$\bar{n}_{chain} = \bar{n}/N_{chain} \qquad (5\text{-}4)$$

5.5 Results and Discussion

5.5.1 Effect of Particle Size on Miniemulsion ATRP.

The polymerization of BMA was carried out in miniemulsion using an ATRP process, mediated with $CuBr_2$-EHA_6TREN, and initiated by the redox pair HPO/AA. Previous work with this system produced high number-average molecular weight (M_n) polymers (up to M_n ~1 000 000 g·mol^{-1}) with a narrow polydispersity index (PDI < 1.25)

at relatively fast rates of polymerization (compared to typical ATRP).[32] In the present investigation, the effect of particle diameter (D_p) on the system was studied by using the cationic surfactant CTAB, with experiments that have surfactant loadings from 0.5-3 wt% based on monomer. Table 5-1 provides a summary of the essential experimental conditions and results.

In experiments 1-5 the effect of surfactant loading was investigated on identically formulated systems ($[BMA]_0/[CuBr_2\text{-}EHA_6TREN]_0/[HPO]_0/[AA]_0$ = 1270:1.6:1.0:0.5). There is a clear trend between the amount of surfactant and the D_p of the final latex (Table 5-1), ranging from 212 nm (expt 1, 0.5 wt% CTAB) to 119 nm (expt 5, 3 wt% CTAB), which correspond to a particle volume of 49.8×10^5 nm^3 and 8.8×10^5 nm^3, and a N_c of 3.5×10^{16} L_{water}^{-1} and 20.0×10^{16} L_{water}^{-1}, respectively.

Figure 5-1a plots M_n versus conversion, which illustrates the linear increase in the molecular weight with conversion, as well as, that the CTAB loading has no discernable effect on the molecular weight of the polymer (or on the number of polymer chains generated) since the evolution of M_n is consistent between experiments. The one exception is experiment 1, with a surfactant loading of 0.5 wt% CTAB, which has a lower M_n until about 60% conversion at which point there is an increase in M_n, where it obtains the same value as experiments 2-5. The comparatively poor control of the polymerization in experiment 1 is also evident in the *PDI* versus conversion plot (Figure 5-1b). The *PDI* reaches a minimum value of 1.39 at approximately 31% conversion, then increases with conversion reaching a value greater than 1.6 before ending at approximately 1.5. For experiments 2-5 the *PDI* has the expected trend of a well-controlled polymerization, which is to continually decrease with conversion (PDI ~1.25).

Table 5-1. Summary of Experiments for the Compartmentalization of ATRP

expt	CTAB (wt%)[b]	$[BMA]_0/[CuBr_2]_0/[HPO]_0/[AA]_0$	*conv*[c] (%)	M_n[d] (g·mol^{-1})	*PDI*[e]	D_p[f] (nm)	SD[g]	k^{app}[h] ($s^{-1}\times10^{-5}$)	N_c[i] ($\times10^{-16}$)	$\bar{n}$[j] ($\times10^{-3}$)	N_{chain}[k] ($\times10^{2}$)	$\bar{n}_{chain}$[l] ($\times10^{6}$)
1	0.5	1270 : 1.6 : 1 : 0.5	69	504700	1.52	212	94	17.2	3.5	59.1	41.4	12.2
2	1.0	1270 : 1.6 : 1 : 0.5	85	644400	1.29	176	48	19.2	6.0	24.2	23.6	10.3
3	2.0	1270 : 1.6 : 1 : 0.5	81	601200	1.20	142	50	9.7	11.4	5.7	12.6	4.5
4	2.0 + 1.0[m]	1270 : 1.6 : 1 : 0.5	73	511300	1.21	141	16	9.5	11.8	5.1	12.7	4.0
5	3.0	1270 : 1.6 : 1 : 0.5	68	496100	1.19	119	16	5.0	20.0	2.0	7.3	2.7
6	1.0	1270 : 1.3 : 1 : 0.5	84	605700	1.27	162	34	23.3	7.7	25.8	19.2	13.5
7	1.0	1270 : 1.0 : 1 : 0.5	82	584000	1.49	159	36	29.2	8.1	24.5	18.5	13.3
8	3.0	1270 : 1.3 : 1 : 0.5	85	684000	1.18	116	22	11.3	20.1	3.6	6.3	5.6
9	3.0	1270 : 1.0 : 1 : 0.5	79	652600	1.21	119	26	17.3	19.5	9.1	6.6	13.7
10	1.0	630 : 1.6 : 1 : 0.5	87	437600	1.42	172	67	20.5	6.4	22.4	33.1	6.8
11	2.0	630 : 1.6 : 1 : 0.5	89	441200	1.31	147	60	16.1	10.1	12.2	21.0	5.8

12	3.0	630 : 1.6 : 1 : 0.5	84	399000	1.18	130	28	14.0	12.0	6.7	15.0	4.5
13	1.0	1590 : 1.6 : 1 : 0.5	75	559300	1.33	155	38	13.0	8.7	15.6	16.4	9.5
14	2.0	1590 : 1.6 : 1 : 0.5	77	711300	1.20	131	27	7.8	14.7	5.5	7.8	7.1
15	3.0	1590 : 1.6 : 1 : 0.5	69	658200	1.18	117	22	5.4	20.1	2.3	5.4	4.3
16	2.5	400 : 1.0 : 0.32[n]	84	91980	1.32	146	25	20.7	10.4	19.5	93.5	2.1
17	0.5	400 : 1.0 : 0.32[n]	79	95240	1.35	196	45	21.7	4.4	44.8	202.3	2.3

[a] based on total monomer. [b] [hexadecane] = 3.8 wt% based on total monomer; 15% solid content. [c] *conv* = conversion, determined gravimetrically. [d] M_n = number-average molecular weight, determined from size exclusion chromatography. [e] *PDI* = polydispersity index, determined from size exclusion chromatography. [f] D_p = weight-average particle diameter, determined with capillary hydrodynamic fractionation (CHDF 2000). [g] SD = standard deviation of the weight-average particle diameter, determined with capillary hydrodynamic fractionation (CHDF 2000). [h] k^{app} = apparent rate constant. [i] N_c = number concentration (number density) of particles (particles·L_{water}^{-1}). [j] $\bar{n}$ = average number of radicals per latex particle (L_{water}^{-1}). [k] N_{chain} = average number of polymer chains per latex particle. [l] $\bar{n}_{chain}$ = average number of radicals per polymer chain (chain^{-1}·L_{water}^{-1}). [m] after passing the solution through the Microfluidizer to form the miniemulsion another 1 wt% CTAB was added to the system. [n] initiated with the azo compound 2,2′-azobis[2-(2-imidazolin-2-yl)propane] dihydrochloride (VA-044).

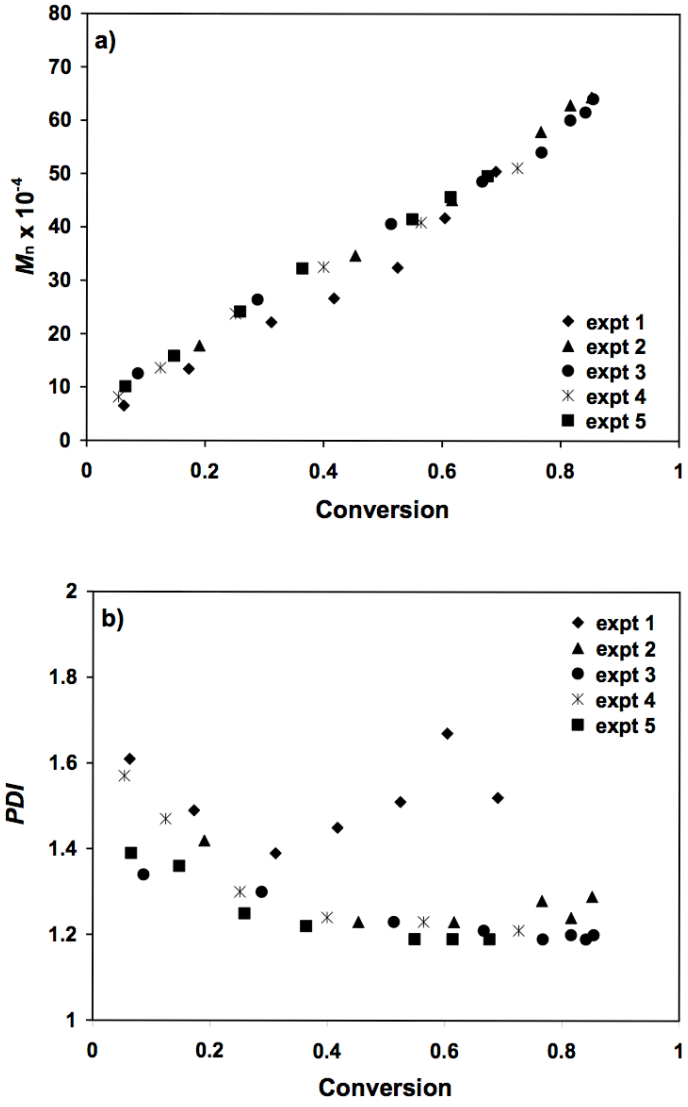

Figure 5-1. Evolution of (a) M_n and (b) *PDI* with conversion for the reverse ATRP of BMA in miniemulsion with varying amounts of CTAB.

expt 1: 0.5 wt% CTAB;

expt 2: 1 wt% CTAB;

expt 3: 2 wt% CTAB;

expt 4: 2+1 wt% CTAB;

expt 5: 3 wt% CTAB.

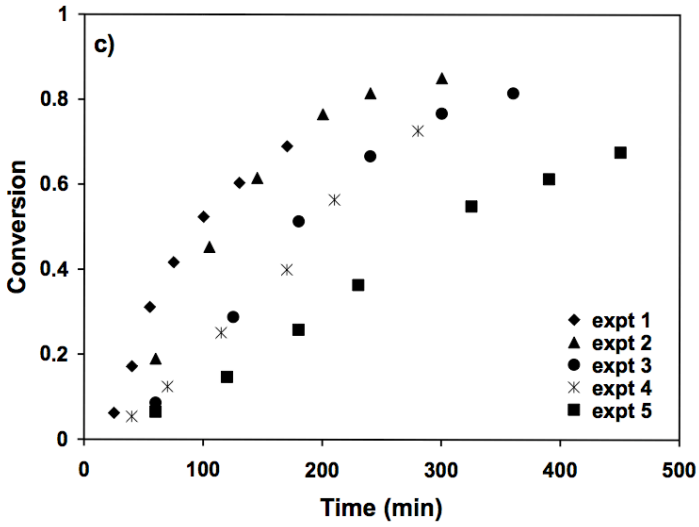

Figure 5-1. Conversion versus time profile (c) for the reverse ATRP of BMA in miniemulsion with varying amounts of CTAB.

expt 1: 0.5 wt% CTAB;
expt 2: 1 wt% CTAB;
expt 3: 2 wt% CTAB;
expt 4: 2+1 wt% CTAB;
expt 5: 3 wt% CTAB.

The poorer control of the polymerization in experiment 1 is believed to result from a decreased influence of compartmentalization, due to the large D_p for the system. This will be further explained later in the text.

It is evident from the conversion versus time plots shown in Figure 5-1c that there is a clear trend of decreasing polymerization rate (R_p) with an increased CTAB loading (decreasing particle size). Modeling of the basic reverse ATRP mechanism for solution/bulk systems, for which heterogeneous systems have typically adhered to, leads to the R_p defined in Equation 5-5. [34, 35, 36]

$$R_p = k_p[M][P^\bullet] = k_p[M]K_{eq}[chain][Cu(I)]/[Cu(II)] = k^{app}[M] \qquad (5\text{-}5)$$

$$\ln\left([M]_0/[M]\right) = k^{app}t \qquad (5\text{-}6)$$

From Equation 5-5 it is expected that the R_p should be consistent between the identically formulated experiments because k_p, [M], K_{eq}, concentration of $CuBr_2$-EHA_6TREN ([Cu(II)]), and concentration of CuBr-EHA_6TREN ([Cu(I)]) should be the same in all experiments. As well, the evolution of M_n with conversion is similar between the experiments, from which it is determined that the concentration of "living" polymer chains ([chain]) is constant among the experiments. The polymerization rates for this investigation are quantified with the apparent rate constant (k^{app}, Equation 5-6, Table 5-1), which has a range of 12.3×10^5 s^{-1} to 5.0×10^5 s^{-1} for a CTAB loading of 0.5 wt% and 3 wt%, respectively.

Experiment 4 was run to ensure that the effects on the polymerization were due to the variation in D_p, and not an unknown interaction with the CTAB. The conditions were identical to experiment 3, however, after passing the solution through the Microfluidizer to form the miniemulsion an additional 1 wt% CTAB was added to the system. This produced a similar D_p for experiment 3 (142 nm) and experiment 4 (141 nm) but with different CTAB loadings of 2 wt% and 3 wt%, respectively. As seen in Figure 5-1 and Table 5-1, the behavior of experiment 3 and experiment 4 are comparable, affirming that it is the D_p influencing the behavior of these systems.

Compartmentalization requires that the amount of a reactant is limited by the volume of the particle, which has two distinct consequences in a radical polymerization. The segregation of the radicals in different particles prevents mutual termination, with the degree of segregation increasing as the particle size decreases. The confined space effect

refers to the size of the particle influencing the reaction rate between radicals, with smaller particles increasing the reaction rate. For ATRP to exhibit compartmentalization the particle needs to be sufficiently small to limit the concentration of the persistent radical ($CuBr_2$-EHA_6TREN) and the active polymeric radical. The use of the initiation system HPO/AA, in experiments 2-5, produces polymers with high M_n (~ 600 000 g·mol^{-1} at 80% conversion) resulting in a range of N_{chain} from 2360 (expt 2) down to 730 (expt 5). The low concentration of polymer chains would limit the availability of both the active polymeric radicals and $CuBr_2$-EHA_6TREN, and coupled with the small D_p results in the observed compartmentalization effects.

It is the confined space effect on experiments 1-5 that causes the reduction in k^{app} with decreasing D_p of the system. To illustrate that the number of active radicals in the system is influenced by the size of the particle, the value of $\bar{n}_{chain}$ was calculated using Equation 5-4 and the data is summarized in Table 5-1. Excluding experiment 1 (due to its poor control), there is a trend of decreasing $\bar{n}_{chain}$ with D_p from experiment 2 ($\bar{n}_{chain}$ = 10.3×10^{-6} L_{water}^{-1}·chain^{-1}, D_p = 176 nm) through experiment 5 ($\bar{n}_{chain}$ = 2.7×10^{-6} L_{water}^{-1}·chain^{-1}, D_p = 119 nm), illustrating that the number of active radicals in the system is influenced by the D_p. The decrease in $\bar{n}_{chain}$ (and subsequently k^{app}) with decreasing D_p is caused by the confined space effect of compartmentalization, which increases the reaction rate between an active polymeric radical and $CuBr_2$-EHA_6TREN.

Previously, compartmentalization has not been seen in a miniemulsion ATRP because the large number of polymer chains in each particle meant that each particle operated as a “nanoreactor”, where the reaction in the particle is identical to that in a bulk system. To show that in a non-compartmentalized system k^{app} and $\bar{n}_{chain}$ are not

dependant on D_p, data from a previous report of miniemulsion ATRP was analyzed in which compartmentalization was not evident.[11] Experiment 16 and experiment 17 in Table 5-1 summarize the results of earlier work on a very similar system in which the azo initiator VA-044 was used instead of HPO/AA. With the exception of varying the amount of CTAB, the experiments were run under identical conditions with $[BMA]_0/[CuBr_2\text{-}EHA_6TREN]_0/[VA\text{-}044]_0$ = 400:1:0.32. The M_n reached a value of ~90 000 g·mol^{-1} at 80% conversion and increased linearly with conversion, while the *PDI* deceased with conversion reaching a final value less than 1.35. In experiment 16 the CTAB loading was 2.5 wt% producing a particle with a D_p of 146 nm with N_{chain} of 9350, where as the larger particle size in experiment 17 (0.5 wt% CTAB, D_p = 196 nm) had a value of N_{chain} = 20 230. The system shows no signs of compartmentalization, illustrated by the nearly identical k^{app} values of 20.7×10^5 s^{-1}and 21.7×10^5 s^{-1}, and $\bar{n}_{chain}$ of 2.1×10^{-6} L_{water}^{-1}·chain^{-1} and 2.3×10^{-6} L_{water}^{-1}·chain^{-1} for experiments 16 and 17, respectively. The relatively high value for N_{chain} and the subsequently high concentration of active polymeric radicals and $CuBr_2$-EHA_6TREN meant that the availability of the reactants were not limited by the volume of the particle and therefore compartmentalization was not present in this system.

The second important aspect of compartmentalization is the segregation of radical species limiting the occurrence of mutual termination. This would be expected to increase the rate of the polymerization because the number of living chains would remain at its maximum and the [$CuBr_2$-EHA_6TREN] would be minimized (Equation 5-5). The large decrease in the k^{app} with decreasing D_p observed experimentally shows that the effect of radical segregation on the kinetics is eclipsed by the confined space effect previously discussed. Radical segregation could manifest itself through improved control of the

polymerization, which would be seen experimentally as a decrease in the *PDI* of the polymer. As well, the increased rate of deactivation from the confined space effect would increase the number of activaton/deactivation cycles the polymer chains would undergo, contributing to a lower *PDI*. A comparison of experiment 1 and experiment 2, clearly depicts the influence that compartmentalization can have on the control of the polymerization. The poorly-controlled polymerization in experiment 1 had a D_p of 212 nm, which contained an average of 4140 polymer chains with an $\bar{n}_{chain}$ value of 12.2×10^{-6} $L_{water}^{-1}\cdot chain^{-1}$, resulting in an M_n that did not grow linearly with conversion and a final *PDI* of 1.52. The D_p in experiment 2 of 176 nm produces a particle with roughly half the volume of experiment 1, containing an average of 2360 chains in the particle with an $\bar{n}_{chain}$ value of 10.3×10^{-6} $L_{water}^{-1}\cdot chain^{-1}$; the well-controlled polymerization had a final PDI of 1.29. The trend of decreased $\bar{n}_{chain}$ and *PDI* with decreased D_p is continued for experiments 3-5 (Table 5-1).

The behavior of experiment 1 is not the typical result expected from the reduced influence of compartmentalization in an ATRP system, and necessitates further discussion. For a typical ATRP system that experiences compartmentalization effects (slower rate of polymerization, narrower *PDI*, higher percentage of "living" chains), as D_p increases the influence of compartmentalization diminishes until the polymerization proceeds as it would in bulk. As such, a system capable of producing a well-controlled polymerization in bulk, which was also well-controlled when the system is compartmentalized, is expected to be well-controlled in a dispersed system containing large particles. The initiation system for this investigation (HPO/AA) prevents the polymerization for being conducted in bulk, and attempts to create a stable latex with a

D_p larger than 212 nm in experiment 1 failed. However, a similar polymerization rate would indicate negligible compartmentalization effects, and occurs when comparing experiment 1 with experiment 2 (Figure 5-1c). Although the polymerization rates are similar, experiment 2 (D_p = 176 nm) exhibits the characteristic of a well-controlled polymerization, while in experiment 1 (D_p = 212 nm) the polymerization is poorly controlled. As outlined in the previous report, the $CuBr_2$-EHA_6TREN/AA/HPO system exhibits significantly faster rates of polymerization (k^{app}/total number of polymer chains) than a typical miniemulsion ATRP. The conclusion was that the HPO/AA system yields an advantageous ratio of [Cu(I)]/[Cu(II)] that allows the polymerization to proceed at higher polymerization rates, with the reasoning that the concentration of the deactivating species ($CuBr_2$-EHA_6TREN) was regulated to very low levels by the presence of the AA. With a relatively low concentration of $CuBr_2$-EHA_6TREN, the system may only be controlled when it is compartmentalized, which is what appears to be occurring is experiment 1-5. As well, for experiments 2-5 the low number of polymer chains, with N_{chain} ranging from 730 to 2400, coupled with the compartmentalization effects, could explain how the system is capable of producing well-controlled higher polymers of much higher M_n (400 000 – 1 000 000 g·mol^{-1}), than has previously been observed. Typically, for linear polymers produced by ATRP the M_n is limited to < 200 000 g·mol^{-1}, after which the effect of the radical side reactions (termination and transfer) become significant and the livingness of the system is decreased.[35, 37]

5.5.2 Effect of [$CuBr_2$-EHA_6TREN]$_0$.

Experiments 1-5 illustrated that compartmentalization reduces the overall polymerization rate and improved control of the polymerization by increasing the rate of deactivation in

the system. Experiments 6-9 (Table 1) were run to examine the effect of the $[CuBr_2\text{-}EHA_6TREN]_0$ on the system, with the other parameters kept constant. The first set of experiments was run at a CTAB loading of 1 wt% (Figure 5-2) and the second set of experiments was conducted at a CTAB loading of 3 wt% (Figure 5-3). The figures show that M_n (and therefore the number of polymer chains) is not affected by $[CuBr_2\text{-}EHA_6TREN]_0$, which is expected since $CuBr_2\text{-}EHA_6TREN$ should only deactivate propagating radicals and not influence the generation of primary radicals.

A CTAB loading of 1 wt% produced a D_p of 176 nm for experiment 2, and approximately 160 nm for experiments 6 and 7. The amount of $CuBr_2\text{-}EHA_6TREN$ was progressively reduced from experiment 2 ($[CuBr_2\text{-}EHA_6TREN]_0/[HPO]_0$ = 1.6:1) to experiment 6 ($[CuBr_2\text{-}EHA_6TREN]_0/[HPO]_0$ = 1.3:1) and finally experiment 7 ($[CuBr_2\text{-}EHA_6TREN]_0/[HPO]_0$ = 1:1). In each of the experiments, the M_n grew linearly with conversion, however, the effect of decreasing the $[CuBr_2\text{-}EHA_6TREN]_0$ could be seen in the evolution of the *PDI* (Figure 5-2a). With the lowest $[CuBr_2\text{-}EHA_6TREN]_0$, the *PDI* in experiment 7 obtains a relatively high minimum value of 1.39 at 62% conversion, before increasing to a final value of 1.49. The lower concentration of $CuBr_2\text{-}EHA_6TREN$ was expected to reduce the level of control over the polymerization.

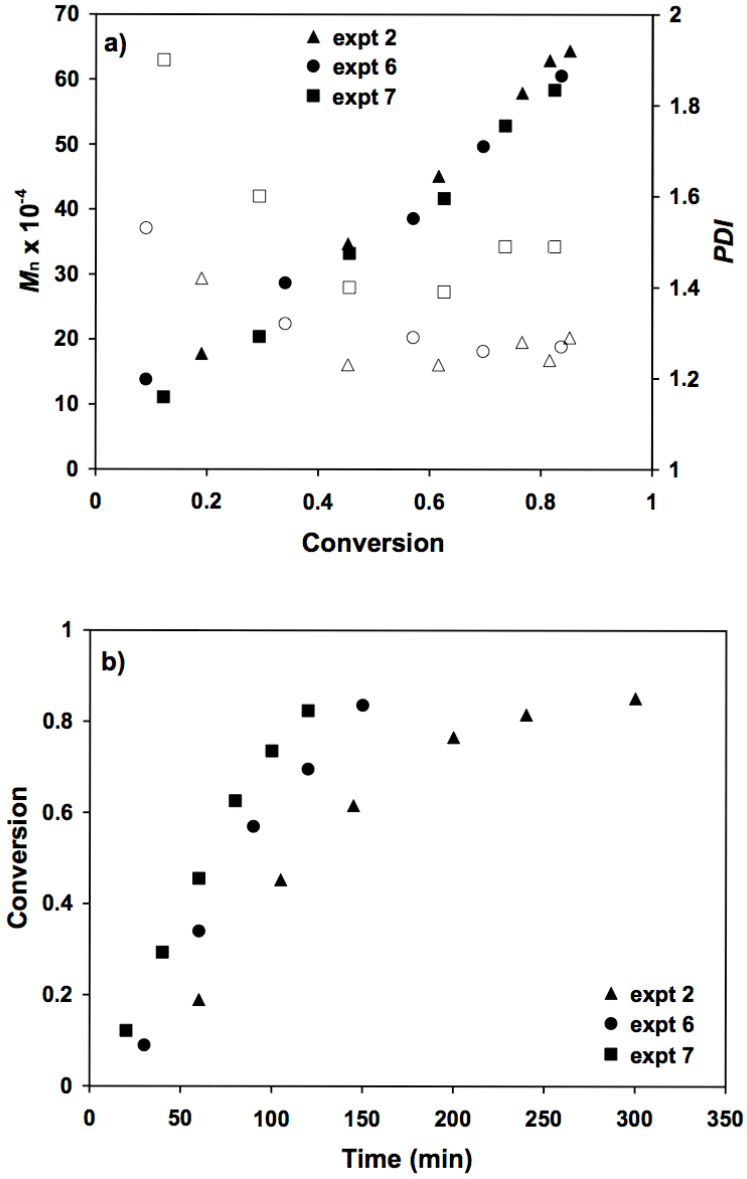

Figure 5-2. Evolution of (a) M_n and *PDI* with conversion and (b) conversion vs. time plots for the reverse ATRP of BMA in miniemulsion with 1 wt% CTAB, varying the $[(CuBr_2\text{-}EHA_6TREN)]_0$.

expt 2: $[BMA]_0/[CuBr_2\text{-}EHA_6TREN]_0/[HPO]_0/[AA]_0$ = 1270:1.6:1:0.5;

expt 6: $[BMA]_0/[CuBr_2\text{-}EHA_6TREN)]_0/[HPO]_0/[AA]_0$ = 1270:1.3:1:0.5;

expt 7: $[BMA]_0/[CuBr_2\text{-}EHA_6TREN]_0/[HPO]_0/[AA]_0$ = 1270:1:1:0.5.

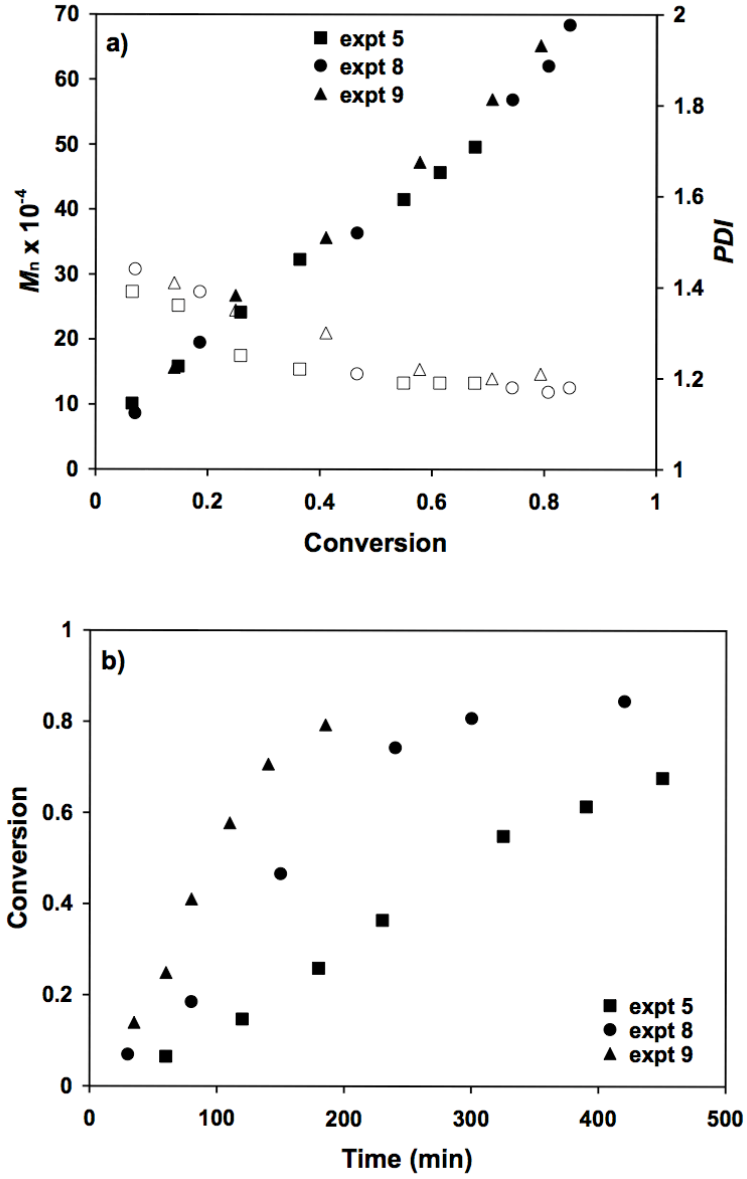

Figure 5-3. Evolution of (a) M_n and *PDI* with conversion and (b) conversion vs. time plots for the reverse ATRP of BMA in miniemulsion with 3 wt% CTAB, varying the $[CuBr_2\text{-}EHA_6TREN]_0$.

expt 5: $[BMA]_0/[CuBr_2\text{-}EHA_6TREN]_0/[HPO]_0/[AA]_0$ = 1270:1.6:1:0.5;

expt 8: $[BMA]_0/[CuBr_2\text{-}EHA_6TREN)]_0/[HPO]_0/[AA]_0$ = 1270:1.3:1:0.5;

expt 9: $[BMA]_0/[CuBr_2\text{-}EHA_6TREN]_0/[HPO]_0/[AA]_0$ = 1270:1:1:0.5.

An identical set of experiments was run with a CTAB loading of 3 wt%, which produced a D_p of approximately 119 nm. In experiment 5 ($[CuBr_2\text{-}EHA_6TREN]_0/[HPO]_0$ = 1.6:1), experiment 8 ($[CuBr_2\text{-}EHA_6TREN]_0/[HPO]_0$ = 1.3:1), and experiment 9 ($[CuBr_2\text{-}EHA_6TREN]_0/[HPO]_0$ = 1:1), the polymerization was well-controlled. Of significance is the comparison of the *PDI* evolution for experiment 7 (final *PDI* = 1.49) with experiment 9, in which the *PDI* decreases with conversion and obtains a final value of 1.21. The improved control of the polymerization in experiment 9 over experiment 7 is the result of an increased degree of compartmentalization in the system. The volume of a particle in experiment 9 (D_p = 119 nm) is approximately 2.4 times smaller than in experiment 7 (D_p = 159 nm). The resulting increased influence of compartmentalization can be seen in the lower N_{chain}, k^{app}, and $\bar{n}_{chain}$.

The difference in the degree of compartmentalization between the set of experiments with 1 wt% CTAB and 3 wt% CTAB is apparent from the conversion versus time profiles (Figure 5-2b and Figure 5-3b) and the magnitude of k^{app} (Table 5-1). The figures illustrate that with 3 wt% CTAB the polymerizations are significantly slower than the runs stabilized with only 1 wt% CTAB. This can also be seen comparing the k^{app}, which are greater for the 1 wt% CTAB experiments (19.2×10^5 s^{-1}, 23.3×10^5 s^{-1}, and 29.2×10^5 s^{-1} for experiments 2, 6 and 7, respectively) than the experiments conducted with 3 wt% CTAB (5.0×10^5 s^{-1}, 11.3×10^5 s^{-1}, and 17.3×10^5 s^{-1} for experiments 5, 8 and 9, respectively).

5.5.3 Effect of M_n (number of chains).

Since compartmentalization was argued to stem from the small particle size and the low number of polymer chains per particle (thereby limiting the concentration of active polymeric radicals and $CuBr_2$-EHA_6TREN) it was of interest to see what influence the number of chains (controlled by the target M_n) would have on the system. In the first set of experiments (expt 10-12) the number of polymer chains was increased by reducing the $[BMA]_0/[CuBr_2\text{-}EHA_6TREN]_0/[HPO]_0$ from 1270:1.6:1 to 630:1.6:1. The resulting decrease in M_n was slightly less than the factor of two expected (indicating a greater efficiency for chain initiation in expt 10-12). The plots of M_n and *PDI* are displayed in Figure 5-4a. All the polymerizations were controlled, with the M_n increasing linearly with conversion and the *PDI* remaining low. For experiment 10 (D_p = 172 nm, *PDI* = 1.42) and experiment 11 (D_p = 147 nm, *PDI* = 1.31) the *PDI* did increase with conversion after ~60% conversion and the final *PDI* was relatively high compared to experiment 12 (D_p = 130 nm, *PDI* = 1.18), a trend that is rationalized by compartmentalization. When the concentration of polymer chains in the system for experiments 10-12 (N_{chain} of 3310-1500) is increased from the levels in experiments 2-5 (N_{chain} of 2360-730), there is an increase in the final *PDI* of the polymer formed, with the exception of experiment 12 (3wt% CTAB). The *PDI* of 1.18 in experiment 12 confirms that the difference in the *PDI* for the experiments with a high concentration of polymer chain versus a low concentration of polymer chains cannot be attributed to the expected trend in an ATRP system of a decrease in *PDI* with higher M_n. Instead, the greater *PDI* is attributed to the higher N_{chain} that serves to reduce compartmentalization effects in the system. The most compelling evidence for this is seen in the small effect that the D_p has on the value of

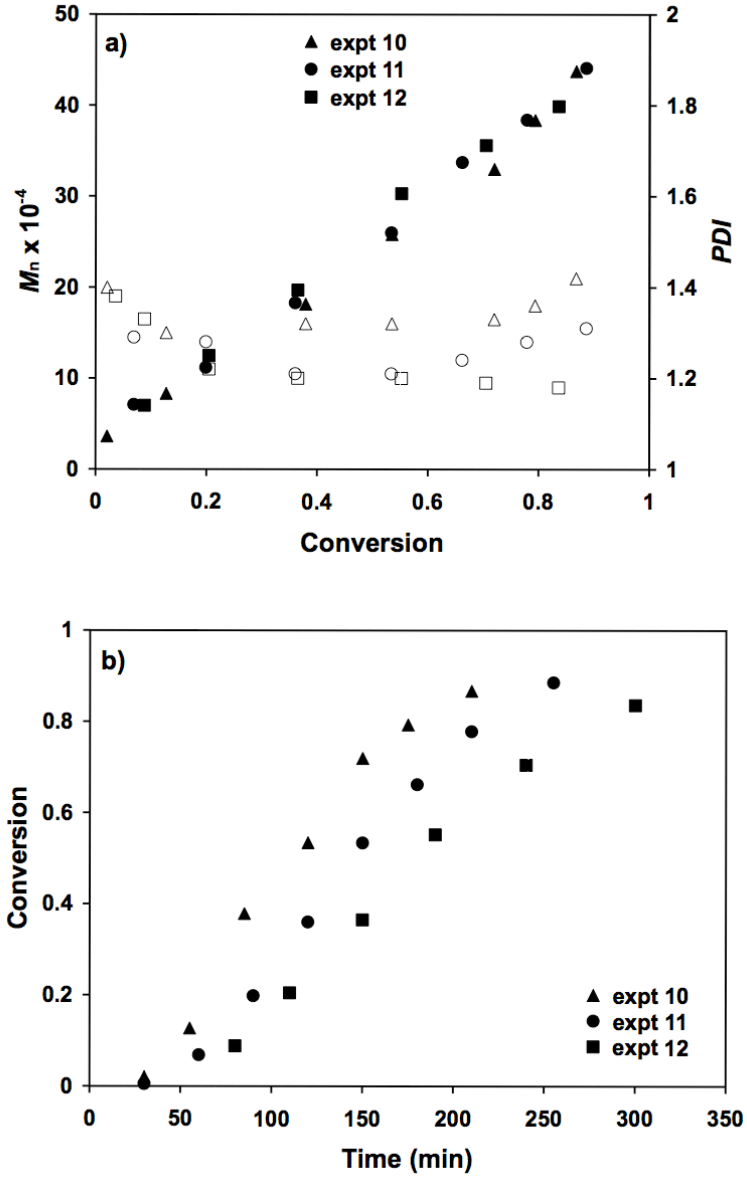

Figure 5-4. Targeting a low M_n (high number of polymer chains). Evolution of (a) M_n and *PDI* with conversion and (b) conversion vs. time plots for the reverse ATRP of BMA in miniemulsion with varying amounts of CTAB.

expt 10: 1 wt% CTAB;

expt 11: 2 wt% CTAB;

expt 12: 3 wt% CTAB.

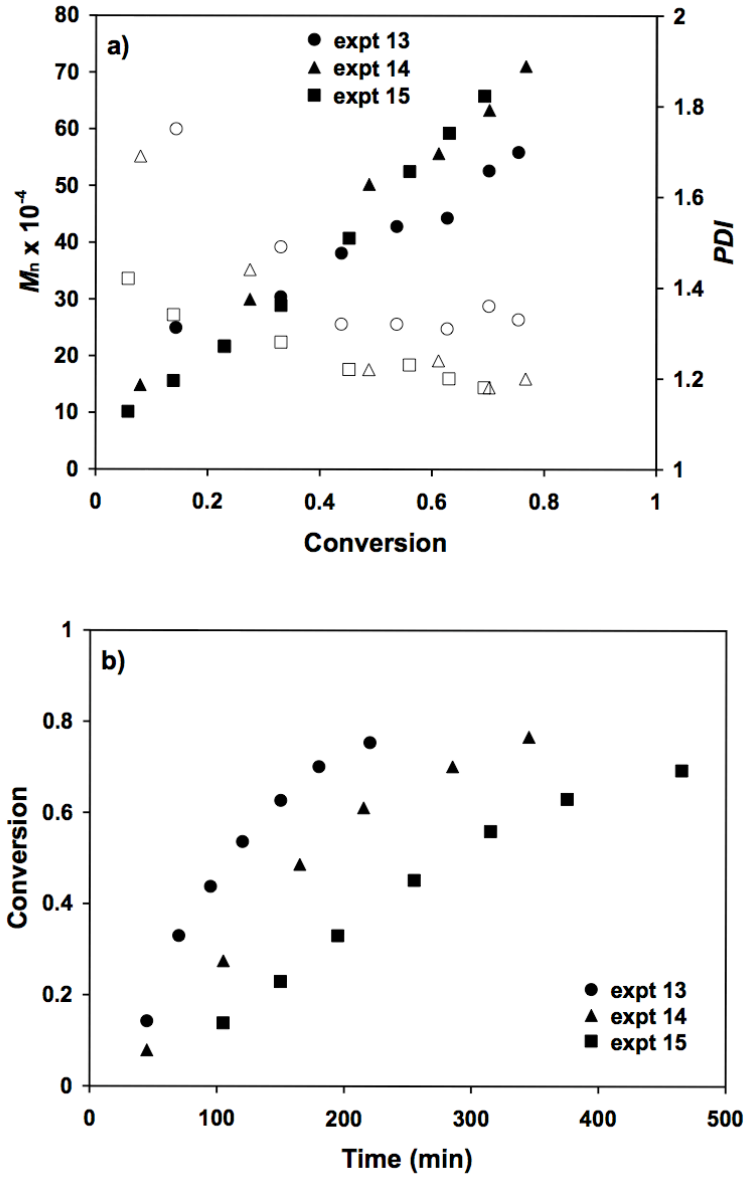

Figure 5-5. Targeting a high M_n (low number of polymer chains). Evolution of (a) M_n and *PDI* with conversion and (b) conversion vs. time plots for the reverse ATRP of BMA in miniemulsion with varying amounts of CTAB.

expt 13: 1 wt% CTAB;

expt 14: 2 wt% CTAB;

expt 15: 3 wt% CTAB.

$\bar{n}_{chain}$ (ranging from 6.8×10^{-6}-4.5×10^{-6} $L_{water}^{-1}\cdot chain^{-1}$) for experiment 10-12 compared with the large variation on $\bar{n}_{chain}$ (from 10.3×10^{-6}-2.7×10^{-6} $L_{water}^{-1}\cdot chain^{-1}$) for the system with a lower chain concentration (experiments 2-5). As well, the conversion vs time profiles of Figure 5-4b and the k^{app} values in Table 1 for experiments 10-12 have a significantly narrower range than the more compartmentalized systems of experiments 2-5.

If a higher concentration of reactants reduces the impact of compartmentalization, than a polymerization with a lower concentration of reactants would be expected to exhibit a greater influence from compartmentalization. In the set of experiments 13-15 the number of polymer chains was decreased by increasing the $[BMA]_0/[CuBr_2\text{-}EHA_6TREN]_0/[HPO]_0$ from 1270:1.6:1 to 1590:1.6:1, resulting in a proportional increase in M_n. From Figure 5-5a, the M_n increased linearly with conversion, and the *PDI* decreased with conversion. The expected compartmentalization trends are seen in the conversion versus time profiles in Figure 5-5b, which depicts the lower polymerization rate with decreasing D_p. As well, the kinetic data in Table 5-1 lists the decrease in k^{app} and $\bar{n}_{chain}$ with D_p. In agreement with the previous results, experiment 13, with the largest D_p (155 nm) exhibited the lowest control over the polymerization. Accompanying the relatively high *PDI* of 1.33 was also a large increase in molecular weight at the beginning of the reaction (M_n = 249 800 $g\cdot mol^{-1}$ at 14% conversion). After the initial increase, the M_n grew linearly with conversion, however, the final M_n (~560 000 $g\cdot mol^{-1}$ at 75% conversion) was significantly lower than in experiments 14 and 15 (M_n = ~ 700 000 $g\cdot mol^{-1}$ at 75% conversion). The large increase in M_n in the early stages of the polymerization suggests a lack of $CuBr_2$-EHA_6TREN to mediate the polymerization,

however with the same formulation, experiments 14 (2 wt% CTAB D_p = 131 nm) and 15 (3 wt% CTAB, D_p = 117 nm) show significantly better control over the polymerization. In the larger reaction volume of experiment 13 the $CuBr_2$-EHA_6TREN cannot effectively mediate the active radicals (that are at their peak concentration at the beginning of the polymerization), causing the polymerization to proceed rapidly, until enough chains have terminated that the [$CuBr_2$-EHA_6TREN] is sufficient to control the polymerization.

5.6 Conclusions

The results from these experiments have shown that compartmentalization can influence miniemulsion reverse ATRP under the right set of conditions. Both the particle size and the number of polymer chains contained in the particle are important parameters to control when formulating a compartmentalized ATRP systems. It was determined that a particle size of less than 200 nm is sufficiently small to affect ATRP provided that each particle contains less than ~ 4 000 polymer chains. The value of N_{chain} is important in miniemulsion ATRP because compartmentalization requires that the reactants (active polymeric radicals and $CuBr_2$-EHA_6TREN) be limited by the volume of the particle. This was confirmed when systems with N_{chain} > 10 000 and D_p between 150-200 nm, showed no evidence of compartmentalization, and explains why compartmentalization has not been previously seen in aqueous based ATRP system. Compartmentalization was found to reduce the overall polymerization rate by increasing the rate of deactivation due to the confined space effect, and compartmentalization was also found to improve the control over the polymerization and reduce the final *PDI* of the polymer.

The difference between a conventional free radical polymerization and ATRP is highlighted by the opposing impact that compartmentalization has on the kinetic of the polymerizations. In a conventional system it is the segregation effects that causes an increase in the polymerization rate, while it was determined that the confined space effect in ATRP that dominates the kinetics and causes the reduction in the polymerization rate. Decreasing the particle volume increases the reaction rate between an active polymeric radical and the persistent radical species, $CuBr_2$-EHA_6TREN, lowering the value $\bar{n}_{chain}$ and subsequently k^{app}.

Both radical segregation and the confined space effect of compartmentalization improve the control over the polymerization. Increased compartmentalization was shown to improve the linearity of growth for M_n with conversion, decrease the *PDI* of the polymer, and maintain better control of the polymerization during the early stage of the polymerization when the radical concentration is at its peak value.

5.7 References

1. Cunningham, M. F. *Prog. Polym. Sci.* **2002,** 27, 1039.
2. Qiu, J.; Charleux, B.; Matyjaszewski, K. *Prog. Polym. Sci.* **2001,** 26, 2083.
3. Matyjaszewski, K.; Shipp, D. A.; Qiu, J.; Gaynor, S. G. *Macromolecules* **2000,** 33, 2296.
4. Qiu, J.; Pintauer, T.; Gaynor, S. G.; Matyjaszewski, K.; Charleux, B.; Vairon, J. -P. *Macromolecules* **2000,** 33, 7310.
5. Li, M.; Matyjaszewski, K. *J. Polym. Sci., Part A: Polym. Chem.* **2003,** 41, 3606.
6. Li, M.; Matyjaszewski, K. *Macromolecules* **2003,** 36, 6028.

7. Li, M.; Min, K.; Matyjaszewski, K. *Macromolecules* **2004,** 37, 2106.
8. Li, M.; Jahed, N. M.; Min, K.; Matyjaszewski, K. *Macromolecules* **2004,** 37, 2434.
9. Min, K.; Gao, H.; Matyjaszewski, K. *J. Am. Chem. Soc.* **2005,** 127, 3825.
10. Kagawa, Y.; Zetterlund, P. B.; Minami, H.; Okubo, M. *Macromolecules* **2007,** 40, 3062.
11. Simms, R. W.; Cunningham, M. F. *J. Polym. Sci., Part A: Polym. Chem.*. **2006,** 44, 1628.
12. Farcet, C.; Lansalot, M.; Charleux, B.; Pirri, R.; Vairon, J. P. *Macromolecules* **2000,** 33, 8559.
13. Farcet, C.; Nicolas, J.; Charleux, B. *J. Polym. Sci., Part A: Polym. Chem.* **2002,** 40, 4410.
14. Pan, G. Sudol, E. D.; Dimonie, V. L.; El-Aasser, M. S. *Macromolecules* **2002,** 35, 6915.
15. Cunningham, M. F. *Comptes Rendus Chimie* **2003,** 6, 1351.
16. Pan, G.; Sudol, E. D.; Dimonie, V. L.; El-Aasser, M. S. *J. Polym. Sci., Part A: Polym. Chem.* **2004,** 42, 4921.
17. Saka, Y.; Zetterlund, P. B.; Okubo, M. *Polymer* **2007,** 48, 1229.
18. Gilbert R. G. *Emulsion Polymerization – A Mechanistic Approach*; Academic Press: New York, 1995.
19. Butte, A.; Storti, G.; Morbidelli, M. *Macromolecules* **2000,** 33, 3485.
20. Monteiro, M. J.; Hodgson, M.; De Brouwer, H. *J. Polym. Sci., Part A: Polym. Chem.* **2000,** 38, 3864.
21. Monteiro, M. J.; de Barbeyrac, J. *Macromolecules* **2001,** 34, 4416.

22. Butte, A.; Storti, G.; Morbidelli, M. *Macromolecules* **2001,** 34, 5885.

23. Prescott, S. W. *Macromolecules* **2003,** 36, 9608.

24. Charleux, B. *Macromolecules* **2000,** 33, 5358.

25. Butte, A.; Storti, M.; Morbidelli, M. *DECHEMA Monographs* **1998,** 134, 497.

26. Zetterlund, P. B.; Okubo, M. *Macromolecules* **2006,** 39, 8959.

27. Nakamura, T.; Zetterlund, P.B.Okubo, M. *Macromol. Rapid Commun.* **2006,** 27, 2014.

28. Maehata, H.; Buragina, C.; Keoshkerian, B.Cunningham, M.F. *accepted for publication in Macromolecules* **2007**.

29. Kagawa, Y.; Zetterlund, P. B.; Minami, H.; Okubo, M. *Macromol. Theory Simul.* **2006,** 15, 608.

30. Klee J. E.; Neidhart F.; Flammersheim H. –J.; Mülhaupt, R. *Macromol. Chem. Phys.* **1999,** 200, 517.

31. Zeng, F.; Shen, Y.; Zhu, S.; Pelton, R. *Macromolecules* **2000,** 33, 1628.

32. Simms, R. W.; Cunningham, M. F. *Macromolecules* **2007,** 40, 860.

33. Beuermann, S.; Buback, M.; Davis, T. P.; Gilbert, R. G.; Hutchinson, R. A.; Kajiwara, A.; Klumperman, B.; Russell, G. T. *Macromol. Chem. Phys.* **2000,** 201, 1355.

34. Matyjaszewski, K.; Patten, T. E.; Xia, J. *J. Am. Chem. Soc.* **1997,** 119, 674.

35. Matyjaszewski, K.; Xia, J. *Chem. Rev.* **2001,** 101, 2921.

36. Zhang, H.; Klumperman, B.; Ming, W.; Fischer, H.; van der Linde, R. *Macromolecules* **2001,** 34, 6169.

37. Kamigaito, M.; Ando, T.; Sawamoto, M. *Chem. Rev.* **2001,** 101, 3689.

CHAPTER 6

6 Nitroxide-Mediated Styrene Surfactant-Free Emulsion Polymerization

6.1 Preface

Although my research focused on ATRP there is enough similarity between the different types of living radical polymerizations to entice researchers to investigate all the techniques. When conducting aqueous based ATRP one of the limiting aspects of the technique is the partitioning of the metal complexes. One has to ensure that the ligand selected is hydrophobic enough to maintain the metal complex in the organic phase because that is where the polymerization occurs. A draw back to this is that the hydrophobic complexes are prevented from transferring across the water phase, preventing the easy adaptation of ATRP to a conventional emulsion system. Nitroxide-mediated systems do not have this constraint because nitroxides will preferential partition into the organic phase while still having sufficient water solubility to allow for transport across the aqueous phase. It was this aspect of nitroxide-mediated polymerizations, coupled with what I had learned while investigating aqueous based ATRP that led me to investigate and develop a surfactant-free, nitroxide-mediated, emulsion polymerization of styrene.

6.2 Abstract

A two-stage nitroxide-mediated surfactant-free polymerization of styrene mediated with SG1 and initiated by the thermal decomposition of the water-soluble initiator potassium persulfate (KPS) has been developed. Heterogeneity of the system broadens the molecular weight distribution, but control is shown by the linear increase in M_n with conversion, evolution of the entire molecular weight distribution, and successful chain extension with butyl acrylate. To stimulate the creation of micelles, the desired loci of polymerization, a multi-stage approach was adopted starting from dilute styrene/water solutions to favor the insitu formation of an SG1 alkoxyamine and short chain SG1-oligomers (stage one) before the addition of the majority of the styrene (stage two).

6.3 Introduction

Living/controlled radical polymerization (L/CRP) provides a facile route to the syntheses of polymers with complex microstructure and narrow molecular weight distributions, once the domain of living ionic polymerizations. The three techniques appearing most frequently in the literature are: reverse addition fragmentation chain transfer polymerization (RAFT),[1] atom transfer radical polymerization (ATRP)[2,3] and stable free radical polymerization (SFRP).[4] Irreversible termination reactions do occur in L/CRP, but the benefits include mild reaction conditions and a tolerance to impurities, including water, which is advantageous because it allows for aqueous based polymerizations.[5,6] Research in heterogeneous SFRP has focused primarily on two nitroxides; 2,2,6,6-tetramethylpiperidinyl-1-oxy (TEMPO) and *N*-*tert*-butyl-*N*-(1-diethylphosphono-2,2-dimethylpropyl) nitroxide (SG1). TEMPO is generally restricted to polymerization of styrenics above 120 ^{o}C, while SG1 has shown more versatility with the ability to control acrylates and styrenics[7] at temperatures as low as 90 ^{o}C.

The original attempts to conduct a nitroxide-mediated emulsion polymerization generally suffered from poor latex stability leading to severe coagulum, probably due to the method of particle nucleation and the partitioning of various species in the system. Adopting a miniemulsion approach allowed for a controlled polymerization in colloidally stable systems, and provided insight into the challenges associated with conducting heterogeneous SFRP.[5,8,9] Nevertheless, the ability to conduct SFRP in an emulsion is desirable because it simplifies the formulation by removing the need for a hydrophobe (which has to be removed from the final product) and the application of high shear to form the initial emulsion. Szkurhan and Georges[10] successfully developed an SFRP

emulsion process that bypasses the particle nucleation steps using a nanoprecipitation technique consisting of TEMPO-terminated oligomers of polystyrene in monomer-swollen particles. As well, considerable progress has been made by Charleux *et al*.[11-13] in developing an SFRP emulsion using a SG1-based water-soluble alkoxyamine. The multi-step emulsion polymerization starts with water-phase initiation of a seed latex (under microemulsion-like conditions) followed by a one-shot monomer addition. The process is capable of synthesizing well-controlled polymers of poly(n-butyl acrylate) and polystyrene, as well as diblock and triblock copolymers. A surfactant-free emulsion polymerization has also been reported using a SG1-terminated poly(sodium acrylate) water-soluble macroinitiator.[14] The batch process allowed for the synthesis of amphiphilic diblock copolymers of both styrene and butyl acrylate that formed stable latexes of hairy nanoparticles. Herein, we report the two-stage nitroxide-mediated surfactant-free polymerization of styrene mediated with SG1 and initiated by the thermal decomposition of the water-soluble initiator potassium persulfate (KPS).

6.4 Experimental

Materials. Potassium persulfate (KPS, Aldrich, > 99%), styrene (Aldrich, > 99%), *n*-butyl acrylate (Aldrich, > 99%), sodium bicarbonate ($NaHCO_3$, Aldrich, > 99.5%), potassium carbonate (K_2CO_3, Aldrich, 99%), and *N*-*tert*-butyl-*N*-(1-diethylphosphono-2,2-dimethylpropyl) nitroxide (SG1, supplied by Arkema, 89%) were all used as received.

Emulsion Polymerization. SG1(0.126 g, 4.27×10^{-4} mol) was added to 1.5 g of styrene and stirred for 10 minutes. The solution was transferred to a 250 mL round-bottom flask fitted with a condenser, containing KPS (0.068 g, 2.52×10^{-4} mol) and K_2CO_3 (0.026 g, 1.91×10^{-4} mol) dissolved in deionized water (90 g). The system was purged with ultra-high-purity nitrogen for 30 min before being immersed in a 90 ^{o}C oil bath with the magnetic stirring speed set to 650 rpm. After 3.5 hours elapsed an additional 8.5 g of deoxygenated styrene was added over 10 minutes. Samples were withdrawn with a deoxygenated syringe and placed in an ice bath. The polymer samples were dried under the air manifold overnight than placed in a vacuum overnight to remove all volatile compounds. All polymerizations were repeated to ensure reproducibility.

Chain Extension. At the completion of the emulsion polymerization the polymer was precipitated in methanol, filtered, washed, and dried under vacuum overnight. The SG1-terminated polymer was dissolved in butyl acrylate (~50 g) in a 100 mL round-bottom flask fitted with a condenser. The system was purged with ultra-high-purity nitrogen for 30 min before being immersed in a 90 ^{o}C oil bath with the magnetic stirring speed set to 300 rpm. After 2.5 hours the flask was removed from the oil bath and the solution cooled to room temperature prior to a sample taken.

Characterization. After the polymerizations were complete the latexes were filtered (Fisherbrand P8 creped) to collect any coagulum. The amount of coagulum was determined gravimetrically. Monomer conversions were determined gravimetrically. Size exclusion chromatography (SEC) was used to measure the molecular weight distribution

of the polymer samples. The SEC was equipped with a Waters 2960 separation module containing four Styragel columns (100, 500, 10^3, 10^4 Å) maintained at 40 ^oC, coupled with a Waters 410 differential refractive index (RI) detector. THF was used as the eluant and the flow rate was set to 1 $mL \cdot min^{-1}$. The RI detector was calibrated with narrowly distributed polystyrene standards ranging from 347-355 000 $g \cdot mol^{-1}$). The particle size was measured using a Matec Applied Sciences Capillary Hydrodynamic Fractionation (CHDF) 2000 unit. The UV detector was set to 220 nm. The eluant was a 20:1 mixture of deionized water/GR500-1X (Matec Applied Sciences). Samples were diluted with the eluant to approximately 3.5 wt% solids and sonicated for 5 minutes. Samples were passed through a 0.5 μm pore size filter prior to injection. The marker was a 2 wt% solution of sodium benzoate. To ensure that there were no particles greater than 0.5 μm the particle size distributions were also measured using a Malvern Mastersizer 2000 equipped with a Hydro 2000S optical unit. The refractive index value for water and polystyrene were 1.33 and 1.56, respectively.

6.5 Results and Discussion

A water-soluble alkoxyamine is formed by the thermal decomposition of KPS to sulfate radicals (and hydroxide radicals)[15] that propagate with the styrene dissolved in the aqueous phase, adding 1-2 styrene units before reversible termination by SG1.[10, 16] The bicomponent (KPS and SG1) system leads to an induction period that continues until the concentration of free SG1 is low enough to allow for a reasonable propagation rate of the alkoxyamine species. Subsequent propagation of the alkoxyamine reduces the water solubility of the oligomeric species, causing the amphiphilic chains to exhibit surfactant-

like behavior (i.e. the species are expected to reside at the organic/aqueous interface as well as form micelles). Once the number of styrene units exceeds a critical length, the chain will be rendered too hydrophobic to desorb into the aqueous phase.

Initial experiments were simple batch emulsion processes that resulted in poorly controlled polymerizations and unstable latexes. To stimulate the creation of micelles, the desired loci of polymerization, a multi-stage approach was adopted starting from dilute styrene/water solutions to favor the formation of the alkoxyamine and short chain SG1-oligomers (stage one) before the addition of the majority of the styrene (stage two). A series of experiments led to the formulation described in the experimental section that produced the well-controlled polymerization depicted in Figure 6-1. The particle distribution was monomodal and the weight-average particle diameter was 121± 21 nm, with ~5 wt% coagulum at the end of the polymerization. The particle sizes were confirmed with a Malvern Mastersizer 2000, which also demonstrated the absence of large particles in the system.

The conversion versus time plot shown in Figure 6-1a depicts an induction period of ~3.5 hours, where little conversion occurs. This corresponds to the first stage of the polymerization where 1.5 g of styrene ($[SG1]_0/[KPS]_0 = 1.5$; $[styrene]_0/[SG1]_0 = 38$) is dispersed in 90 g of water, and the dominant product is SG1-terminated oligomers (with less then 5 styrene units based on SEC analysis) presumably with primarily sulfate end groups. The polymerization proceeded rapidly after the addition of 8.5 g of styrene (stage two) at the 3.5 hour mark of the polymerization. The duration of the first stage corresponds roughly to the time required for the complete thermal decomposition of KPS at 90 ^{o}C.[15] Attempts at decreasing the allotted time for stage one resulted in poor behavior

of the polymerization and an unstable latex. Similarly, increasing the duration of the first stage to 8 hours had detrimental effects on the system. After 3.5 hours the conversion (of the 1.5 g of styrene) was less than 15%, but an additional 5.5 hours of reaction time yielded no further conversion. When stage one was run for 8 hours the second stage of the polymerization proceed very slowly, with a significantly higher number-average molecular weight (M_n), indicating that polymer chains were irreversibly terminated during the extended time of stage one.

Given the low conversion at the end of stage one, and that Szkurhan and Georges[10] were able to produce TEMPO-terminated styrene oligomers (with 1-2 units) from a styrene saturated aqueous solution of KPS and TEMPO, the effect of the $[\text{styrene}]_0/[\text{SG1}]_0$ ratio was investigated. Attempts were made at reducing the amount of styrene to ~0.2 g ($[\text{styrene}]_0/[\text{SG1}]_0 = 5$) which would saturate the aqueous phase with styrene but limit the presence of styrene droplets. This adversely affected the formation of the SG1-terminated oligomers and the polymerization, which proceeded slowly (or not at all) and produced high M_n (> 20 000 $g \cdot mol^{-1}$) at less than 10% conversion with significant coagulum formation. The situation was not improved by increasing the styrene content to 0.75 g ($[\text{styrene}]_0/[\text{SG1}]_0 = 19$), indicating that the excess styrene (forming monomer droplets in the system) may contribute to the successful formation of SG1-terminated oligomers. The process developed by Farcet *et al.*[16] used the KPS-SG1 bicomponent system to effectively initiate a nitroxide-mediated styrene miniemulsion (ie. in the presence of excess styrene).

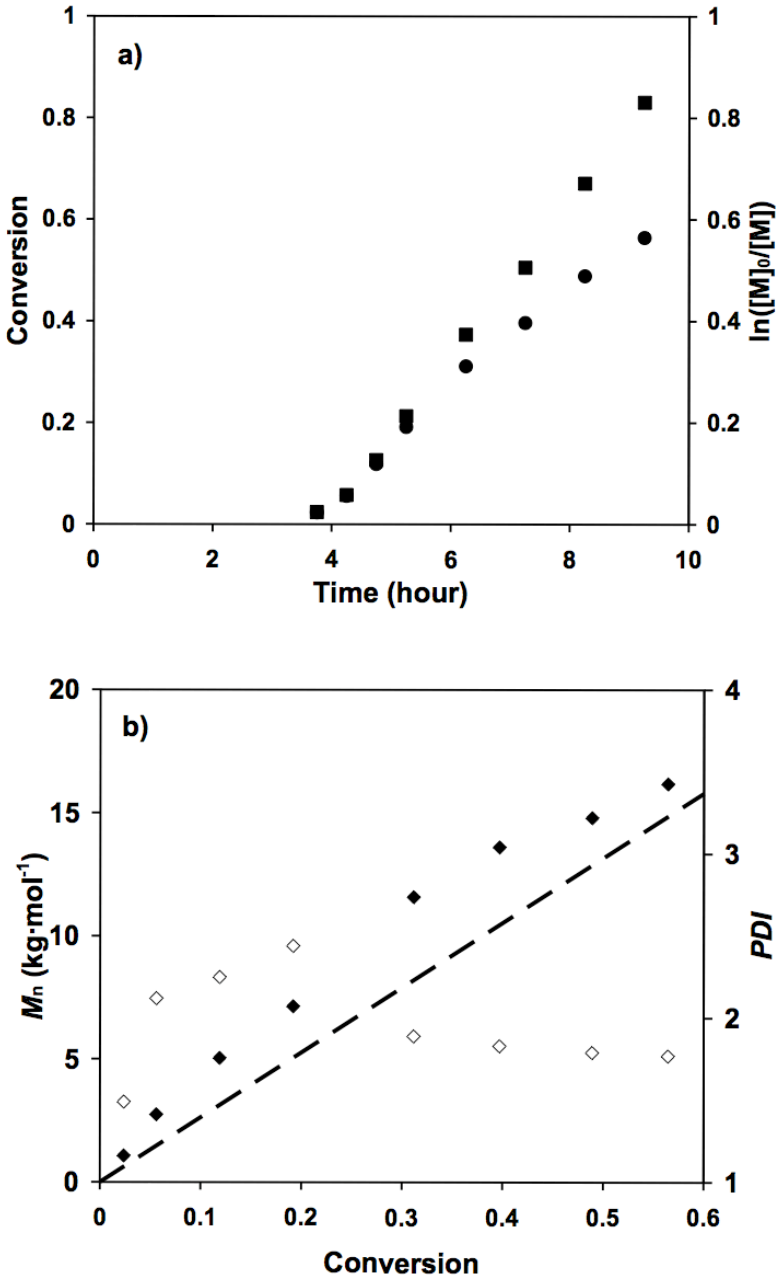

Figure 6-1. (a) Conversion vs. time (●) and kinetic plot (■), and (b) M_n (◆) and PDI (◇) with conversion for the KPS initiated, SG1 mediated emulsion polymerization of styrene. Dashed line represents the theoretical M_n based on SG1 ($M_{n,theory}$ = conversion × $[styrene]_0/[SG1]_0$).

Figure 1b shows that the M_n increased with monomer conversion, however the polydispersity index (*PDI*) remained high for a living polymerization. The *PDI* increases with conversion reaching a value of 2.44 at ~20% conversion before steadily decreasing to a final value of 1.77. A large *PDI* does not negate the living nature of polymerization, as evidenced from the evolution of the entire molecular weight distributions with monomer conversion and the chain extension to form a polystyrene-*b*-poly(butyl acrylate) copolymer (Figure 6-2). Although polymer chains are initiated over a span of hours, the bicomponent system ensures that propagation begins only after most of the chains have been formed. With the majority of chains formed at a monomer conversion less than 3% the long initiation period cannot solely account for the broad distribution of the polymer. A contributing factor to the large *PDI* is the heterogeneity of the system. When the styrene is introduced in the second stage of the polymerization the resulting emulsion contains monomer-swollen micelles and droplets of various sizes (up to microns in diameter), stabilized by the sulfate end group of the surfactant-like SG1-oligomers. After several activation/deactivation cycles the polymer chains are no longer water-soluble, and are tethered to the particle surface by the sulfate end group. Consequently, the number (or concentration) of polymer chains in a particle is a function of the surface area of the particle, while the amount of free SG1 (assumed to rapidly establish phase equilibrium)[16,17] is dependent on the volume of the particle. Hence, the [chains]/[SG1] ratio, responsible for the polymerization rate and degree of control over the polymerization, is a function of the particle size, and it is this effect that is believed to contribute to the large *PDI*. The living polymer chains seem to have different rates of polymerization depending on the size of the particle. During the development of this

system, failed experiments consistently had both broad (and usually bimodal) particle distributions with broad monomodal molecular weight distribution at low conversion that grew into bimodal (or developed a distinct shoulder) molecular weight distributions as the polymerization proceeded. The importance of a uniform particle size in providing an identical environment in aqueous based nitroxide-mediated polymerizations is further highlighted by the confirmation of compartmentalization effects and its influence over the propagation rate and control in aqueous based SFRP, with smaller particles resulting in lower rates of polymerization and significantly higher chain livingness.[18-21]

The ability to conduct living polymerizations of styrene at 90 ^{o}C mediated with SG1 is a consequence of its relatively high dissociation rate constant[7] and its inherent instability in water, which is accelerated at lower pH.[16] The thermal decomposition of KPS produces sulfate radicals that add to a styrene unit or react with water to form HSO_4^- and HO•.[15] When the system was not buffered (final pH ~2.8) the polymerizations were uncontrolled presumably because of the low concentration of SG1, which readily decomposes at low pH.[16] The addition of 1.91×10^{-4} moles of K_2CO_3 ($[KPS]_0/[K_2CO_3]_0$ = 1.32) produced a latex with a final pH of ~6.1 and the polymerization was well controlled, while excess K_2CO_3 ($[KPS]_0/[K_2CO_3]_0$ = 1.05, final pH ~8.3) limited the polymer conversion to less than 10%, attributed to the build up of SG1 that is stable at higher pH. The use of $NaHCO_3$ as a buffer was also investigated, requiring approximately twice the loading of K_2CO_3 to achieve a comparable final pH of the latex. While the progress of the polymerization was similar to the K_2CO_3 buffered experiment, the poor colloidal stability and significant coagulum formation was attributed to the additional electrolyte that reduced the effectiveness of the stabilizing sulfate end groups.

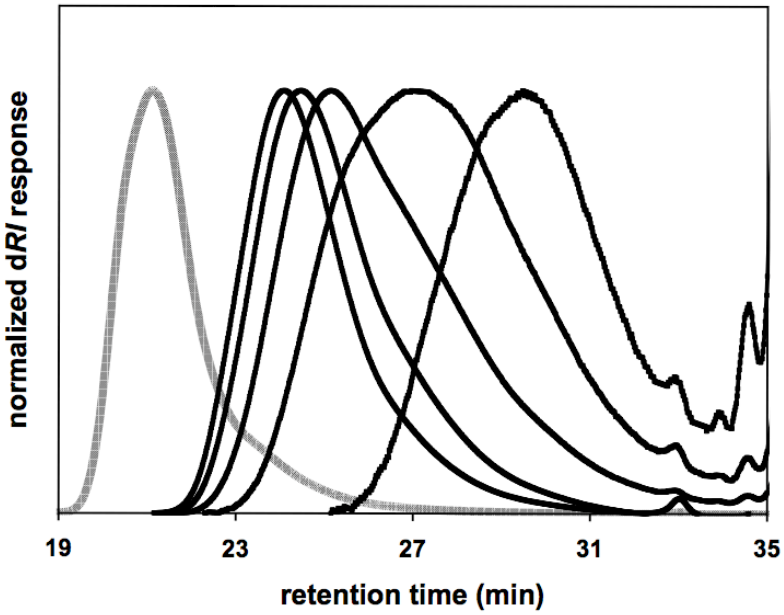

Figure 6-2. SEC traces for the surfactant-free emulsion polymerization of styrene mediated with SG1. See Figure 6-1 for conditions.

Conversion increases from right to left;

conversion = 3%, M_n = 1070, *PDI* = 1.49;

conversion = 6%, M_n = 2750, *PDI* = 2.12;

conversion = 12%, M_n = 5040, *PDI* = 2.25;

conversion = 31%, M_n = 11580, *PDI* = 1.89;

conversion = 56%, M_n = 16180, *PDI* = 1.77;

(grey line) chain extension with butyl acrylate.

6.6 Conclusions

A two-stage nitroxide-mediated surfactant-free emulsion polymerization of styrene was successfully carried out using the water-soluble initiator KPS and the nitroxide SG1. An initial SG1:KPS ratio of 1.5 was required to produce a well-controlled polymerization, provided that the pH of the latex (latex buffered with K_2CO_3) was approximately 6. An excess amount of K_2CO_3 caused the pH of the latex to remain above 8 and no polymerization occurred, while a lack of K_2CO_3 resulted in a low pH that produced poorly controlled polymerization. The living polymer chains seem to have different propagation rates depending on the size of the particle. The heterogeneity in the particle size leads to an increase in PDI, but control is shown by the increase in M_n with conversion, the evolution on the entire molecular weight distribution with conversion, and successful chain extension with butyl acrylate.

6.7 References

1. Chiefari, J.; Chong, Y. K.; Ercole, F.; Krstina, J.; Jeffery, J.; Le, T. P. T.; Mayadunne, R. T. A.; Meijs, G. F.; Moad, C. L.; Moad, G.; Rizzardo, E.; Thang, S. H. *Macromolecules* **1998**, 31, 5559.
2. Kato, M.; Kamigaito, M.; Sawamoto, M.; Higashimura, T. *Macromolecules* **1995,** 28, 1721.
3. Wang, J.; Matyjaszewski, K. *J. Am. Chem. Soc.* **1995,** 117, 5614.
4. Georges, M. K.; Veregin, R. P. N.; Kazmaier, P. M.; Hamer, G. K. *Macromolecules* **1993,** 26, 2987.

5. Qiu, J.; Charleux, B.; Matyjaszewski, K. *Prog. Polym. Sci.* **2001,** 26, 2083.
6. Cunningham, M. F. *Prog. Polym. Sci.* **2002,** 27, 1039.
7. Benoit, D.; Grimaldi, S.; Robin, S.; Finet, J. -P.; Tordo, P.; Gnanou, Y. *J. Am. Chem. Soc.* **2000,** 122, 5929.
8. Cunningham, M. F. *Comptes Rendus Chimie* **2003,** 6, 1351.
9. Cunningham, M.; Lin, M.; Smith, J.; Ma, J.; McAuley, K.; Keoshkerian, B.; Georges, M. *Progr. Colloid Polym. Sci.* **2004,** 124, 88.
10. Szkurhan, A.; Georges, M. K. *Macromolecules* **2004,** 37, 4776.
11. Nicolas, J.; Charleux, B.; Guerret, O.; Magnet, S. *Angew. Chem. Int. Ed.* **2004,** 43, 6186.
12. Nicolas, J.; Charleux, B.; Guerret, O.; Magnet, S. *Macromolecules* **2005,** 38, 9963.
13. Nicolas, J.; Charleux, B.; Magnet, S. *J. Polym. Sci., Part A: Polym. Chem.* **2006,** 44, 4142.
14. Delaittre, G.; Nicolas, J.; Lefay, C.; Save, M.; Charleux, B. *Chem. Commun.* **2005**, 614.
15. Kolthoff, I. M.; Miller, I. K. *J. Am. Chem. Soc.* **1951,** 73, 3055.
16. Farcet, C.; Lansalot, M.; Charleux, B.; Pirri, R.; Vairon, J. P. *Macromolecules* **2000,** 33, 8559.
17. Ma, J. W.; Cunningham, M. F.; McAuley, K. B.; Keoshkerian, B.; Georges, M. K. *Macromol. Theory and Simul.* **2002,** 11, 953.
18. Maehata, H.; Buragina, C.; Keoshkerian, B.Cunningham, M.F. *accepted for publication in Macromolecules* **2007**.
19. Butte, A.; Storti, M.; Morbidelli, M. *DECHEMA Monographs* **1998,** 134, 497.

20. Charleux, B. *Macromolecules* **2000,** 33, 5358.

21. Zetterlund, P. B.; Okubo, M. *Macromolecules* **2006,** 39, 8959.

CHAPTER 7

7 Summary and Conclusions

Aqueous based systems were developed for the three main living/controlled radical polymerization techniques, reversible addition fragmentation transfer (RAFT)/ macromolecular design via interchange of xanthates) MADIX, atom transfer radical polymerization (ATRP) and stable free radical polymerization (SFRP). From this research the main conclusions are as follows.

The controlled polymerization of vinyl acetate can be conducted in an aqueous based system when a miniemulsion system is employed and the xanthate methyl (ethoxycarbonothioyl)sulfanyl acetate (MESA) is used as the mediating agent. The resulting latexes were stable, with no coagulum present. The controlled polymerization of vinyl acetate with MESA in miniemulsion is influenced by the aqueous phase kinetics, evident from the inhibition period at the start of the polymerization (ie. no polymer formation), retardation of the polymerization rate compared to the equivalent free radical polymerization, and the incorporation of only 55% of the MESA into polymer chains. The high solubility of both the MESA and the vinyl acetate monomer suggest that termination in the aqueous phase plays an important role in these systems.

It had previous been reported that ionic surfactants (anionic and cationic) adversely affected the ATRP, thereby limiting aqueous based ATRP to non-ionic surfactants as the sole stabilizing agent. Our research found that the miniemulsion reverse ATRP of butyl methacrylate can be conducted with the cationic surfactant cetyltrimethylammonium bromide (CTAB) as the stabilizer. The use of CTAB produced a colloidally robust miniemulsion, with no coagulum. The formulation was a true miniemulsion (ie. the surfactant loading was below the critical micelle concentration of

the system), allowing for the easy manipulation of particle size (between 100-200nm) by varying the surfactant loading between 0.5-3 wt%. Using the ionic surfactant CTAB allows aqueous based ATRP to be conducted at temperatures up to 90 ^{o}C while maintaining the colloidal stability of the system. Systems stabilized with non-ionic surfactants are usually limited to 60 ^{o}C, after which coagulation becomes an issue because the performance of the non-ionic surfactant decreases at higher temperatures. The benefits of operating reverse ATRP at higher temperatures include and increased polymerization rate, and a more ideal initiation (with all the polymer chains produced in a shorter time frame).

The reverse ATRP of butyl methacrylate in miniemulsion initiated with the redox pair hydrogen peroxide/ascorbic acid and mediated with $CuBr_2$-EHA_6TREN produced high-molecular weight poly(butyl methacrylate) (M_n = 989 900, PDI = 1.25). Typically, for linear polymers produced by ATRP the M_n is limited to ~200 000, after which the effect of the radical side reactions become significant and the livingness of the system is decreased. The use of the redox initiation system dramatically reduced the induction period at the start of the polymerization. The inhibition time of less than 20 minutes is attributed to the initiation of the majority of the polymer chains early in the polymerization, which consumes the $CuBr_2$-EHA_6TREN to levels where polymerization can proceed at an appreciable rate. From the apparent rate constants calculated from the kinetic plots and normalized with respect to the number of polymer chains, the redox initiated systems are five times faster than systems initiated with azo-based compounds. As the k_p and K_{eq} values should not be influenced by the initiation system, the conclusion is that the HPO/AA system yields an advantageous ratio of [Cu(I)]/[Cu(II)] that allows

the polymerization to proceed at higher rates and to much higher molecular weights, while preserving control, than has previously been observed. The miniemulsions were stabilized with the non-ionic surfactant Brij 98, at a loading of 10 wt%. Typically, the final latexes were monomodal and ranged in particle size from 90-110 nm, with less than 2 wt% coagulum at the end of the polymerization. The particle sizes were confirmed with a Malvern Mastersizer 2000, which also verified the absence of large particles in the system.

Combining the results from the work into cationic surfactants (which allows the particle size in the system to be varied) and the ability to create high molecular weight polymers I was able to show that compartmentalization can influence miniemulsion reverse ATRP under the right set of conditions. Both the particle size and the number of polymer chains contained in the particle are important parameters to control when formulating a compartmentalized ATRP system. The number of chains is important in miniemulsion ATRP because compartmentalization requires that the reactants (active polymeric radicals and $CuBr_2$-EHA_6TREN) be limited by the volume of the particle. It was determined that a particle size of less than 200 nm is sufficiently small to affect ATRP provided that each particle contains less than 4 000 polymer chains. The differences between a conventional free radical polymerization and ATRP are highlighted by the opposing impact that compartmentalization has on the kinetics of the polymerizations. In a conventional system the segregation effect dominates and causes an increase in the polymerization rate, while it was determined that the confined space effect dominates the kinetics in ATRP and cause a reduction in the polymerization rate. Compartmentalization was shown to improve the linearity of growth for M_n with

conversion, decrease the PDI of the polymer, and maintain better control of the polymerization during the early stage of the polymerization when the radical concentration is at its peak.

Finally, with the knowledge gained from working with ATRP a two-stage nitroxide-mediated surfactant-free polymerization of styrene mediated with SG1 and initiated by the thermal decomposition of the water-soluble potassium persulfate (KPS) was developed. To stimulate the creation of micelles, the desired loci of polymerization, a multi-stage approach was adopted starting from dilute styrene/water solutions to favor the formation of the alkoxyamine and short chain SG1-oligomers (stage one) before the addition of the majority of the styrene (stage two). The polymers have broad a PDI attributed to the heterogeneity of the system, but control is shown by the increase in M_n with conversion, the evolution on the entire molecular weight distribution, and successful chain extension with butyl acrylate. The surfactant-free polymerization links the number of polymer chains to the amount of stabilizing agent the system and therefore the process was found to be dependant on the amount and ratio of SG1, KPS, and K_2CO_3. The amount of styrene in the first stage of the polymerization was found to influence the formation of the SG1-terminated oligomers.

CHAPTER 8

8 Recommendations for Future Work

1. The L/CRP of vinyl acetate was shown to be viable in miniemulsion, but the system can be further developed. Optimization and expansion to different surfactants, xanthates and initiators (oil-soluble and water-soluble) may allow for better control of the polymerization.
2. Determine whether the low MADIX efficiency results from the formation of short chain water-soluble MADIX compounds, or an unknown side reaction that consumes the MADIX compound. Exploring the system (see point 1) may provide some insight. As well, developing new xanthates with a long chain alkyl Z-group would help to probe the issue and illustrate the influence of controlling agents (ie. xanthate) solubility in aqueous based MADIX systems.
3. The formation of block polymers, and particles with core-shell morphology could also be developed. The vinyl acetate shell could be hydrolyzed to produce a poly(vinyl alcohol) "hairy" particle. Further modification could entail ionizing the poly(vinyl alcohol) to create pH sensitive nanoparticles.
4. The high water solubility of the xanthate and kinetics of MADIX create the potential for an emulsion-based system to be developed, eliminating the need for the hyrdophobe and the application of high shear.
5. The use of CTAB proved that ionic surfactants are compatible with ATRP. There is the opportunity to explore additional cationic surfactants and mixed (ionic and non-ionic) surfactant systems which would provide insight into the effect (if any) of the surfactant on ATRP. As well, there remains the question of whether the other

initiation mechanisms (simultaneous reverse and normal initiation, AGET) are compatible with cationic surfactants.

6. Understand the cause of the rapid increase in the molecular weight at the beginning of reverse ATRP. A limited number of experiments show a rapid increase also occurs in bulk experiments with AIBN. Does it really occur or can a suitable formulation eliminate it. Is it the same phenomenon in bulk and miniemulsion, or are the aqueous phase kinetics playing a significant role. This could be investigated by developing a bulk system that is transferred to a miniemulsion process.
7. All the research has focused on very hydrophobic ATRP mediating complexes (to maintain the copper in the organic phase). There could be (based on other L/CRP techniques) significant aqueous phase kinetics at work early in the ATRP miniemulsion system. Using a water soluble mediating agent at very low monomer concentration (target degree of polymerization less than 10 monomer units) or a mixed ATRP system, with a water-soluble mediating agent and an oil-soluble mediating agent could provide insight into the aqueous phase kinetic at work in ATRP systems.
8. When ATRP is initiated with the redox initiation system HPO/AA there appears to be an advantageous ratio of Cu(I)/Cu(II) which allows for fast rate of polymerization. An additive that increases the polymerization rate for ATRP systems would be beneficial. Adding HPO and/or AA to an ATRP miniemulsion that was initiated with a azo-based initiator could allow for rate enhancement, and help to determine the role of HPO and AA in ATRP.

9. The compartmentalization needs to be further explored. It would be beneficial if a bulk ATRP system could be adapted to an emulsion-based with a range of particle sizes from 100nm to 500nm. The number of chains in a particle was argued to be an important criterion for compartmentalization. Developing a system with particle sizes less than 100 nm would help explore this. Alternatively, using hexadecane to dilute the number of chains in a miniemulsion droplet may also allow this issue to be probed for systems with lower target molecular weights.